Experimental Investigation on the Formation of Carbon-Bearing Molecules in the Interstellar Medium via Neutral−Neutral Reactions

Ralf I. Kaiser*

Department of Chemistry, University of York, YO10 5DD, U.K.

Received August 15, 2001

Contents

I. Introduction

The physical and chemical processes leading to the formation of molecules in the interstellar medium (ISM)—the vast voids between the stars—fascinated scientists since the first detection of CH, CH^+, and CN radicals in extraterrestrial environments 60 years ago. Although more than one-half of a century has passed by and 121 species from molecular hydrogen (H_2) to polyatomics such as the sugar glycolaldehyde ($HOCH_2CHO$), benzene (C_6H_6), cyanopentaacetylene ($HC_{11}N$), and possibly the amino acid glycine (H_2NCH_2COOH) have been identified so far, the enigma 'How are these molecules actually formed under the harsh conditions in the interstellar medium?' is still under debate.[1]

This review focuses on the newly emerging field of astrochemistry and anthologizes the latest trends in laboratory experiments on the formation of carbon-bearing molecules in the interstellar medium via neutral−neutral reactions. To introduce this topic to the general chemical community and novices, the first sections provide an overview of the chemical composition (atoms versus molecules; neutrals versus ions; gas phase versus solid state) and the physical properties (temperatures and number densities) of various interstellar environments (sections I.A and I.B). This provides the crucial background to understand the basic molecular processes and prerequisites of how molecules might be synthesized in the strongly diverse regions of the interstellar medium (section

Ralf I. Kaiser was born on May 24, 1966, in Unna, Germany. He received his Ph.D. degree in Chemistry from the University of Münster (Germany) and Nuclear Research Center (Jülich). He did postdoctoral work on the formation of astrophysical molecules in the interstellar medium at UC Berkeley (Department of Chemistry). From 1997 to 2000 he received a fellowship from the German Research Council (DFG) to perform his *Habilitation* at the Department of Physics (University of Chemnitz, Germany) and Institute of Atomic and Molecular Sciences (Academia Sinica, Taiwan). His research interests include chemical reaction dynamics (gas phase and solid state), planetary chemistry, and laboratory studies relevant to astrochemistry.

* E-mail: rik1@york.ac.uk.

10.1021/cr970004v CCC: $39.75
Published on Web 04/11/2002

Table 1. Classification of Neutral Species and Ions Detected in the Interstellar Medium via Microwave Spectroscopy Unless Noted Otherwise[a]

1. diatomic molecules

H_2(IR) CC(IR) CN CP* CO CS* SiC* SiN* SiO SiS NP NO NS SO

2. halides and pseudohalides

HF HCl
NaCl* KCl NaCN
MgCN MgNC
AlF* AlCl*
SiCN

3. hydrides

CH_4(IR) NH_3 H_2O CH NH(UV) OH SH
SiH_4*(IR) H_2S CH_2 NH_2
CH_3

4. closed shell hydrocarbons

CH_4(IR) C_2H_4*(IR) C_2H_2(IR) CH_3CCH CH_3CCCCH
HCCCCH# HCCCCCCH#
C_6H_6#

5. long chain molecules

$CH_3(C{\equiv}C)_nH$	n = 1, 2
HC_n	n = 1-8
$H(C{\equiv}C)_nH$	n = 2#, 4#
C_n	n = 2(IR), 3(IR; UV), 5(IR)*
$H(C{\equiv}C)_nCN$	n = 1-5
$(C{\equiv}C)_nCN$	n = 1, 2*
$CH_3(C{\equiv}C)_nCN$	n = 1, 2
H_2C_n	n = 3, 4, 6*
C_nO	n = 1, 2, 3, 5
C_nS	n = 1, 2, 3*, 5(?)
C_nSi	n = 1, 4*

6. cyclic molecules

SiC_2 SiC_3 C_3H C_2H_4O C_3H_2

7. oxygen and carbon containing molecules

CH_3OH H_2CO HCOOH
C_2H_5OH CH_3CHO CH_3COOH
$HCOOCH_3$
C_2H_3OH
H_2CCO HCCCHO CH_3COCH_3 CH_3OCH_3 $HOCH_2HCO$
CO CO_2 HCO C_2O C_3O C_5O

8. sulfur and carbon containing molecules

CH_3SH H_2CS CS C_2S C_3S

9. nitrogen and carbon containing molecules

HCN CHCN*
CH_2CN
CH_3CN C_2H_3CN C_2H_5CN H_2NCN
CH_3NH_2 H_2CNH
H_2CN

10. structural isomers

c-C_3H_2	l-C_3H_2
c-C_3H	l-C_3H
HCN	HNC
CH_3CN	CH_3NC
HCO^+	HOC^+
MgCN	MgNC

HCCCN HCCNC HNCCC
CH_3COOH $HCOOCH_3$ $HOCH_2HCO$
CH_3CHO c-C_2H_4O C_2H_3OH

11. other molecules

SO_2 OCS N_2O HNO
$HCONH_2$ HNCO HNCS
H_2NCH_2COOH(?)

12. ions

CH^+(VIS) CO^+ SO^+
HCO^+ HCS^+ HNN^+ HOC^+ H_3^+(IR)
$HCNH^+$ $HOCO^+$ H_3O^+
H_2COH^+ HC_3NH^+

[a] IR, infrared; UV, ultraviolet; VIS, visible; ?, tentative identification; *, observation only in carbon-rich circumstellar envelopes; #, observation only in carbon-rich planetary nebulae.

I.C). Since carbon is the fourth most abundant element in the universe and the basis of all life as we know it, an understanding of elementary chemical reactions involving carbon-bearing species is of particular importance to expose the chemical processing of interstellar matter. Selected reaction classes which are of paramount significance to key questions in astrochemistry and astrobiology are examined in sections II.A−D. The subsequent sections review modern experimental techniques to untangle the rate constants (kinetics; section III), intermediates involved, products, and the reaction mechanisms (dynamics; section IV) of these important neutral−neutral reactions. The last sections summarize these findings, evaluate the benefits and limitations of currently operating experimental setups critically, and emphasize future research directions to study important classes of neutral−neutral reactions in the interstellar medium. Finally, implications for solar system sciences and terrestrial stages such as combustion processes and chemical vapor deposition are addressed.

A. Interstellar Medium

The ISM contains about 10% of the mass of our galaxy and consists of gas (99%) and submicrometer-sized grain particles (1%) with averaged number densities of 1 H atom cm^{-3} and 10^{-11} grains cm^{-3}, respectively.[2−5] These data translate to pressures of about 10^{-18} mbar at 10 K, which is beyond any ultrahigh vacuum achieved in terrestrial laboratories so far. The chemical composition of the interstellar medium is dominated by neutral hydrogen (93.38%) and helium (6.49%), whereas biogenic elements oxygen, carbon, and nitrogen contribute 0.11% (O:C:N $\approx$ 7:3:1).[6] The third-row elements neon, silicon, magnesium, and sulfur are less copious (0.002%) and have relative abundances of 8:3:3:2; all remaining elements furnish only 0.02%.

This elementary classification is well-reflected in the molecular composition of the interstellar medium. Molecules, radicals, and ions are ubiquitous in extraterrestrial environments and have been detected in extraordinary diversity ranging from small molecules such as hydrogen (H_2) to astrobiologically important species such as the simplest sugar glycolaldehyde ($HOCH_2CHO$) and possibly the amino acid glycine (H_2NCH_2COOH). Table 1 compiles all species identified in the interstellar medium so far, many of them thermally unstable and extremely reactive in

terrestrial laboratories.[7] The majority of these molecules were detected by radio telescopes observing their rotational transitions in emission; to a minor extent, infrared (IR), visible (VIS), and ultraviolet (UV) astronomy fostered their identification. Diatomic molecules with second- and third-row elements are particularly prevalent; in particular, carbon (C_2, CN, CO, CS) and silicon (SiC, SiN, SiO, SiS) bearing species have to be named. CP and PN are the only phosphorus-containing molecules identified so far; NO, NS, and SO represent the sole extraterrestrial radicals carrying atoms of the fifth and sixth period.

Halides and pseudohalides represent a second important class of molecules. Quite surprisingly, two halogen hydrides HF and HCl together with three alkali carrying species NaCl, KCl, and NaCN present a significant component of the interstellar medium; in particular, the open-shell species MgCN, MgNC, AlF, AlCl, and SiCN denote crucial tracers of metals and semi-metals bound in molecular form.

Di-, tri-, and tetravalent hydrides methane (CH_4), silane (SiH_4), ammonia (NH_3), water (H_2O), and hydrogen sulfide (H_2S) are very important species as they implicate the parent molecules of CH, CH_2, CH_3, NH, NH_2, OH, and SH radicals. Note that neither phosphine (PH_3) nor silicon-bearing radicals SiH_3, SiH_2, and SiH have been identified in the interstellar medium; however, phosphine, its higher homologue arsine (AsH_3), and germane (GeH_4) designate substantial trace constituents in the atmospheres of Jupiter and Saturn. Methane—the simplest, closed-shell and fully saturated hydrocarbon molecule—leads us to olefines and alkynes. Here, ethylene (C_2H_4), acetylene (C_2H_2), methylacetylene (CH_3CCH), and methyldiacetylene (CH_3CCCCH) contribute significantly to the cosmic carbon budget. Very recently, diacetylene (C_4H_2), triacetylene (C_6H_2), and benzene (C_6H_6) were detected as well. The search for allene (H_2CCCH_2)—a structural isomer of methylacetylene—has been unsuccessful so far.

These hydrocarbons stand in strong contrast to hydrogen-deficient, linear carbon chain molecules. Here, hydrogen-terminated carbon clusters from the ethinyl radical (C_2H) to octatetraynyl (C_8H), the bare carbon clusters C_2, C_3, and C_5, cummulene carbenes (H_2CCC, H_2CCCC, $H_2CCCCCC$) together with oxygen (C_2O, C_3O, C_5O)-, sulfur (C_2S, C_3S)-, and silicon (C_4-Si)-terminated carbon chains are very abundant in space. Likewise, cyanopolyacetylenes ($H(CC)_nCN$), together with their radicals ($(CC)_n-CN$), and methylcyanopolyacetylenes ($CH_3-(CC)_nCN$) present important molecules which are to some extent considered as precursors to amino acids. These linear species expose a beautiful contrast to cyclic molecules silicon dicarbide (SiC_2), silicon tricarbide (SiC_3), tricarbonhydride (c-C_3H), cyclopropenylidene (c-C_3H_2), and ethylene oxide (C_2H_4O).

The latter connects to complex, organic molecules observed in the interstellar medium. Particular attention has been devoted to alcohols (methanol (CH_3-OH), ethanol (C_2H_5OH), and vinyl alcohol (C_2H_4O)),[8] aldehydes (formaldehyde (H_2CO), acetaldehyde (CH_3-CHO)), acids (formic acid (HCOOH), acetic acid (CH_3-COOH)), and their fully oxidized product carbon dioxide (CO_2). Further, formic acid methylester ($HCOOCH_3$), acetone (CH_3COCH_3), dimethyl ether (CH_3OCH_3), ketene (H_2CCO), propynal (HCCCHO), and the formyl radical (HCO) are present in detectable quantities. Two of these species possess interstellar sulfur counterparts, namely, thioformaldehyde (H_2CS) and thiomethanol (CH_3SH).

Besides cyanopolyacetylenes and their radicals, rather saturated, nitrogen-carrying molecules are of crucial importance to the interstellar nitrogen budget. Here, methyl- and ethylcyanide (CH_3CN, C_2H_5-CN) together with the CH_2CN and CHCN radicals have to be addressed. Likewise, hydrogen cyanide (HCN) and the isocyanide isomer (HNC), their reduced forms H_2CN, H_2CNH, and CH_3NH_2, plus H_2-NCN are worth mentioning. Vinylcyanide (C_2H_3CN) completes the homologous row from the bare, nitrogen-terminated cluster CCCN via cyanoacetylene (HC-CCN) to ethylcyanide (C_2H_5CN). As the molecular complexity rises, molecules with four different types of atoms have been detected in the interstellar medium in small quantities; these are $HCONH_2$, HNCO, and HNCS.

Structural isomers—molecules with the same chemical formula but distinct connectivities of atoms—and molecular ions received special fascination. As the relative abundances of isomers should depend strongly on the physical and chemical conditions in the interstellar medium, isomers act as tracers to elucidate temperature- and density-dependent formation routes to extraterrestrial molecules. Species of the gross formula C_2H_4O, $C_2H_4O_2$, and HC_3N represent the only cases where three isomers have been observed, namely, ethylene oxide, acetaldehyde, and vinyl alcohol (system 1), acetic acid, formic acid methylester, and glycolaldehyde (system 2), as well as cyanoacetylene, isocyanoacetylene, and the carbene structure HNCCC (system 3). Six isomer pairs of cyclic (c) and linear (l) C_3H, c/l-C_3H_2, HCN/HNC, CH_3CN/CH_3NC, MgCN/MgNC, and HCO^+/HOC^+ have been assigned as well. Ions, especially H_3^+, are thought to be important ingredients to drive a rich chemistry in those extraterrestrial environments in which neutral particles are sparse. Notice that, on average, 97% of all molecules are neutral whereas only 3% are positively charged; so far, no anion has been identified unambiguously in the interstellar medium.

B. Extraterrestrial Environments

The majority of the volume of the interstellar medium is very hot ($T > 10\,000$ K) and does not contain any molecules at all. Hence, interstellar molecules, radicals, and ions detected so far are not distributed homogeneously but are confined to distinct environments. These can be categorized thoroughly into six classes based on their size (large-scale structures versus point sources), physical parameters (density, average translational temperature), and the chemical characteristics (Table 2 and Figure 1).[9−23] The interstellar medium is composed primarily of three types of large-scale structures which are often called 'clouds'. These are diffuse clouds, translucent

Table 2. Overview of Physical Parameters in Important Interstellar Environments

region	molecules	density, cm^{-3}	temp, K
diffuse clouds	simple molecules H_2, CH^+, CH, CN, C_2, OH, CO, HCO^+, HCN	10^1-10^2	100−120
translucent clouds	simple molecules H_2, CH^+, CH, CN, C_2, OH, CO, HCO^+, HCN, C_3	10^2-10^3	50−100
dense clouds (molecular clouds) (cold clouds)	carbon-rich, linear and cyclic molecules with up to 13 atoms	10^2-10^4	10−15
hot molecular cores	1. saturated molecules CH_3OH, C_2H_5OH, C_2H_5CN, CH_3COCH_3, CH_4, NH_3, H_2O 2. no carbon-rich linear molecules 3. vibrationally excited $HCCCN/C_2H_3CN$ 4. large deuterium fractionation	10^6-10^9	100−300
circumstellar envelopes	carbon rich: carbon clusters and hydrogen-terminated clusters oxygen rich: small oxygen bearing species	variable	10−4500
planetary nebulae	carbon rich: di- and triacetylene, benzene	variable	200−3000

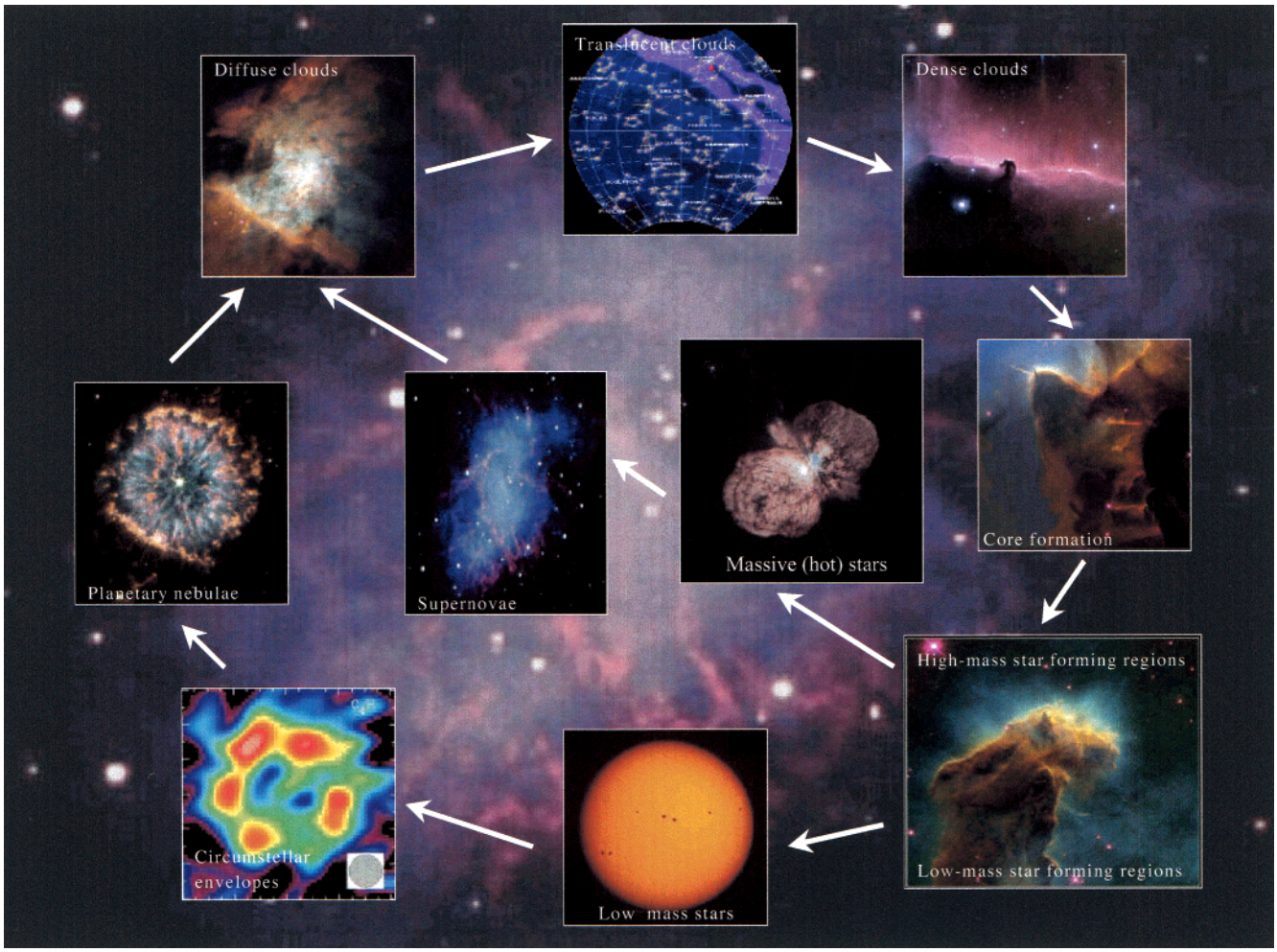

Figure 1. Cycling of matter in the interstellar medium: diffuse clouds, translucent clouds, molecular clouds, core formation, high- and low-mass star-forming regions, supernovae, circumstellar envelopes, and planetary nebulae.

clouds (semitransparent clouds), and dense clouds (cold clouds; molecular clouds).[24] The nomenclature is based on an increasingly denser medium rising from 10^1 to10^4 atoms cm^{-3} as the temperature drops simultaneously from 120 to about 10 K. As the density rises further to 10^9 atoms cm^{-3}, we move toward star-forming regions with hot molecular cores and young stellar objects (YSO) which resemble stars in their very early phase of life.[25−27] This class presents the link between large-scale structures and pointlike sources such as circumstellar envelopes (CSE) and planetary nebulae (PNe). The latter classification is in line with an increasingly aging star. As stars evolve and reach the end of their lives, they develop winds which return part of their stellar matter back into the interstellar medium (low-mass stars with masses $M < 1$ $M_\odot$ ($M_\odot$ = solar mass)) or they end their life violently in a supernova explosion (massive stars; $M > 1-10$ $M_\odot$).[28−32] These ejecta contain elements heavier than helium; a fraction of these ejecta is incorporated into solid matter (dust grains); the rest remains in the gas phase. The following sections (sections I.B.1−6) examine the physical and chemical characteristics of each region.

This sets the stage to discuss the ongoing chemistry in the interstellar medium (section I.C).

1. Diffuse Clouds

Diffuse clouds are tenuous concentrations of interstellar matter with typical number densities of 10^1-10^2 atoms cm^{-3} and average translational temperatures of the gas of 100−120 K.[33] They contain up to a few thousand solar masses. ζOph (Ophiuchi), and ξ Per (Persei) represent typical examples of diffuse clouds. These structures are called 'diffuse' because the interstellar ultraviolet radiation easily penetrates. UV photons play a significant role in the chemistry of diffuse clouds as they ensure photodissociation of molecules. Further, atoms and molecules with ionization potentials (IP) less than of atomic hydrogen (13.59 eV) can be photoionized. This limit represents the highest energy available to photodissociate and photoionize; shorter wavelengths are absorbed by interstellar hydrogen atoms and, hence, are confined to regions around brightest stars.[34] Therefore, most of the atomic carbon $C(^3P_j)$ (11.26 eV), silicon $Si(^3P_j)$ (8.15 eV), sulfur $S(^3P_j)$ (10.36 eV), and magnesium $Mg(^1S_0)$ (7.64 eV) is expected to be ionized; nitrogen $N(^4S_{3/2})$ (14.53 eV) and oxygen $O(^3P_j)$ (13.62 eV) should exist in their atomic form. So far the diatomics H_2, CH, CH^+, CS, CN, C_2, OH, HCl, and CO have been detected unambiguously. The only triatomic species identified are HCN, HNC, C_2H, and HCO^+.[35] Very recently, C_3 has been observed toward ζOph and ξ Per.[36] These molecules accommodate strong carbon−hydrogen, carbon−carbon, and carbon−nitrogen backbones. Formaldehyde (H_2CO) and the aromatic species cyclopropenylidene (c-C_3H_2) have been detected as well. Although large molecules are also thought to be present in diffuse clouds as polycyclic aromatic hydrocarbon (PAH)-like structures, the latter are not formed in situ but are injected into the interstellar medium from winds of dying, carbon-rich stars or indirectly via erosion of carbonaceous solid-state matter (section II.D).

2. Translucent Clouds

Translucent clouds are suggested to form the bridge between diffuse and dense structures. These clouds are defined by moderate number densities of 10^2-10^3 atoms cm^{-3} and relatively low kinetic temperatures of 50−100 K compared to diffuse structures.[37] The molecular composition of translucent clouds such as Cyg OB2 No.12, HD 29647, HD 147889, and Cas A is well-reflected by small diatomics H_2, CH, CH^+, CS, CN, C_2, OH, and CO together with larger species HCN, HNC, C_2H, HCO^+, and H_2CO. The tricarbon molecule C_3 was tentatively identified toward HD 147889. Further, the abundance of interstellar CH_2 is significantly enhanced in a cold translucent cloud compared to low-density regions. So far, no signatures of early stars, so-called pre main sequence stars, have been found in these environments.

3. Dense Clouds

Dense clouds are formed from low-density clouds and characterized by typical number densities of 10^2-10^4 atoms cm^{-3}. Due to their low kinetic gas temperatures of only 10−15 K,[38] these dense structures are also referred to as cold clouds. Whereas in diffuse and translucent clouds the formation of molecules is dominated by photochemistry and photoionization, interstellar dust particles—submicrometer-sized silicate- and carbonaceous-based grain nuclei—inside dense clouds shield complex molecules from the destructive short wavelength radiation field. Therefore, the flux of the interstellar UV radiation field drops from 10^8 photons cm^{-2} s^{-1} to a residual flux of only 10^3 photons cm^{-2} s^{-1}. The latter is dictated by the cosmic ray particle—mostly energetic protons and helium nuclei-driven ionization of molecular hydrogen followed by a recombination of an electron from the cosmic radiation field with H_2^+ to form excited hydrogen. These excited states decay radiatively and emit photons in the UV and VIS range of the electromagnetic spectrum. Note, however, that compared to the inner regions of molecular clouds, the outer rims are more diffuse (10^2 atoms cm^{-3}) and hence bombarded by a significantly higher photon flux. Due to the efficient extinction of UV and VIS light by dust, dense clouds block entirely the light of stars, which lie behind them. Therefore, dense clouds are also known as dark clouds because they often appear on images as black patches. These clouds contain an unprecedented variety of neutral molecules and hence are dubbed molecular clouds. The chemistry of the Taurus Molecular Cloud 1 (TMC-1) has been studied extensively. Its composition is dominated by molecular hydrogen (H_2); only trace amounts of atomic hydrogen of about 1 atom cm^{-3} exist. In strong contrast to diffuse clouds, the fractional ionization in dense clouds is only $10^{-6}-10^{-8}$. This is well-reflected in a significant density of neutral carbon atoms $C(^3P_j)$ as detected toward the molecular clouds Orion A,[39] TMC-1,[40,41] L134N, and IC 5146[42] with ratios of 0.05−0.2 compared to carbon monoxide (CO). The latter furnishes the second most abundant molecule with fractional abundances f of 8×10^{-5} compared to hydrogen, followed by the hydroxyl radical (OH; $f = 10^{-7}$). Dense clouds contain further a rich variety of hydrogen-deficient carbon chains cyanopolyynes, cummulene carbenes, methylated molecules, as well as H-, N-, O-, and S-terminated carbon clusters (Table 1). In particular, the large fractional abundances of the cyclic molecule c-C_3H_2 ($f \leq 2 \times 10^{-8}$) and c-C_3H ($f \leq 10^{-9}$) should be highlighted. Cyanopentaacetylene ($HC_{10}CN$) presents the largest single molecule identified so far in TMC-1.

4. Star-Forming Regions, Young Stellar Objects, and Hot Molecular Cores

Dense clouds are in a precollapse phase and contain the basic ingredients to form massive and low-mass stars.[43] Dense clouds represent therefore the formation sites of stars such as our Sun. Whereas spectral lines observed toward the dense cloud TMC-1 show little evidence of cloud rotation or collapse, the theory of star formation requires that the core of a quiescent molecular cloud collapses under its own gravity. These cores have masses of typically 10^4 solar masses and are denser than the outer regions

of the molecular clouds. The very first step toward the core collapse is thought to be the condensation of gas-phase species onto the cold mantles of grains inside dense clouds.[44] This aggregation continues for about 10^5 years, until the force of gravity overcomes the resistance provided by the gas pressure and magnetic pressure. As the core collapses, it fragments into clumps of about 10−50 solar masses. Note that the Orion Molecular Cloud (OMC) has two of these clumps in the direction of the Kleinman−Low (KL) Nebula—the hot core and the compact ridge.[45]

Once a clump has broken free from the other parts of the cloud core, it has its own gravity. The dynamic collapse proceeds, and angular momentum turns the clump into a rotating disk: a protostar and an accretion disk are formed onto which material from the surrounding matter falls down. The infalling gas releases its kinetic energy in the form of heat, hence the temperature and pressure in the center of the protostar increase. As its temperature approaches a few thousand Kelvin, it becomes an infrared source, which is indicative of a young stellar object (YSO). The whole process might take up to 10^7 years and is accompanied by a significant change of the physical parameters. The density increases from 10^4 atoms cm^{-3} in cold clouds up to 10^9 atoms cm^{-3} in the circumstellar disk still surrounding the young stellar object. Temperatures range from 10 K in the collapsing envelope to a few thousand Kelvin in the gas shocked by the impact. After the new star has formed, its radiation heats the surrounding matter and molecules sublime from the remaining icy grain mantles back into the gas phase. The infall of mass is stopped when thermonuclear fusion (hydrogen burning) begins. This phase is accompanied by strong stellar wind, usually more or less parallel to the rotation axis. Since they occur at the northern and southern poles of the young stars perpendicular to the accretion disk, they are often dubbed as 'bipolar outflows'. These outflows drive strong shock waves to the surrounding gas, which can be heated to 1000 K or more; this presents a second source to sublime molecules from the grain mantles into the gas phase. This early phase of the life of the star is called 'T Tauri' phase.[46] T Tauri stars such as the Trapezium Cluster in the Orion Nebula are always embedded in the clouds of gas from which they were born and can lose up to one-half of its mass before becoming a main sequence star. This ultimate mass loss leads to the cleaning stage where the envelope is dispersed. Once the main sequence is reached, no massive loss of matter occurs. The mass of the star is fixed as long as the hydrogen burning in its center continues. Young main sequence stars are often hot (OB stars) and influence the molecular abundances by photodissociation and ionization-forming areas of ionized hydrogen, so-called HII regions.[47]

The energetic environment surrounding a protostar is called the hot molecular core (HMC) containing several tens of solar masses. HMCs are found in regions of massive star formation such as the ρ Ophiuchi complex with 300 young stellar objects.[48,49] The thermal radiation from the central star heats the grain particles and sublimes the ice mantles progressively.[50,51] This phase is characterized by densities up to 10^8 atoms cm^{-3} and kinetic temperatures of gas-phase molecules of 100−300 K as found in the hot core Sgr B2(N), Cepheus A, Orion A, and W51.[52,53] It is apparent that this thermal sublimation should lead to a distinct molecular composition of hot molecular cores compared to dense clouds. This has been confirmed. The molecular inventory of hot cores is dominated by saturated molecules (CH_3OH, C_2H_5OH, CH_3OCH_3, C_2H_5CN, CH_3COCH_3, CH_4, H_2O, and NH_3) which are enriched by a factor of 10^3−10^5 compared to quiescent molecular clouds.[54−58] These environments contain further a great variety of complex epoxides, aldehydes, ketones, and acids, for instance the cyclic molecule ethylene oxide (C_2H_4O),[59−61] acetaldehyde (CH_3CHO), formic acid (HCOOH), acetic acid (CH_3COOH), glycolaldehyde ($HOCH_2CHO$), carbon dioxide (CO_2), and possibly glycine (H_2NCH_2COOH).[62−67] The only unsaturated molecules detected so far are vibrationally excited cyanoacetylene (HCCCN) toward G10.47+0.03[68,69] and vinyl cyanide (C_2H_3CN) in Sgr B2(N).[70] With the exception of the ethinyl radical (C_2H), no hydrogen-terminated carbon chains C_nH ($n = 3$−8) have been found in hot cores.

Since current gas-phase processes cannot reproduce the observed number densities of saturated molecules, these species are suggested to be synthesized on interstellar grains at 10 K in the molecular cloud stage and then released into the gas phase by sublimation in hot molecular cores. This hypothesis has been supported very recently employing formaldehyde (H_2CO) and deuterated molecules as tracers. Depending on whether the nuclear spin of both protons is parallel or antiparallel, formaldehyde can exist in an ortho (o) or para (p) form. Since the conversion from one to the other spin state by collisional processes is strictly forbidden, o/p abundances yield information on the molecular formation temperature.[71−73] At elevated temperatures of 300 K as found in the hot molecular core L1498, the ratio of the statistical weight of o-H_2CO/p-H_2CO of 3 would be expected, if formaldehyde is synthesized in the gas phase. However, the actually observed ratios in hot cores L723 and L1228, which have typical temperatures of 300 K, of 1.5−2.1 suggest a thermalization and hence formation of formaldehyde at a lower kinetic temperature. This finding strongly suggests a synthesis of formaldehyde on 10 K grains, followed by a sublimation into the gas phase during the HMC stage.[74] Second, a significant deuterium enrichment as found in HDO, NH_2D, HDCO, and D_2CO which exceeds the cosmic D/H ratio of 10^{-5} by a factor of 10^2−10^3 supports the hypothesis that molecules in hot cores sublime from grains.[75] Since the process of D fractionation depends on small zero-point vibrational energy differences, the observed fractionation in HMCs must have occurred at $T < 20$ K but not in the hot gas of the molecular cores.[76,77] An explosive desorption of molecules from grains, which is triggered by radical recombination on grains at 10 K or upon heating to $T > 30$ K, presents a nonequilibrium scenario to replenish molecules from the grains back into the gas phase.[78]

As YSOs present bright and natural infrared sources, they allow a detection of molecules in their envelopes along the line-of-sight to terrestrial or space born telescopes. The identification of gaseous hydrogen cyanide (HCN), acetylene (C_2H_2), carbon dioxide (CO_2), and methane (CH_4) in the infrared regime employing the Infrared Space Observatory (ISO)[79,80] clearly demonstrates the unique power of this technique.[81] Most important, the molecular composition of ices can be unraveled once the YSO forms in the infrared regime utilizing the ISO; recall that molecules frozen on grains show no rotational spectrum and hence cannot be probed via radio telescopes. W33A and NGC7538:IRS9 denote the best studied protostellar and high-mass young stellar objects, respectively.[82−85] So far, only eight simple molecules have been identified unambiguously in ices toward protostellar and YSOs.[86,87] This is based on the relatively insensitive IR detection method compared to microwave spectroscopy. The identification of minor species of concentrations less than 0.01 relative to water remains a tremendous challenge for the future. However, once those species are released into the gas phase, radio telescopes can observe these molecules—if they bear a permanent dipole moment. The water molecule (H_2O) is by far the dominating ice component, whereas carbon monoxide (CO; 0.08−0.15) and carbon dioxide (CO_2; 0.12) are about 1 order of magnitude less abundant.[88−93] Methane (CH_4; 0.004−0.019), ammonia (NH_3; 0.15), formaldehyde (H_2CO; 0.06), and carbonylsulfide (COS, 0.018) present only minor components. The abundance of methanol (CH_3OH) depends strongly on the history of the ice (unprocessed versus photolyzed/bombarded ices) and can vary significantly (0.03−0.3) from its averaged value of 0.18.[94−98] The assignment of formic acid (HCOOH; 0.07), the $HCOO^-$ anion (0.008), and acetaldehyde (CH_3CHO; 0.1) must be regarded as tentative.[99,100] Further, the 4.62 μm band which was suggested to correlate with charged particle processed ices has been attributed to OCN^- (0.04); however, this assignment remains to be investigated in depth. Note that molecules in ices around YSOs are not distributed homogeneously but highly fractionated. In cold outer envelopes of YSO, where typical temperatures of 10−20 K reside, ices contain a significant fraction of nonpolar carbon monoxide (CO) and carbon dioxide (CO_2) (apolar ices). As we move closer to the inner warm envelope, the temperature rises to 20−90 K and molecules such as methane (CH_4) and carbon monoxide (CO) are too volatile to exist in ices; therefore, polar ices of methanol and water are very abundant. Most likely, this fractionation could be the result of a successive sublimation of apolar ice constituents with rising temperature.

5. Circumstellar Envelopes

Once the contraction of a protostar is finished, the star evolves only slowly burning hydrogen into helium.[101,102] Our Sun presents a typical example of these main sequence stars. The continuing nuclear fusion leads to structural changes of the star as the radius and the luminosity increase steadily. Once hydrogen is exhausted in the central core, the evolution accelerates rapidly. Hydrogen is now fused in a shell surrounding the inert helium core. In turn, the core increases its density and temperature via contraction until helium ignites. In the center, helium fusion via metastable ^{8}Be to ^{12}C and ^{16}O is the central energy source. The cycle of core and shell burning with increasing densities and temperatures in the core continue until the most stable ^{56}Fe nuclei are formed. Elements heavier than iron cannot be formed by nuclear fusion as these processes are endoergic. The final fate of the star depends on its mass and leads to a white dwarf, neutron star, or black hole.

During the helium fusion, the star expands its shell. Under certain circumstances, a red giant is formed, where the carbon−oxygen core is surrounded by a helium-burning shell, a helium buffer layer, and a hydrogen-burning shell. These stars are becoming increasingly unstable and leave the main sequence to become an asymptotic giant branch (AGB) star.[103,104] Recall that each low and intermediate mass star having 1−5 solar masses goes in its evolution through the AGB stage. At this stage of its life, the star returns matter in steady winds back into interstellar space. Since these ejecta contain elements heavier than hydrogen, the chemical composition of the interstellar medium is enriched in these heavy atoms. New stars are formed from this material, and their return will enrich the interstellar medium even further. These late-type AGB stars lose significant amounts of their mass once they left the main sequence and are surrounded by expanding matter, which is often called the circumstellar shell or the circumstellar envelope (CSE).[105−107] AGB stars are know to be surrounded by expanding shells. Circumstellar envelopes consist of gas-phase molecules and submicrometer-sized grain particles. Therefore, these stars must be regarded as a source of interstellar grain material: once dust is formed, it is subjected to radiation pressure from the central star and accelerated outward from the circumstellar envelope into the interstellar medium. Depending on the oxygen-to-carbon ratio of the out-flowing matter, AGB stars can be divided into three classes: M-, C-, and S-type stars. S-type stars are defined by a carbon-to-oxygen ratios C/O = 1. M-type stars depict C/O < 1, and all the carbon is locked in carbon monoxide (CO). The IR spectra of these stars show features of amorphous silicate grains—most probably olivine-like matter $(Fe,Mg)_2SiO_4$. As expected from an oxygen-rich environment, M-type stars favor the production of silicates and the gas-phase chemistry is dictated by simple oxygen-carrying molecules. In C-type stars, the situation is reversed and defined by C/O > 1. Therefore, these stars are called carbon stars. All oxygen resides in carbon monoxide (CO); C-type stars display a prominent feature of silicon carbide (SiC).

The carbon star IRC+10216 is the brightest carbon-rich object in the infrared sky.[108] It has an extended envelope in which more than 60 species have been observed. This object is particularly carbon rich, as many carbon clusters C_n (n = 2, 3, 5), hydrogen-deficient carbon chains C_nH (n = 2−8), cyanopolyynes ($HC_{2n}CN$ (n = 1−4)), their radicals $C_{2n}CN$ (n = 1−2),

cummulenes C_nH_2 (n = 3, 4, 6), and hydrocarbons (CH_4, C_2H_2, C_2H_4) have been detected in its circumstellar envelope. Note that the molecules around stars are nearly arranged in onion-like shell structures around the central star. The identification of methane, acetylene, ethylene, together with silane (SiH_4) makes this star especially valuable. These molecules have no permanent dipole moment and are not detectable with radio spectroscopy; therefore, powerful IR background sources together with cutting-edge IR telescopes such as ISO are crucial. IRC+10216 depicts further an unprecedented variety of metal-bearing species such as NaCl, AlCl, AlF, KCl, NaCN, MgNC, and MgNC, whose vibrational temperatures have been determined to be 700−1500 K.[109] With the exception of SiC_2, SiC_3, and SiC_4, all molecules in CSE have been observed in interstellar clouds. No ion has been identified so far in any CSE.

However, this simplified categorization of a carbon- and oxygen-dominated chemistry in S- and C-stars, respectively, is incomplete. Herpin and Cernicharo presented compelling evidence that two oxygen-bearing species, water (H_2O) and the hydroxyl radical (OH), are abundant in the innermost region of the circumstellar envelope of the carbon-rich, preplanetary nebula CRL 681.[110] As the inner regions are very close to the photosphere of the central star, the ubiquitous carbon monoxide molecule (CO) can be photodissociated to carbon and oxygen atoms.[110,111] The latter were suggested to react with molecular hydrogen (H_2) to form H_2O and OH radicals. Likewise, the methanol molecule (CH_3OH) as detected in the CSE of IRC+10216 could be the product of the reaction of oxygen atoms with methane.

Finally, the dust formation needs to be addressed briefly. Dust forms in high mass losing AGB stars.[112−114] Typically, the temperature and densities at the outer edge of the star's photosphere reach up to 4500 K and 6×10^{15} atoms cm^{-3}. Since the star can be approximated as a point source, the number density drops roughly with the inverse square of the radius from the center. If a region above the photosphere is cooled to about 1700−2000 K, gas-phase molecules are allowed to seed to dust grains. In the inner regions of the CSE, the dust cools to 1000−1200 K. Carbon-rich grains are of particular importance, and two mechanisms have been postulated on how they can be formed. They involve either a successive build-up of neat carbon clusters via sequential addition steps or are speculated to comprise the acetylene molecule to form benzene—the very first aromatic molecule—via multiple reactions (sections II.A and II.D).[115]

6. Planetary Nebulae

Planetary nebulae (PNe) are the descendants from AGB stars.[116,117] This phase is characterized by a very efficient mass loss of the dying star. The reshaping of the circumstellar envelope which is initially formed by material expelled during the AGB phase over 10^6 years is dictated by high-velocity winds from the central star. An increasing photon flux in the UV range accompanies this process as the remaining hydrogen shell burns up by nuclear fusion. While the ejecta move away from the central star, the enhanced photon emission will gradually photodissociate and -ionize the circumstellar shell which at the same time is growing as more material is swept up.[118,119] These fast stellar winds and photon field sweep the circumstellar envelope into the ring-shaped, planetary-like structure we see in planetary nebulae. At some stage of their evolution, dust erosion might play an important role. Despite their unique name, these objects are not correlated to planets. When the stellar hydrogen envelope is burned up completely, the core will cool, decreases in luminosity, and becomes a white dwarf. During this phase, the circumstellar matter expands more, finally replenishing into the intercloud regions. Due to the low density of the latter (<1 atom cm^{-3}), most of the atoms are ionized, if their ionization potential is less than 13.59 eV, and translationally suprathermal (10^3−10^4 K). This completes the cyclization of matter in the interstellar medium (Figure 1).

Planetary nebulae disclose a unique chemistry. The molecular inventory is imposed by photodissociation and -ionization processes leading to detectable amounts of CH^+, CO, CO^+, HCO^+, CH, OH, H_2, and possibly H_2O as observed around NGC 7027. The temperature decreases from 3000 K in regions close to the star down to 200 K in the outer edges of the shell. A temperature of 200 K is interpreted as an averaged temperature of the shocked gas behind the shock front of the out-flowing gas.[120] The planetary nebula CRL 618 presents a particular wealth of complex hydrocarbons, as diacetylene (C_4H_2), triacetylene (C_6H_2), and benzene (C_6H_6) have been identified for the very first time outside our solar system.[121,122] Note that the carbon star IRC+10216 has nondetectable amounts of these molecules. This might be attributed to the fact that CRL 618 has higher fractional abundances of ethinyl radicals (C_2H) due to photodissociation of acetylene, which are thought to be key ingredients for the formation of polyacetylenes and benzene (sections II.C and II.D).

C. Formation of Molecules

The preceding sections provided an overview of the chemical composition and physical properties of various interstellar environments (Tables 1 and 2; Figure 1). This furnishes the basic input data and sets the stage for unraveling the chemical processing of the interstellar medium. The broad heterogeneity of temperatures ranging from 10 K to a few thousand Kelvin together with an extraordinary diversity of number densities extending over 8 orders of magnitude (10^1−10^9 atoms cm^{-3}) demonstrates clearly that interstellar chemistry is expected to be remarkably diverse. To ascertain whether a chemical reaction is feasible in distinct interstellar environments, two basis set of information are crucial. These are (i) the rate constant to categorize how 'fast' a chemical reaction is (kinetics)[123−131] and (ii) the chemical reaction dynamics investigating, for example, entrance and exit barriers, intermediates involved, reaction products, and the energy partition into translational and internal degrees of freedom.[132−138]

For simplicity, let us consider a bimolecular reaction of one species A with a second atom, molecule,

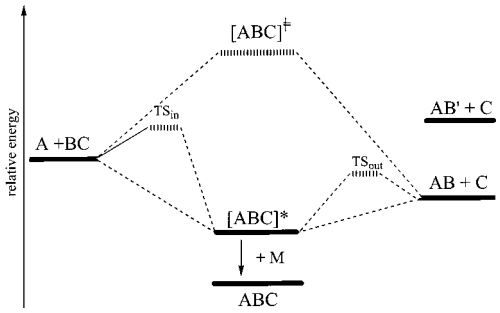

Figure 2. Schematic potential energy surface of a bimolecular reaction A + BC forming AB + C and AB′ + C products via indirect and direct reaction mechanisms. AB′ denotes a structural isomer of AB, [ABC]‡ a transition state, [ABC]* an internally excited intermediate, and ABC an intermediate stabilized by a three-body reaction with a collider M. Reactants, products, and the intermediate of an indirect reaction are connected via transition states TS_{in} (entrance channel) and TS_{out} (exit channel to AB + C); transition states to form AB′ + C are omitted for clarity.

or radical BC which leads to the generic products AB and C or AB′ plus C (Figure 2). On the basis of the energetics, two cases can be distinguished. If the free energy of the products is lower than the free energy of the separated reactants, the reaction is exoergic (AB + C); if the situation is reversed, the reaction is endoergic (AB′ + C). Besides the energetics, two limiting cases of the reaction dynamics have to be addressed. If A and BC react via a transition state [ABC]‡ to the products, this reaction is called 'direct'. On the other hand, the reaction can go through an intermediate [ABC]*; these dynamics are called 'indirect'. The intermediate can be formed either barrierless or via an entrance barrier (TS_{in}). Compared to the separated reactants, [ABC]* is lower in energy. Due to energy and momentum conservation, the free reaction energy must channel into the internal (rotation, vibration, electronic) degrees of freedom. Hence, this intermediate is internally excited and can undergo various reactions. First, a unimolecular decay might form AB + C or AB′ + C. These fragmentations may proceed via an exit transition state (TS_{exit}) or without exit barrier. Second, if the number density of the gas-phase molecules and hence the collision frequency is large, the intermediate can collide with another bath molecule M. This three-body collision diverts the excess energy of the energized intermediate into the translational/internal degrees of freedom of the third-body collider forming a stable ABC species. This process is of particular importance in dense planetary atmospheres or in the solid state. In solids, the internally excited intermediate can couple with the phonons of the solid target. Lastly, [ABC]* can react back to the reactants or might be stabilized via photon emission; the latter process converts (parts of) the internal energy into electromagnetic radiation. Note that [ABC]* might isomerize prior to fragmentation or stabilization. Multiple electronic surfaces and/or intersystem crossing may complicate the scenario. This simplified treatment of a chemical reaction helps to extract generalized concepts on the astrochemical processing of distinct interstellar environments.

1. Solid State

Although the dust component embodies only 1% of the interstellar matter, these predominantly silicate- and carbonaceous-based grain nuclei play a key role in the formation of new molecules. Deep in the interior of dense clouds, grain particles effectively shield newly synthesized molecules in the gas phase from the destructive external UV radiation field. Most important, these submicrometer-sized particles present valuable nurseries to synthesize new molecules. In dense clouds, these grains have typical temperatures of 10 K.[139,140] Once molecules, radicals, or atoms from the gas phase collide with the solid particle, they are accreted on the grain surface, resulting in an icy mantle up to 0.1 μm thick. At ultralow temperatures, all species except H, H_2, and He hold sticking coefficients of unity. This means that each collision of a gas-phase species with a cold surface leads to an absorption and hence thickening of the ice layer. Here, solid mixtures containing H_2O (100), CO (7−27), CH_3OH (<3.4), NH_3 (<6), CH_4 (<2), and CO_2 (15) were identified unambiguously via IR spectroscopy toward the dense cloud TMC-1 employing the field star Elias 16 as a blackbody source;[141] the numbers in parentheses indicate the relative abundances compared to water ice. Rather complex ice mixtures have been identified in the vicinity of young stellar objects (section I.B.4).

However, what reactions are feasible at ultralow temperatures of 10 K? On the basis of the schematic potential energy surface, reactions should have a negligible entrance barrier and are expected to be exoergic. A 'direct' reaction via a transition state [ABC]‡ involves often a significant barrier which cannot be overcome at low temperatures of 10 K. Therefore, barrierless and exoergic reactions which proceed via an intermediate should dominate (Figure 3). Note that light atoms such as hydrogen and

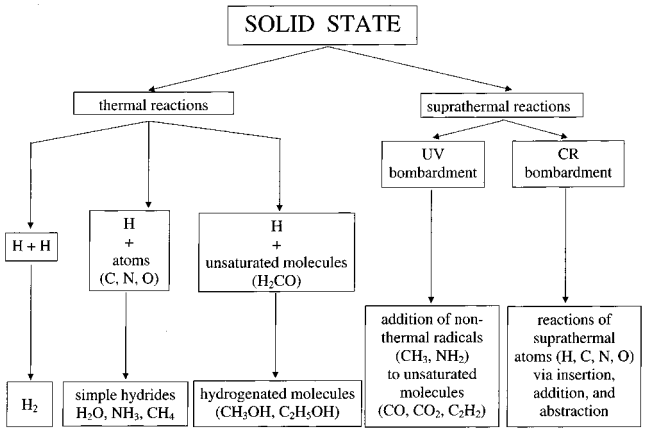

Figure 3. Overview of thermal and suprathermal chemical reactions in the solid state; examples of reactants and synthesized molecules are given in parentheses.

deuterium are suggested to tunnel through entrance barriers up to 20 kJ mol^{-1} and might pass them. These considerations dictate that thermal processes must involve hydrogen or deuterium atoms.

The formation of molecular hydrogen via a recombination of mobile hydrogen atoms is supposed to be the prototype of a barrierless reaction not only on

low-temperature icy grains, but also on carbonaceous and silicate grain particles.[142−153] Recall that reactions between two atoms or radicals do not involve any entrance barrier. Gas−grain models suggest that the recombination of two hydrogen atoms is the central source of molecular hydrogen,[154−157] which has been detected via pure rotational lines[158,159] in emission around T Tauri stars,[160] in the Orion bar,[161] in supernova remnants,[162] toward star-forming regions,[163] around circumstellar accretion disks of young stars,[164] and toward young stellar objects.[165] Vibrationally excited hydrogen has been identified further in emission toward the diffusive cloud ζ Ophiuchi.[166] The surface recombination of two adsorbed hydrogen atoms via the Langmuir−Hinshelwood mechanism might account for the molecular hydrogen abundances as found in dense clouds. Since the H−H bond is 4.5 eV strong, the H_2 molecule which is formed on the grain surface is vibrationally excited and hence can be desorbed from the grain into the gas phase.[167,168] Alternatively, an Eley−Rideal mechanism, which involves the collision between one gas-phase hydrogen atom and another on a surface[169] or a negative ion route via H^- [170,171] present alternative routes to molecular hydrogen. The reader should keep in mind that the grain acts as a 'catalyst' for the recombination of two hydrogen atoms; in the gas phase this reaction is not feasible, as the newly formed hydrogen molecule is highly rovibrationally excited and cannot get rid of its internal energy via a three-body reaction due to the low-density medium (Table 2). Therefore, any internally excited H_2 molecule which is formed in the gas phase will dissociate back to the reactants. However, interaction of the internally excited hydrogen molecule on the grain with the phonons can transfer a significant amount of internal energy to the solid matter, thus stabilizing the newly formed H_2 species on the grain or releasing it into the gas phase.

The mechanism to form molecular hydrogen is suggested to be closely related to the synthesis of simple hydrides on icy grains. Since atomic hydrogen is even mobile at temperatures as low as 10 K, hydrogen atoms can react with accreted heavier atoms such as C, N, and O via multiple reaction sequences. Reactions 1 and 2 present a typical example to form the water molecule on interstellar grains

$$O(^3P_j) + H(^2S_{1/2}) \rightarrow OH(X^2\Pi_\Omega) \quad (1)$$

$$OH(X^2\Pi_\Omega) + H(^2S_{1/2}) \rightarrow H_2O(X^1A_1) \quad (2)$$

These processes can explain the formation of CH_4, NH_3, and H_2O together with their deuterated counterparts.[172−174] It should be stressed that currently no scientific proof exists which supports that species heavier than deuterium are mobile on grain surfaces at 10 K. Hence, reaction networks[175−177] involving surface reactions of thermalized C, N, and O atoms as well as polyatomic radicals such as HCO, CH, CH_2, CH_3, OH, NH, and NH_2 with species except H and D atoms must be regarded as purely speculative.[178]

The addition of hydrogen atoms to unsaturated molecules represents a third important class of thermal reactions involving mobile hydrogen atoms. Although the initial addition step to closed-shell species such as C_2H_2, C_2H_4, CO, and HCN involves entrance barriers of up to 20 kJ mol^{-1}, the latter can be overcome due to the unique ability of hydrogen atoms to tunnel through barriers.[179] These successive hydrogenation processes can lead ultimately to fully saturated molecules on grain surfaces and could synthesize, for example, CH_3OH and CH_3NH_2 via H_2-CO and CH_2NH, respectively. The suggested formation route to methanol via hydrogenation of carbon monoxide and formaldehyde is outlined in reactions 3−6[179]

$$CO(X^1\Sigma^+) + H(^2S_{1/2}) \rightarrow HCO(X^2A') \quad (3)$$

$$HCO(X^2A') + H(^2S_{1/2}) \rightarrow H_2CO(X^1A_1) \quad (4)$$

$$H_2CO(X^1A_1) + H(^2S_{1/2}) \rightarrow H_2COH(X^2A'') \quad (5)$$

$$H_2COH(X^2A'') + H(^2S_{1/2}) \rightarrow CH_3OH(X^1A') \quad (6)$$

It should be emphasized that only H and D atoms can tunnel through entrance barriers. Reactions of, for example, CH_3 and NH_2 radicals adding to double and triple bonds involve significant entrance barriers of up to 30 kJ mol^{-1}. Even if current models should underestimate the mobility of these radicals, the latter cannot overcome the entrance barrier via tunneling. Therefore, reactions of thermalized CH_3 and NH_2 species with closed-shell molecules are clearly irrelevant at temperatures as low as 10 K and can be disregarded.

However, interstellar space is interspersed with ultraviolet photons ($\leq$13.59 eV) and energetic particles from T-Tauri winds, stellar jets, carbon stars, and galactic cosmic ray particles. Therefore, pristine ice mantles are processed chemically by the cosmic ray-induced internal ultraviolet radiation present even in the deep interior of dense clouds ($\phi = 10^3$ photons cm^{-2} s^{-1}) and, in particular, through particles of the galactic cosmic radiation field. This can lead to the formation of new molecules in the solid state via nonequilibrium (nonthermal) chemistry even at temperatures as low as 10 K. The particle component of the cosmic ray radiation field consists of 97−98% protons (p, H^+) and 2−3% helium nuclei (α-particles, He^{2+}) in the low-energy range of 1−10 MeV (1 MeV = 10^6 eV) with $\phi = 10$ particles cm^{-2} s^{-1} and higher energies up to the PeV limit (1 PeV = 10^{15} eV) ($\phi = 10^{-12}$ particles cm^{-2} s^{-1}). The chemical evolution of interstellar ices by bombardments with ultraviolet (UV) photons[180−184] and cosmic ray (CR) particles is well established.[185−200] A photon can be absorbed by a single molecule in the ice; this process is followed predominantly by a selective bond rupture of a single bond. If a hydrogen atom is released in this photodissociation, it can hold kinetic energies up to a few electronvolts. The radical formed is internally excited and might react with a neighboring molecule. Since the internal energy of the radical can be coupled into the reaction coordinate, entrance barriers could be passed. For example, vibrationally excited CH_3 and NH_2 radicals could now add to

double and triple bonds; this is in strong contrast to their thermal reactions in which the entrance barriers cannot be overcome.

Compared to UV photons which are absorbed within about 0.05 μm of the ice, CR particles such as a 10 MeV H^+ penetrate the grain easily and deposit up to 1 MeV inside the icy mantle. Since chemical bonds are up to 10 eV strong, this energy exceeds the stability of the molecule. For instance, a CR particle can interact with a methanol molecule and knocks off an H atom which carries kinetic energy up to 10 keV. The CH_2OH or CH_3O counterfragment remains excited internally. This H atom interacts in subsequent collisions with the solid target and releases its excess energy to the target atoms in successive collisions via elastic and inelastic interactions to generate further high-energy carbon, hydrogen, and oxygen atoms. Here, the elastic process transfers energy to the nuclei of the target atoms igniting *p*rimary *k*nock-*o*n particles (PKOs; first generation of knock-on particles) if this amount is larger than the binding energy of the atom. MeV α-particles, for example, generate carbon PKOs with kinetic energies up to 10 keV. These knock-on particles can transfer their energy in consecutive encounters to the target atoms resulting in a collision cascade of secondary, tertiary, and higher knock-on atoms. Moderated to about 1−10 eV—the so-called chemical energy range—these atoms are not in thermal equilibrium with the 10 K target (hence, nonequilibrium or suprathermal particles) and can react finally with the target molecules via elementary steps of bond insertion, addition to double or triple bonds, or hydrogen abstraction. The power of suprathermal reactions to form new molecules at temperatures even as low as 10 K is based on their ability to overcome reaction barriers in the entrance channel easily, since suprathermal species can impart their excess kinetic energy into the transition state of the reaction. Even reactions endoergic at 10 K are feasible and extend the synthetic power of this reaction class beyond thermal processes on interstellar grains. These unique aspects of suprathermal reactions result in reaction rate constants k orders of magnitude larger than their thermal counterparts. Detailed calculations on the reactions of 1 eV suprathermal hydrogen atoms with H_2O and CH_4 to form H_2 and OH as well as CH_3, respectively, depict k(1 eV H, H_2O) = 1.7×10^{-11} cm^3 s^{-1} and k(1 eV H, CH_4) = 5.0×10^{-11} cm^3 s^{-1} versus thermal rate constants of k(293 K, H + H_2O) = 9.6×10^{-27} cm^3 s^{-1} and k(293 K, H + CH_4) = 2.5×10^{-19} cm^3 s^{-1}, a difference of up to 16 orders of magnitude.[201] Irradiating, for example, solid CH_4, C_2H_2, and C_2H_4 samples with MeV protons or helium nuclei leads to a broad product spectrum of synthesized species such as atomic and molecular hydrogen, H and H_2,[202] CH_n (n = 1−4), C_2H_n (n = 1−6), C_3H_n (n = 4−8),[203] larger alkanes and alkenes with up to 18 carbon atoms, as well as polycyclic aromatic hydrocarbons (PAHs) up to coronene.[204] Once molecules are formed on interstellar grains, grain heating can redistribute these molecules into the gas phase.[205−209]

Lastly, basic differences between photon and charged particle processing of interstellar ices should be addressed. Compared to a photon, a CR-triggered bond rupture does not follow optical selection rules. Furthermore, a CR particle generates suprathermal carbon and oxygen particles from, for instance, methanol via an elastic interaction potential. These species cannot be formed via photolyses. Hence, photon and CR processing of ices are expected to synthesize different molecules. A comparison of MeV particle processing with photolyzed CH_4 ices at 10 K offers further insights in the crucial role of suprathermal atoms such as carbon in ices. UV irradiation experiments indicate that 38% of the CH_4 was converted to methyl radicals (0.01%), C2 species ethylene (2.6%) and ethane (8%), the C3 species propane, and higher hydrocarbons holding structural units R−CH_3, R−CH_2−R, R_2C=CH_2, R_2C=CRH, as well as HCCR; 'R' indicates an organic group. Most importantly, neither acetylene, C_2H_2, nor vinyl radicals, C_2H_3, could be sampled. Since, however, C_2H_2 molecules were formed in MeV irradiation via an initial insertion of a suprathermal carbon atom into a carbon−hydrogen bond of a methane molecule, we must conclude that UV exposure of CH_4 cannot generate suprathermal C atoms. Here, UV photons interact in single quantum processes with a CH_4 molecule and are unable to ignite collision cascades to form suprathermal carbon atoms. In strong coincidence, Gerakines and co-worker postulated the formation of ethylene and ethane via reactions of UV photon-induced CH_2 and CH_3 radicals. Since CH_2 as well as CH_3 are not mobile at 10 K, these processes must be restricted to neighboring radicals in the UV-processed CH_4 target. Although calculations show that the CR particle flux in dense molecular clouds is 2 orders of magnitude lower than the internal ultraviolet flux, each particle can generate about 100 suprathermal species in a 0.1 μm thick icy layer. Hence, the flux advantage of the UV field is clearly eliminated by the ability of one CR to induce up to 100 energetic particles.

2. Gas Phase

The chemistry in the gaseous interstellar medium depends strongly on the effective physical parameters. Since the kinetic energy of interstellar species is confined from typically 0.8 (diffuse clouds) to 0.08 kJ mol^{-1} (dense clouds) on average, gas-phase reactions under thermodynamical equilibrium conditions in interstellar clouds should be exoergic or only slightly endoergic, exhibit little or no entrance barriers, and involve exit barriers which are lower in energy than the separated reactants. Further, due to the low density of the interstellar cloud media, only two-body collisions (binary reactions) are relevant. A three-body reaction occurs only once in a few 10^9 years and is negligible considering typical lifetimes of dense clouds of 10^5−10^6 years. Circumstellar envelopes of carbon stars and planetary nebulae depict a more diverse chemistry. Here, the temperatures can rise to a few thousand Kelvin close to the photosphere of the central star. Therefore, reactions which are either endoergic or involve an entrance barrier become increasingly significant. The en-

hanced number density of up to 10^{15} atoms cm^{-3} in the outer edge of the carbon star's photosphere dictates further that three-body encounters are important.

The classical Arrhenius equation postulates that the rate constant k of a chemical reaction depends on the temperature T according to eq 7

$$k(T) = A \times e^{-(Eact/RT)} \quad (7)$$

Here, A denotes the preexponential factor, R the gas constant, and E_{act} the classical activation energy. If this relation holds even down to typical interstellar temperatures as low as 10 K and the activation energy is positive, rate constants of gas-phase reactions would be vanishingly small in interstellar clouds and no chemical processing should occur. However, the large number of molecules detected so far suggests that this consideration is not entirely accurate.

2.1. Ion−Molecule Reactions. In the early 1970s, a significant step forward was made to account for the formation of simple interstellar molecules and ions. It was postulated that bimolecular, exoergic ion−molecule reactions have no entrance barrier and proceed within orbiting limits. This hypothesis fulfills all basic requirements for a reaction to occur in interstellar clouds. Early chemical equilibrium models of interstellar clouds incorporated this assumption and focused on ion−molecule reactions, radiative associations, and dissociative recombination between cations and electrons of the cosmic radiation field to advance interstellar chemistry.[210−230] These models proposed a cosmic ray (CR) driven ionization of molecular hydrogen followed by an H_3^+ ion-dominated chemistry to form small molecules via proton transfer to an acceptor molecule X[231−234]

$$H_2 + CR \rightarrow H_2^+ + e^- \quad (8)$$

$$H_2^+ + H_2 \rightarrow H_3^+ + H \quad (9)$$

$$H_3^+ + X \rightarrow H_2 + HX^+. \quad (10)$$

Since the proton affinity of H_2 is low, H_3^+ donates H^+ with a large variety of astrochemically important molecules such as CO, H_2O, NH_3, and CH_4 as well as nitrogen and oxygen atoms. These models explain surprisingly well the formation of small molecules such as water, ammonia, and methane, in particular in diffuse clouds with their high number densities of ions. At this stage, neutral−neutral reactions have been considered to be unimportant because they were thought to involve significant entrance barriers. Note that the key molecule in ion−molecule reaction schemes—H_3^+—was detected only very recently in the interstellar medium.[235−239]

However, the following years revealed that not all ion−molecule reactions are barrierless. For instance, the reaction of c-$C_3H_3^+$ with atomic nitrogen, which was thought to be the key route to interstellar nitrogen chemistry, is strictly forbidden in the cold interstellar medium.[240] As complex hydrogen-deficient molecules were detected in dense clouds and in the outflow of carbon stars, it became clear that ion−molecule reactions alone cannot reproduce the observed gas-phase abundances of complex, carbon-bearing molecules. The formation of interstellar isomers, in particular those of C_3H, C_3H_2, and HC_3N, presented a severe problem.,[241−243] Ion−molecule reaction schemes incorporating a dissociative recombination of HC_3NH^+ with an electron followed by an isomerization of the neutral HC_3NH molecule prior to dissociation predicted that HCCCN, HNCCC, and HCCNC should be present in relative amounts of 240:1:8 toward the dense cloud TMC-1.[244] However, actual observations depicted a ratio of 1000:1:8—a lower production of the thermodynamically most stable cyanoacetylene isomer. Therefore, important production routes to cyanoacetylene—possibly via hitherto neglected reactions of two neutral species—are obviously missing.

2.2. Neutral−Neutral Reactions. The inclusion of alternative, bimolecular exoergic neutral−neutral reactions into chemical models of, for instance, the dark cloud TMC-1 occurred only gradually,[245] predominantly because laboratory data were absent and entrance barriers were assumed to hinder even exoergic reactions. Kinetic experiments verified that this scenario holds particularly for reactions of ground-state nitrogen ($N(^4S_{3/2})$)[246−252] and oxygen ($O(^3P_j)$) atoms with closed-shell hydrocarbon molecules.[253−267] Likewise, reactions of CH_3, CH_2, NH_2, and NH in their electronic ground states with hydrocarbons were found to have significant entrance barriers as high at 35 kJ mol^{-1}.[268,269] Note, however, that oxygen and nitrogen reactions with hydrocarbon radicals[270−272] and reactions of two hydrocarbon radicals were found to be barrierless.[273−275]

As dense clouds and evolved carbons stars contain a great variety of highly unsaturated carbon-bearing molecules and nitriles, particular attention has been devoted on how these complex species can be formed in the interstellar medium via neutral−neutral reactions. Very often, kinetic models of distinct interstellar environments are designed and the output of these reaction networks is then compared with actual astronomical observations. However, each network relies heavily on laboratory data. These are (i) temperature-dependent rate constants over a broad temperature range from 10 K in dense clouds to high temperatures in circumstellar envelopes, (ii) reaction products, (iii) branching ratios, and (iv) intermediates involved. Kinetic measurements at room temperature and ultralow temperatures (section III) improved the understanding on the role of neutral−neutral reactions in extraterrestrial environments. These kinetic studies demonstrated explicitly that reactions of ground-state carbon atoms, cyano radicals, and ethinyl radicals with unsaturated hydrocarbons are indeed rapid and barrierless and proceed with almost unit collision efficiency within gas kinetics limits. Although these kinetic experiments provided unprecedented information on temperature-dependent rate constants, their crucial drawback is the lacking information on intermediates involved, reaction products, and branching ratios. Therefore, information on the chemical reaction dynamics under single-collision

conditions as provided in crossed molecular beam experiments are crucial to provide these information (section IV). These experiments give an intimate insight into the underlying reaction mechanisms at the molecular level—a crucial piece of information to untangle the chemical processing of distinct interstellar environments. Here, the neutral−neutral reactions of $C(^3P_j)$, $C_2(X^1\Sigma_g^+)$, $C_3(X^1\Sigma_g^+)$ the isoelectronic radicals $CN(X^2\Sigma^+)$ and $C_2H(X^2\Sigma^+)$, and phenyl radicals $C_6H_5(X^2A')$ with unsaturated hydrocarbons and hydrogen sulfide are of particular importance in astrochemistry.

II. Key Reactants in the Interstellar Medium

A. Atomic Carbon, $C(^3P_j)$, Dicarbon, $C_2(X^1\Sigma_g^+)$, and Tricarbon, $C_3(X^1\Sigma_g^+)$

Atomic carbon is the fourth most abundant element in universe and ubiquitous in the interstellar medium. The 609 μm $^3P_1 - {}^3P_0$ transition presents a valuable probe to detect $C(^3P_j)$ in significant amounts in circumstellar envelopes of evolved carbon stars IRC+10216 and α Orionis.[276−279] A further identification was made toward the protoplanetary nebulae CRL 618 and CRL 2688,[280] the diffuse cloud ζOph,[281] and the dense cloud OMC-1.[282] The dicarbon and tricarbon molecules $C_2(X^1\Sigma_g^+)$ and $C_3(X^1\Sigma_g^+)$ have been detected in diffuse clouds ζOph and ξ Per,[283−285] in translucent clouds such as HD147889,[286,287] and in the circumstellar shell of carbons stars such as IRC+10216.[288−292] Additionally, tricarbon was found to be abundant toward the hot core source SgrB2.[293] Note that C_2 and C_3 molecules have been assigned in comets as well.[294−298]

Investigating the dynamics of these reactions is strongly expected to provide a unique knowledge on the formation of hydrogen-deficient carbon molecules in the interstellar medium such as hydrogen-terminated carbon clusters C_nH, cummulenes C_nH_2, and hydrogen-deficient, sulfur-carrying molecules (Table 1).[299−311] These investigations are of further importance to resolve synthetic routes to interstellar cyclic molecules C_3H and C_3H_2 together with their linear isomers CCCH and $CCCH_2$. Linear and cyclic C_3H radicals are ubiquitous in the interstellar medium and hold high fractional abundances, up to 10^{-9} relative to atomic hydrogen. l-C_3H was detected in 1985 by Thaddeus et al. via microwave spectroscopy toward the dark Taurus molecular cloud 1 (TMC-1) and the carbon star IRC+10216.[312] Two years later, Yamamoto et al. identified rotational transitions of the cyclic isomer in TMC-1 prior to laboratory synthesis via radiofrequency discharge of $He/CO/C_2H_2$ mixtures.[313] The aromatic c-C_3H_2 molecule is very stable toward decomposition; hence, it is observable not only toward shielded regions as dense clouds such as TMC-1 [c-C_3H/c-C_3H_2 = 0.1; c-C_3H_2/l-C_3H_2 = 5−13],[314−319] but also in diffuse clouds,[320] around the circumstellar envelope of IRC+10216, and in the hot molecular cores SgrB2 [c-C_3H_2/l-C_3H_2 = 150:1].[321,322] The cummulene isomer H_2CCC is less abundant than the cyclic structure, and isomer ratios of c-C_3H_2/l-C_3H_2 = 100:1 have been determined in TMC-1.[323] These hydrogen-deficient radical species are thought to be key intermediates in the synthesis of polycyclic aromatic hydrocarbons (PAHs) and their derivatives, carbonaceous grain particles in circumstellar envelopes of carbon and planetary nebulae, and possibly fullerenes.[324−326] Note that so far no fullerene molecules have been detected in the gas phase of the interstellar medium unambiguously. However, on the basis of the $^3He/^4He$ isotopic composition of endohedral helium trapped inside a sample of C_{60} obtained from a meteorite, the authors provided compelling evidence of an extraterrestrial evidence of C_{60}.[327] Nevertheless, the synthetic routes to form fullerenes in the interstellar medium remain elusive.

B. Cyano Radicals, $CN(X^2\Sigma^+)$

Ever since the very first detection of cyanoacetylene (HCCCN) in interstellar environments, the synthesis of highly unsaturated cyanopolyynes up to $HC_{10}CN$ has been a challenge for astronomers and chemists. Since early models of interstellar cloud chemistry employing ion−molecule reactions cannot reproduce the abundances of these long-chain molecules, neutral−neutral reactions of cyano radicals with unsaturated hydrocarbons were suggested as a potential alternative. These elementary reactions might verify not only the synthetic routes to polycyanoacetylenes, but also astronomically observed nitriles vinylcyanide (C_2H_3CN) and cyanomethylacetylene (CH_3CCCN) in the circumstellar envelope surrounding the carbon star IRC+10216, hot molecular cores, and dark molecular clouds such as TMC-1. Therefore, detailed laboratory investigations unraveling the chemical reaction dynamics are crucial to test this hypothesis. The cyano radical is ubiquitous in the ISM and has been observed in the dense clouds TMC-1[328,329] and OMC-1[330] and around circumstellar envelopes of IRC+ 10216.[331,332] Note that these reactions have strong ties to our solar system as cyanoacetylene together with unsaturated hydrocarbons acetylene, ethylene, and methylacetylene have been observed in Saturn's moon Titan. Understanding the formation of nitriles has further importance to astrobiological problems since nitriles are suggested to represent precursors to amino acids which can be formed in multiple reaction pathways via hydrolysis and aminolyses.[333−337]

C. Ethinyl Radicals, $C_2H(X^2\Sigma^+)$

The ethinyl radical is isoelectronic to the cyano radical. After its first detection[338] it became clear that C_2H is ubiquitous in the interstellar medium and might be the key species involved in the formation of the polyynes $CH_3C{\equiv}C-C{\equiv}C-H$ and $H(C{\equiv}C)_n$ as detected in cold molecular clouds TMC-1 and OMC-1[339] as well as in circumstellar envelopes around carbon-rich asymptotic giant branch stars such as the red giant star IRC+10216.[340] Further, diacetylene (HCCCCH) has been observed in the atmosphere of Saturn's moon Titan[342] and in Saturn.[341] Whereas the main source of the interstellar and planetary ethinyl radicals have been unambiguously identified as a photolyses of acetylene (C_2H_2)[342] and to a minor amount of diacetylene, the mechanisms to synthesize

the observed polyacetylenes is far less clear. Neutral−neutral reactions of ethinyl radicals with unsaturated hydrocarbons have been postulated as a possible source, and experiments will be discussed in section IV.

D. Phenyl Radicals, $C_6H_5(X^2A')$

Elementary reactions of phenyl radicals are suggested to play a major role in the formation of polycyclic aromatic hydrocarbons (PAHs),[343−360] their cations,[361−385] hydrogenated[386] and dehydrogenated PAHs,[387−391] and possibly PAHs with aliphatic side chains[392−395] in circumstellar envelopes of carbon-rich stars and planetary nebulae. The very first postulation of their interstellar relevance as the missing link between small carbon clusters C_2-C_5 and carbon-rich grain material fueled enormous scientific research. Currently, PAH-like species are presumed to tie up about 18% of the cosmic carbon.[396,397] These species are further thought to be the carrier of diffuse, interstellar absorption bands (DIBs) covering the visible spectrum from 440 nm to the near-infrared[398] and may contribute to the infrared emission features in the spectrum of comet P/Halley.[399] PAH-like species also might be the emitter of unidentified infrared bands (UIRs) observed at 3030, 2915, 2832, 1612, 1300, 1150, and 885 cm^{-1}.[400] These bands dominate the spectra of a great variety of objects such as T Tauri Stars,[401] HII regions,[402] planetary nebulae,[403−405] circumstellar envelopes of carbon stars,[406−411] young stellar objects,[412,413] and even in the diffuse interstellar medium.[414] The survival of aromatic units in the harsh conditions of the interstellar radiation field suggests that distinct PAH-like structures could be stable toward ionizing radiation and possibly toward photodissociation.[415−417] These large molecules may survive the harsh photon flux because they have a sufficiently high density of states to undergo internal conversion; these rovibrationally excited species are considered for these UIRs as discussed above. However, this stability depends strongly on the molecular structure of the individual aromatic species and in particular on the charge state.[418−429] PAH-like molecules are further considered as precursors leading ultimately to carbon-rich interstellar grain material with various degrees of hydrogenation,[430−438] possibly fullerenes and their ions,[439−444] and perhaps interstellar diamonds as detected toward carbon-rich preplanetary nebulae.[445−447] Note that although no individual PAH molecules have been identified in the interstellar medium so far, aromatic moieties have been detected in meteorites.[448−450]

However, despite the crucial importance of PAH (like) molecules in various extraterrestrial environments, experimentally and theoretically well-defined mechanisms to synthesize these species in the gas phase have not been elucidated. All chemical reaction networks modeling PAH formation suggest a stepwise extension of monocyclic rings via benzene (C_6H_6), phenyl (C_6H_5), and/or cyclopentadienyl radicals (C_5H_5) to polycyclic systems.[451−459] However, even the most fundamental data on the formation of these very first cyclic building blocks—possibly via small C2−C4 radicals such as propargyl,[460−465] allyl,[466] or C_4H_3 and C_4H_5 intermediates[467−476] as investigated in crossed molecular beam experiments—and their subsequent reactions are lacking. Alternative formation routes might involve metal-catalyzed reactions in circumstellar envelopes[477] as supported by laboratory experiments[478] and maybe ion−molecule reactions in dense clouds.[479] Therefore, not only kinetic studies of phenyl radical reactions,[480−484] but in particular a systematic investigation of reaction paths leading to these small precursor molecules and the elementary reactions of cyclic building blocks such as phenyl on the most fundamental, microscopic level are of paramount importance. Before plunging into the reaction dynamics, the kinetics of these important neutral−neutral reactions are discussed briefly.

III. Kinetics

A. Room-Temperature Kinetic Studies

Kinetic studies on the reactivity of ground-state carbon atoms $C(^3P_j)$ with unsaturated hydrocarbons revolutionized the conventional thinking of astrochemists.[485−492] Husain et al. provided for the very first time sound experimental data on the potential importance of neutral−neutral reactions in the interstellar medium and determined absolute reaction rate constants at room temperature ($T = 300$ K).[493] The schematic setup is shown in Figure 4. In the

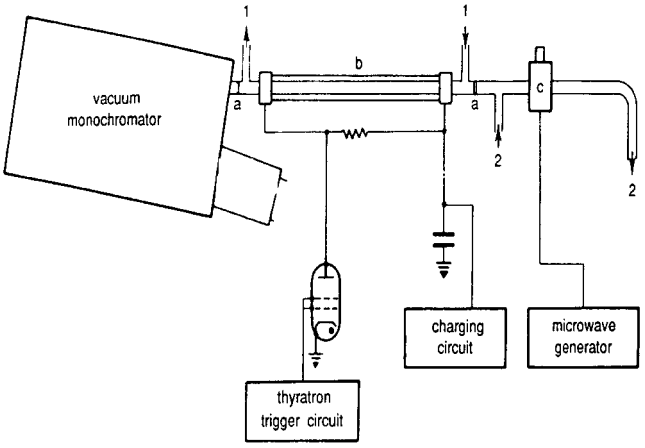

Figure 4. Experimental setup and simplified reactor design employed in kinetic investigations of reactions of ground-state carbon atoms with various unsaturated hydrocarbons at 300 K.

early measurements, two lithium fluoride (LiF) optical windows (a) sealed both ends of a square shaped Pyrex cell (b) through which a pulsed photolysis of precursor to atomic carbon was initially effected ($\lambda > 120$ nm). Subsequently, a coaxial cylindrical lamp and reactor assembly was employed with photolysis through high-purity quartz ($\lambda > 160$ nm). The gas mixture, which contained the carbon atom precursor (carbon suboxide; C_3O_2), helium buffer (He), and the reactant gas, was introduced through port 1 into the reactor. The actual experiments employed the principle of time-resolved atomic absorption spectroscopy with monitoring of atomic carbon $C(^3P_j)$ in the vacuum ultraviolet at 166 nm following a pulsed irradiation of carbon suboxide in the presence of

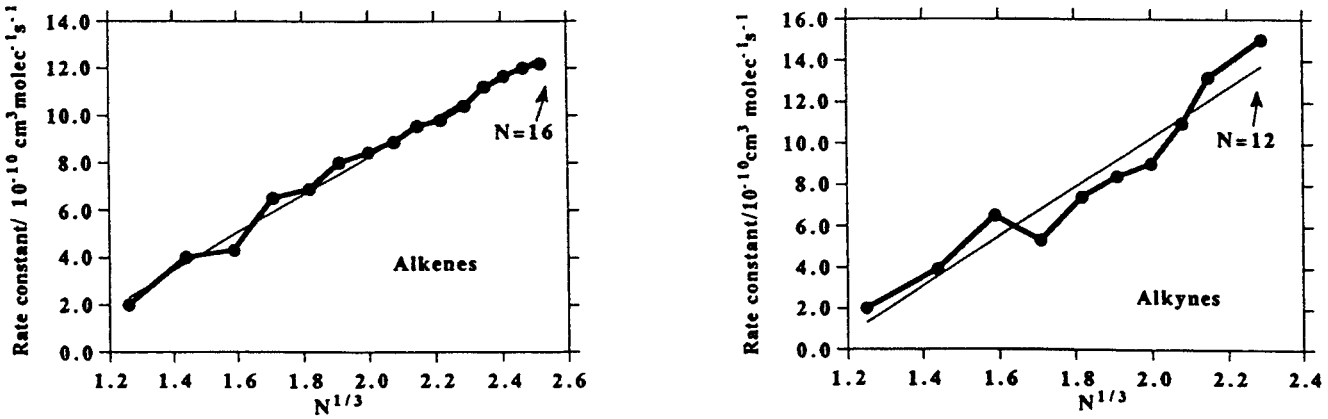

Figure 5. $N^{1/3}$ dependence (N = number of carbon atoms) of rate constants of atomic carbon reactions with alkenes and alkynes at 300 K.

Table 3. Rate Constants of Reactions of Carbon Atoms with Unsaturated Hydrocarbons at 300 K

reactant	rate constant, 10^{-10} cm^3 s^{-1}
alkenes	
ethylene	2.0 ± 0.1
propylene	4.0 ± 0.2
1-butene	4.3 ± 0.1
1-pentene	6.5 ± 0.3
1-hexene	6.9 ± 0.4
1-heptene	8.0 ± 0.4
1-octene	8.5 ± 0.5
1-nonene	8.9 ± 0.5
1-decene	9.6 ± 0.5
1-undecene	9.8 ± 0.5
1-dodecene	10.4 ± 0.6
1-tridecene	11.2 ± 0.6
1-tetradecene	11.7 ± 0.6
1-pentadecene	12.0 ± 0.6
1-hexadecene	12.2 ± 0.7
dienes	
allene	8.0 ± 0.1
1,3-butadiene	11 ± 1.0
1,4-pentadiene	11 ± 1.0
1,5-hexadiene	12 ± 1.0
1,6-heptadiene	12 ± 1.0
1,7-octadiene	12 ± 1.0
1,8-nonadiene	13 ± 1.0
1,9-decadiene	14 ± 1.0
alkyne	
acetylene	2.0 ± 0.1
methylacetylene	3.9 ± 0.2
dimethylacetylene	6.5 ± 0.4
2-butyne	7.0 ± 0.4
1-pentyne	5.3 ± 0.3
1-hexyne	7.4 ± 0.4
1-heptyne	8.4 ± 0.5
1-octyne	9.0 ± 0.5
4-octyne	10.3 ± 0.5
1-nonyne	11.0 ± 0.6
1-decyne	14.2 ± 0.7
1-dodecyne	15.0 ± 0.8
diynes	
1,7-octadiyne	11.0 ± 1.0
1,8-nonadiyne	11.0 ± 1.0
aromatic molecules	
benzene	4.8 ± 0.3
toluene	5.5 ± 0.3

excess helium buffer gas. Vacuum ultraviolet photons were generated from a microwave-powered discharge in a microwave cavity (c) and monitored in absorption via a photomultiplier tube (PMT); port 2 served as the gas inlet into the microwave cavity.[485]

The experiments indicated that all reactions proceeded with second-order kinetics, barrierless, and very rapidly ($k = 2.0 \times 10^{-10}$ to 1.5×10^{-9} cm^3 s^{-1}; Table 3). Clary et al. presented a systematic data analysis combining the absolute rate constants with classical capture theory dominated by an isotropic dispersion term.[494] In the case of alkenes and alkynes, this approach leads to an expression in which the rate constant k scales with one-third power of the polarizability of the colliding molecule and hence with $N^{1/3}$ (N = number of carbon atoms in the alkene or alkyne; Figure 5). Note that C(^{3}P$_j$) showed no reaction toward water and methane, suggesting that possibly only unsaturated molecules reacted rapidly with carbon atoms.[488−494] This hypothesis was supported very recently. Kinetic studies on the collisional removal of ground-state carbon atoms with formaldehyde, acetaldehyde, and acetone at room temperature illustrated that these reactions are indeed very fast ($k = 3.8-6.6 \times 10^{-10}$ cm^3 s^{-1}) and proceed without barriers.[495]

These kinetic data demonstrated explicitly that at least at elevated temperatures prevailing in hot molecular cores, circumstellar envelopes of carbon stars, and planetary nebulae, reactions of atomic carbon with unsaturated molecules can occur. The absence of any entrance barrier underlines further the potential role of these neutral−neutral reactions in dense clouds where temperatures of 10 K prevail. However, their actual effect on the interstellar hydrocarbon chemistry at low temperatures depends on the absence of even minor entrance barriers and the unambiguous identification of the reaction products. Therefore, further investigations are clearly necessary and should acquire data on low-temperature rate constants and the primary reaction products of astrochemically important neutral−neutral reactions.

Very recently, Bergeat et al. extended Husain's investigations of reactions involving atomic carbon to detect the atomic hydrogen reaction product via resonance fluorescence.[496,497] Figure 6 depicts a schematic view of the experimental setup. The low-pressure fast-flow reactor consisted of a hollow stainless steel block in which a Teflon tube is inserted. Ports for the atomic resonance fluorescence detection of carbon and hydrogen atoms were located downstream. Atomic carbon, C(^{3}P$_j$), was generated in situ passing tetrabromomethane (CBr_4) in helium

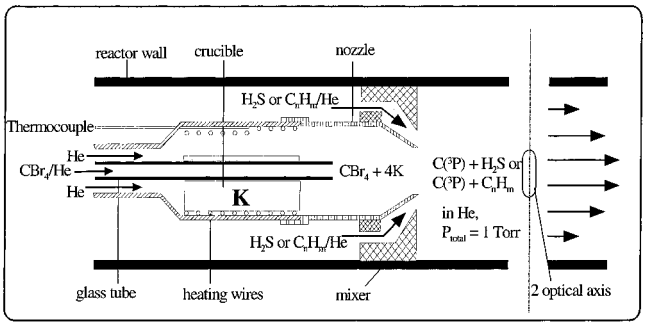

Figure 6. Schematic design of a low-pressure fast flow reactor employed in kinetic investigations of atomic carbon reactions with unsaturated hydrocarbons and hydrogen sulfide monitoring the $C(^3P_j)$ reactant and the $H(^2S_{1/2})$ product via resonance fluorescence.

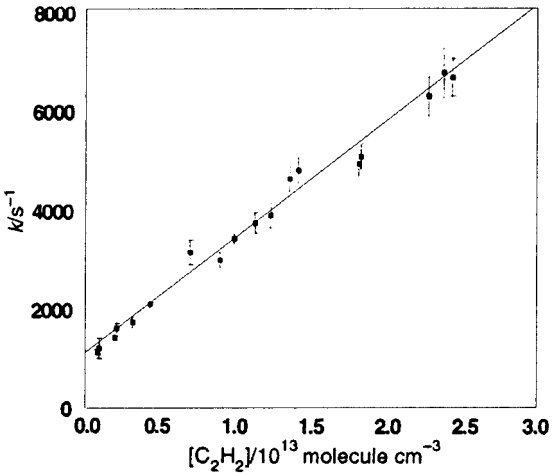

Figure 7. Plot of the pseudo-first-order rate constant of the reaction of $C(^3P_j)$ with acetylene, $C_2H_2(X^1\Sigma_g^+)$ versus the acetylene concentration. The gradient of the fitted line yields the second-order rate constant, $k = 2.4 \pm 0.5 \times 10^{-10}$ cm^3 s^{-1}.

carrier gas at 1.4 Torr through an excess of atomic potassium vapor in a furnace through the exit nozzle. The carbon atoms were then mixed at room temperature with the reactant in helium buffer gas and allowed to react. The overall rate constants were determined by following the decay of the carbon atom via a resonance fluorescence signal employing $C(^3P_j)$ transitions at 156.1 and 165.7 nm (Table 4). Absolute $H(^2S_{1/2})$ atom production yields were estimated probing the hydrogen atom resonance fluorescence at 121.6 nm and scaled to C/H_2S[498] and C/C_2H_4 reactions which serve as reference systems. A typical set of data is shown in Figure 7 for the $C(^3P_j)/C_2H_2$ system.

These experiments verify Husain et al.'s findings that reactions of atomic carbon with unsaturated hydrocarbons are fast ($k = 1.9-2.9 \times 10^{-10}$ cm^3 s^{-1}) and hence proceed close to the gas kinetics limits. The authors did not provide only room-temperature rate constants but also contributed valuable information on relative H atom production yields. For instance, the collision of $C(^3P_j)$ with allene was suggested to produce exclusively atomic hydrogen plus a C_4H_3 isomer. All remaining reactions were found to have lower H atom production yields ranging from 0.92 ± 0.08 (ethylene) to only 0.16 ± 0.08 (benzene). These data could indicate additional reaction channels besides the carbon versus atomic hydrogen exchange pathway. However, as the authors quoted, these kinetic investigations were not performed under single-collision conditions, and three-body collisions might influence the atomic hydrogen yield significantly. Hence, collision-induced intersystem crossings or a three-body reaction leading to a stabilization of the internally excited reaction intermediate have to be taken into consideration. In addition, the detection of the light hydrogen atom does not mean a priori that the carbon versus atomic hydrogen exchange mechanism produces these H atoms. Here, a secondary decomposition of an internally 'hot' product might be an additional source of H atoms. Consequently, an explicit detection of the hydrocarbon reaction products under single-collision conditions, where it is possible to observe a reaction between only two reactant species, is imperative to investigate the complete product spectrum of astrochemically important reactions.

B. Low-Temperature Kinetic Studies

Following the pioneering kinetic studies of Husain et al., the next logical step forward was to validate the astrochemical implications at lower temperatures. This desire was triggered by astrochemists to investigate the role of neutral−neutral reactions not only in hot cores and in circumstellar shells, but also in dense cloud regions where temperatures as low as 10 K prevail. Therefore, rate constants at ultralow temperatures had to be provided. Over the past few years, rate coefficients of elementary reactions important in dense clouds had been measured down to temperatures of 7 K employing continuous flow CRESU (Cinetique de Reaction en Ecoulement Supersonique Uniforme) apparatuses in Rennes and Birmingham (Figure 8).[499−508] These machines utilized an expansion of a preselected gas mixture

Table 4. Rate Constants and Relative Ratios of Atomic Hydrogen Production of Reactions of Ground-State Carbon Atoms with Various Molecules at 300 K and 1.4 Torr as Derived from Low-Pressure Fast Flow Reactor Studies

reactant	rate constant k, 10^{-10} cm^3s^{-1}	relative H-atom production compared to H yield in the C/C_2H_4 system	relative H-atom production scaled to the C/H_2S system
hydrogen sulfide (H_2S)	2.1 ± 0.5	1.09 ± 0.06	1.00 ± 0.06
acetylene (C_2H_2)	2.4 ± 0.5	0.58 ± 0.04	0.53 ± 0.04
ethylene (C_2H_4)	2.1 ± 0.4	1.00	0.92 ± 0.08
methylacetylene (CH_3CCH)	2.9 ± 0.4	0.86 ± 0.06	0.79 ± 0.08
allene (C_3H_4)	2.7 ± 0.5	1.04 ± 0.04	0.95 ± 0.05
propylene (C_3H_6)	2.6 ± 0.4	0.53 ± 0.06	0.49 ± 0.08
trans-butene (C_4H_8)	1.9 ± 0.6	0.32 ± 0.06	0.29 ± 0.06
benzene (C_6H_6)	2.8 ± 0.8	0.17 ± 0.05	0.16 ± 0.08

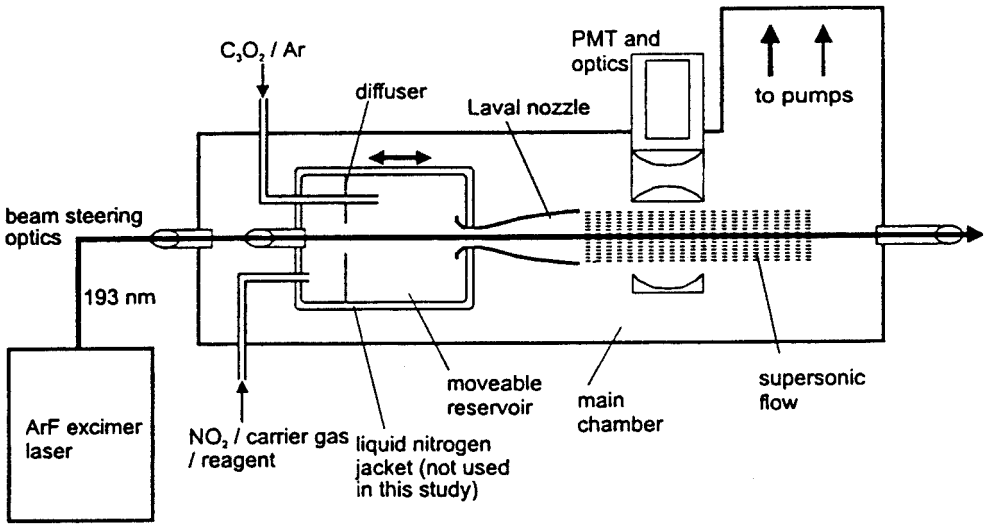

Figure 8. Schematic diagram of the CRESU apparatus adapted for the study of $C(^3P_j)$ reactions by the pulsed laser photolysis−chemiluminescense method.

through an axisymmetric, converging−diverging Laval nozzle, which generated a cold and uniform supersonic flow of gas. This expansion formed a relatively dense medium ($10^{16}-10^{17}$ cm^{-3}) in which the temperature, number density, and velocity were constant along the axis of the flow. Each nozzle was designed to produce a specific density and selected temperature of a carrier gas such as helium, argon, and nitrogen. The supersonic flow regime could be maintained if additional gases are admixed to 1−2%. Employing a liquid nitrogen-cooled gas reservoir, temperatures as low as 7 K could be achieved; without precooling, typical temperatures of 13−15 K were feasible. The recent commission of a pulsed CRESU setup[509] provided a vital improvement, although only temperatures down to 103 K have been achieved so far.[510,511] Due to the immense gas load of continuous beams, reactions with expensive, deuterated, or toxic chemicals were excluded from being studied. However, the significantly reduced gas load of the pulsed setup now permits the exploration of the kinetics of even expensive and hazardous reactants. Generally speaking, both the pulsed and continuous CRESU technique allowed determining rate constants larger than 10^{-12} cm^3 s^{-1}. This order of magnitude was dictated by three factors, i.e., the concentration of the co-reagent which is limiting under pseudo-first-order kinetic conditions in the beam, the supersonic flow which was uniform over a distance of a few tens centimeters, and the velocity of the continuous beam. This translated into a time scale of 100−500 μs in which a detectable change of concentration of the atom/radical reactant had to occur.

These CRESU setups provided a versatile method to measure rate constants at ultralow temperatures. Most commonly, the atom or radical reactant in the gas mixture was generated via pulsed laser photolyses of an admixed precursor molecule. This technique had been applied to produce astrochemically important species, for instance, atomic carbon $C(^3P_j)$, ethinyl radicals ($C_2H(X^2\Sigma^+)$), methylidene ($CH(X^2\Pi_\Omega)$), and cyano radicals $CN(X^2\Sigma^+)$ via photolyses of carbon suboxide (C_3O_2), acetylene (C_2H_2), bromoform ($CHBr_3$), and nitrosocyanide/cyanoiodide (NCNO/ICN), respectively. Subsequently, the changes in the number density of these radicals or atoms was followed with a second laser via laser-induced fluorescence of the reactant as relaxation occurs; this approach had been employed successfully to probe the temporal development of $C(^3P_j)$ and $CN(X^2\Sigma^+)$. Alternatively, the chemiluminescence marker technique could be applied. Here, a fraction of nitrogen dioxide (NO_2) was added to the CRESU flow; $C(^3P_j)$ reacted then at a constant rate with NO_2, which was in large excess over the carbon suboxide to form CO plus NO. The observed chemiluminescense was collected from the $NO(B^2\Pi)$ or $NO(A^2\Sigma^+)$ state as function of time. Likewise, $C_2H(X^2\Sigma^+)$ could be monitored via the reaction with molecular oxygen to form carbon monoxide and the methylidene radical following the $A^2\Delta - X^2\Pi$ chemiluminescense of the latter species.

Table 5 compiles the rate constants of those $C(^3P_j)$, $C_2H(X^2\Sigma^+)$, $CH(X^2\Pi_\Omega)$, and $CN(X^2\Sigma^+)$ reactions with astrochemically important hydrocarbons which have been studied so far. The magnitudes of the rate constants of $1.1-4.8 \times 10^{-10}$ cm^3 s^{-1} close to the gas kinetic limits suggest that even at ultralow temperatures of dense clouds, atomic carbon, methylidene, as well as ethinyl and cyano radicals react barrierless and rapidly with unsaturated molecules. The reactions of carbon atoms follow the general trend of slightly increasing rates as the temperature drops (Figure 9); this was proposed to be consistent with the formation of an initial collision complex. Here, $C(^3P_j)$ might attack the unsaturated bond of the reactant with a rate determined by a capture process. These results correlate nicely with recent ab initio and statistical calculations on minimum energy reaction pathway calculating rate coefficients reaching 2.6×10^{-10} cm^3 s^{-1} with almost no temperature dependence up to 1000 K.[512] Likewise, Herbst et al.'s capture calculations converge with the experiments at lower temperatures.[513] The low-temperature studies propose further that all three spin−orbit states of the carbon atom [$C(^3P_0) = 0$ cm^{-1}; $C(^3P_1) = +16.4$ cm^{-1} (23 K); $C(^3P_2) = +43.4$ cm^{-1} (62 K)] react at comparable rates with unsaturated hydrocarbons.

Table 5. Compilation of Rate Constants of Carbon Atoms, Methylidene, as Well as Cyano and Ethinyl Radicals with Astrochemically Important Hydrocarbon Molecules Obtained at the Minimum Experimental Temperature

reagent	co-reagent	min temp T, K	$k(T)$, 10^{-10} cm^3 s^{-1}
CN($X^2\Sigma^+$)	C_2H_2	25	4.6 ± 0.25
	C_2H_4	25	4.35 ± 0.24
	C_2H_6	25	1.13 ± 0.21
	CH_3CCH	15	3.8 ± 0.7
	H_2CCCH_2	15	4.4 ± 1.1
C_2H($X^2\Sigma^+$)	C_2H_2	15	2.27 ± 0.29
	C_2H_4	15	2.17 ± 0.17
	C_3H_6	15	1.14 ± 0.32
	H_2CCCH_2	63	3.5 ± 0.4
	CH_3CCH	63	2.9 ± 0.3
C(^3P_j)	C_2H_2	15	4.76 ± 0.56
	C_2H_4	15	4.79 ± 0.79
	C_3H_6	15	2.88 ± 0.60
	CH_3CCH	15	3.9 ± 1.6
	H_2CCCH_2	15	2.91 ± 0.58
CH($X^2\Pi_\Omega$)	CH_4	23	3.16 ± 0.25
	C_2H_6	23	2.47 ± 0.27
	C_2H_2	23	3.85 ± 0.23
	C_2H_4	23	3.92 ± 0.22
	C_4H_8 (but-1-ene)	23	3.95 ± 0.65

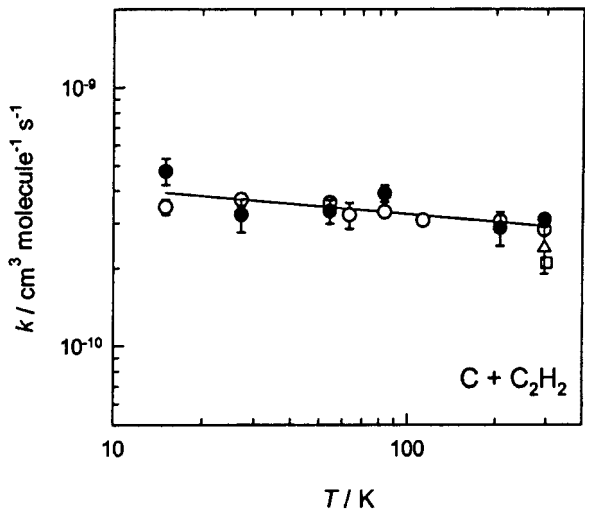

Figure 9. Rate coefficients k for the reaction of atomic carbon with acetylene as a function of temperature T plotted on a log−log scale. The continuous line is the fit to all CRESU data.

The kinetics of the ethinyl radical reactions are similar to those of the cyano species. The authors proposed a barrierless addition of the radical center to the unsaturated bond of the alkyne or alkene via capture to form an intermediate which is followed by a loss of atomic hydrogen. Note, however, the lower rate coefficients of the ethinyl reactions compared to those of the cyano radicals. The rate of cyano radical reactions with acetylene and ethylene is essentially constant in the range of 25−75 K.[501,502] For reactions of CH radicals with olefines, maximum rates of about 70 K were obtained which decrease then slightly at lower temperatures. A similar effect was observed for CH_4 and C_2H_6 with a maximum observed at 40 K; regarding C_2H_2, the maximum is less pronounced at about 70−80 K.[504,506,508,514] Low-temperature rate constants of the CN/C_2H_2 system are in agreement with previous calculations.[515]

These kinetic measurements yielded compelling evidence that atomic carbon, cyano, and ethinyl radicals react rapidly with unsaturated hydrocarbon molecules even at ultralow temperatures. Therefore, these bimolecular reactions are likely to play a considerable role in dense (cold, molecular) clouds where temperatures as low as 10 K dominate. However, despite valuable kinetic data, these techniques cannot furnish information on reaction products and intermediates involved explicitly. Therefore, experiments supplying these data are crucial.

IV. Dynamics: Crossed Molecular Beam Studies

A. Principle

The crossed molecular beam method is a powerful experimental technique to provide reaction products, intermediates involved, and branching ratios of bimolecular reactions.[135−137,516−521] Since the complex networks of chemical processes occurring in the interstellar medium and in planetary atmospheres consist of multiple elementary reactions that are a series of bimolecular encounters between atoms, radicals, and closed-shell species, a detailed knowledge of the elementary processes involved at the most fundamental, microscopic level is imperative. This scenario holds especially in diffuse, translucent, and dense clouds where the low number densities of less than 10^4 atoms cm^{-3} support only binary reactions; three-body encounters do not take place considering typical lifetimes of dense clouds of about 10^9 years. However, in denser media like circumstellar envelopes, planetary nebulae, or planetary atmospheres, three-body collisions may occur and any reaction intermediate [ABC]* (Figure 2) might be stabilized or, since these transient species are often radicals, react leading to more complex molecules. Therefore, it is clearly necessary to obtain two kinds of information to get a global picture on the chemical processing of the interstellar medium and our solar system. These are (i) the nature of the primary reaction products especially structural isomers and (ii) the intermediates involved. These data can be employed then to elucidate the reaction mechanisms, to compare the experimental findings with actual astronomical observations of molecules, and to predict where in extraterrestrial environments hitherto unobserved species can be formed.

The main advantage of the crossed beam technique is that it allows one to study binary collisions under well-defined velocity, velocity- and angular-spread, and internal quantum states. In fact, in contrast to a bulk experiment, the colliding species are confined into distinct beams which cross each other at a specific angle and collision energy. In other words, the species of each beam are made to collide only with the molecules of the other beam and the products formed fly undisturbed toward the detector. Each beam is so dilute that collisions within are negligible. These features provide an unprecedented approach to observe the consequences of a single molecular collision, preventing secondary collisions and wall effects. These single-collision conditions are essential to achieve this goal because in a binary collision of,

for instance, a cyano radical and a generic hydrocarbon molecule, RH, a cyano radical will react only with one single hydrocarbon molecule either 'indirectly' via a reaction intermediate [RHCN]* (reaction 11) or in a direct fashion through a transition state [RHCN]‡ (reaction 12)

$$CN(X^2\Sigma^+) + RH \rightarrow [RHCN]^* \rightarrow RCN + H, \quad (11)$$

$$CN(X^2\Sigma^+) + RH \rightarrow [RHCN]^{\ddagger} \rightarrow RCN + H \quad (12)$$

These requirements avoid that the potential [RHCN]* intermediate is stabilized and that the primary products react successively via a three-body reaction. Therefore, crossed beam experiments allow us to identify the nascent reaction products and to infer the intermediates.

B. Experiment

Only recently, technological improvements in the production of the unstable atom and radical beams together with an enhanced vacuum technology have allowed the study of elementary reactions of astrochemical interest such as those reported here. These experimental setups differ mainly in the source geometry (fixed sources as applied here versus rotatable sources) and detection scheme of the products (rotatable quadrupole mass spectrometric detector (QMS) versus spectroscopic detection via laser induced fluorescence (LIF)). Two important machine designs employed to study reactions of astrochemical interest are discussed. The experiments utilize fixed sources coupled with a rotatable QMS; setups with rotatable sources are associated with spectroscopic LIF detection and present an alternative approach. Both setups are highly complementary and permit one to (i) perform reactive scattering experiments over a wide range of collision energies covering 4 orders of magnitudes from 0.38 kJ mol^{-1} to 150 kJ mol^{-1}, (ii) infer the reaction intermediates involved, (iii) detect reaction products with (a) unknown spectroscopic properties such as polyatomic hydrocarbon radicals via a rotatable quadrupole mass spectrometer and (b) well-known spectroscopic transitions such as laser-induced fluorescence of hydrogen atoms, and (iv) determine the excitation function, i.e., the relative collision energy-dependent reaction cross sections together with branching ratios if multiple reaction channels are open.

1. Fixed Sources with Rotatable Quadrupole Mass Spectrometer

Figure 10 displays a top view of the 35″ crossed molecular beam machine. The setup consisting of two source chambers fixed at 90° crossing angle, a stainless steel scattering chamber, and an ultrahigh vacuum-tight, rotatable triply differentially pumped quadrupole mass spectrometric detector. The scattering chamber is evacuated by oil-free turbo molecular pumps to about 10^{-7} mbar and operated at typically 10^{-6} mbar during the reactive scattering experiments. In the primary source, pulsed supersonic atom/radical beams are produced via laser ablation techniques ($C(^3P_j)$, $C_2(X^1\Sigma_g^+)$, $C_3(X^1\Sigma_g^+)$, CN-

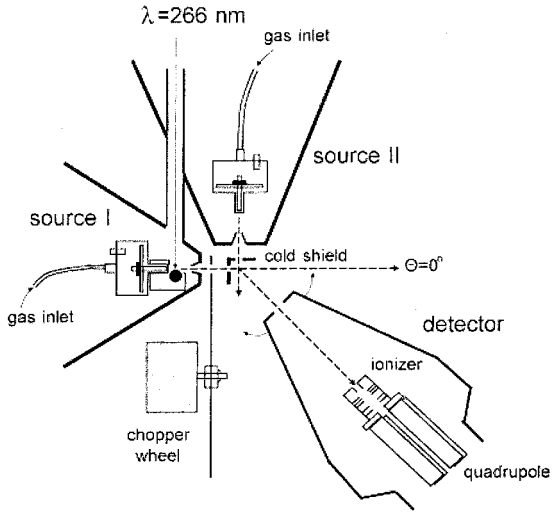

Figure 10. Schematic top view of the 35″ crossed beam apparatus with fixed sources, chopper wheel, laser ablation source, cold shield, and universal detector.

($X^2\Sigma^+$), $C_2D(X^2\Sigma^+)$; due to reasons explained later, no C_2H was used) or flash pyrolysis (C_6H_5 (X^2A')). It should be pointed out that at higher velocities, the carbon beam contains ground-state ($X^1\Sigma_g^+$) and electronically excited ($a^3\Pi_u$) dicarbon. At lower velocities, the $a^3\Pi_u$ state which lies only 718.32 cm^{-1} above the ground state is quenched efficiently. A neodymium yttrium aluminum garnet (Nd:YAG) laser operates at a 30 Hz repetition rate at 266 nm and is focused very tightly on a rotating carbon rod. The ablated carbon species $C(^3P_j)$, $C_2(X^1\Sigma_g^+)$, and $C_3(X^1\Sigma_g^+)$ were then seeded into helium or neon nitrogen carrier gas released by a pulsed valve. Relative concentrations of the ablated carbon species can be adjusted by carefully controlling the laser power, the backing pressure of the carrier gas, and the delay time between the pulsed valve and the laser.[522] Cyano, $CN(X^2\Sigma^+)$, and d_1-ethinyl, $C_2D(X^2\Sigma^+)$, radical beams are generated in situ by laser ablation of graphite and subsequent seeding of the liberated species in molecular nitrogen or deuterium which also serve as reactants.[523] Alternatively, the ablation source can be replaced by a pyrolytic source in which a mixture of <0.1% C_6H_5NO seeded in pulsed helium was expanded through a resistively heated silicon carbide tube. The temperature of 1300−1400 K of the latter splits the weak carbon−nitrogen bond homolytically to produce nitrogen oxide and the phenyl radical. Note that very recently a continuous carbon source has been developed. This beam contains ground-state and electronically excited carbon in its $^1D_2$ state.[524]

The pulsed primary beam passes though a skimmer into the main chamber of the machine. A four-slot chopper wheel is located after the skimmer and rotates at 240 Hz. It selects a 9 μs slice of well-defined velocity and velocity spread from the pulsed beam which reaches the interaction region. At this point, the primary reactant collides at a right angle with the second pulsed beam of an unsaturated hydrocarbon, hydrogen sulfide, or a hydrocarbon radical (vinyl, $C_2H_3(X^2A')$) or propargyl, $C_3H_3(X^2B_1)$). Both radicals were generated by photolyzing a helium/vinyl bromide or helium/propargyl bromide mixture

at 193 nm after the nozzle of the second pulsed valve. Typically, supersonic beams are characterized by very low translational temperatures ($T < 10$ K) and rotationally and vibrationally cold reagents. Note that both beams collide in the interaction region at a crossing angle Θ at distinct collision energies E_c of about 8−150 kJ mol^{-1} depending on the velocities v(A) and v(BC) and the masses m_A and m_{BC} of the reactants A and BC (eq 13). Hence, experiments are characterized by a well-defined collision energy but not by a kinetic temperature of the reactants (Maxwell−Boltzman distribution). If both beams cross perpendicular at $\Theta = 90°$, the cosine term vanishes and eq 13 reduces to eq 14

$$E_C = {}^1/_2(m_A \times m_{BC})/(m_A + m_{BC}) \times (v(A)^2 + v(BC)^2 - 2v(A)v(BC)\cos(\Theta)) \quad (13)$$

$$E_C = {}^1/_2(m_A \times m_{BC})/(m_A + m_{BC}) \times (v(A)^2 + v(BC)^2) \quad (14)$$

The reactively scattered species are registered by a rotatable and triply differentially pumped detector at an extreme ultrahigh vacuum of $<8 \times 10^{-13}$ mbar consisting of a liquid nitrogen-cooled electron impact ionizer followed by a quadrupole mass detector and a Daly-type detector. Any species scattered from the interaction region after a single-collision event took place can be ionized in the electron impact ionizer, and in principle, it is possible to determine the mass (and the gross formula) of all the products of a bimolecular reaction by varying the mass-to-charge ratio, m/e, in the mass filter. A considerable advantage of the crossed beam setup with respect to common flow reactors coupled with a mass spectrometer is the possibility to measure the velocity distribution of the products. The so-called 'time-of-flight' (TOF) operation of the QMS detector records the time-dependent ion current of a preselected m/e ratio taking the crossing time of both beams in the interaction region as a well-defined time zero. Ions of the selected m/e arriving early are fast, whereas ions arriving late have low velocities; this allows one to derive the amount of the total energy available to the products and, therefore, the energetics of the reaction. This is crucial when more isomers with the same gross formula, but different enthalpies of formation, can be produced. Since the QMS is rotatable between −25.0° and 72.0° in the scattering plane as defined by both beams, taking these TOF spectra at one m/e at different laboratory angles and integrating these data provides the laboratory angular distribution (LAB), i.e., the integrated intensity of a TOF spectrum versus the laboratory angle Θ. Second, reaction products with often unknown spectroscopic properties such as polyatomic, open-shell hydrocarbon radicals have to be probed. Hence, the majority of interesting unsaturated products cannot be scrutinized by optical detection schemes, such as laser-induced fluorescence (LIF) or resonance-enhanced multiphoton ionization (REMPI), and the universal mass spectrometric detection scheme is advantageous. Note that some problems such as dissociative ionization and background noise at certain m/e ratios from the residual gas in the ionizer region restrict the sensitivity of the method. This holds especially if low-mass hydrocarbon reaction products have to be probed and the dissociative ionization of the parent molecules contributes significantly to the background at the low-mass hydrocarbon product of interest. Despite the triply differential pumping setup, molecules desorbing from wall surfaces lying on a straight line to the electron impact ionizer cannot be avoided. Their mean free path is on the order of 10^3 m compared to maximum detector dimensions of about 1 m. To reduce this background, a copper plate attached to a two-stage closed-cycle helium refrigerator is placed right before the collision center and cooled to 4.5 K (Figure 10). Now the ionizer views a cooled surface (cold shield) which traps all the species with the exception of molecular hydrogen and helium.

For a detailed physical interpretation of the reaction mechanism, assignment of the intermediates involved, and identification of the reaction products, it is necessary to transform the laboratory (LAB) angular distribution and the TOF spectra into the center-of-mass (CM) system using a forward-convolution routine. This procedure initially assumes trial angular, $T(\theta)$, and translational energy, $P(E_T)$, distributions in the CM reference frame. TOF spectra and LAB distributions are then calculated from these $T(\theta)$ and $P(E_T)$ averaging over the apparatus and beam functions. The procedure is repeated until a satisfying fit of the laboratory data is achieved; the CM functions so determined are called "the best-fit CM functions". The ultimate output data of the experiments is the generation of a product flux contour map which reports the differential cross section (the intensity of the reactively scattered products), $I(\theta,u) \sim P(u) \times T(\theta)$, as the intensity as a function of angle θ and product center-of-mass velocity u. The function $I(\theta,u)$ is called the reactive differential cross section. This contour map can be seen as the image of the reaction and contains all the information on the scattering process. Whereas the intermediates involved are inferred indirectly, the reaction products are identified—in the simplest case—from the $P(E_T)$ distribution.

These contour plots of a bimolecular reactive scattering process allows us (a) to identify the primary reaction products, (b) to determine the branching ratios of competing reaction channels, (c) to untangle the microscopic reaction mechanisms, (d) to quantify the product energy release, and hence (e) to gain information on the underlying potential energy surfaces (PESs), which govern the transformation from reactants to products. To get a picture on the energetics, we must take a closer look at the center-of-mass velocity u of the products; here, all the information we gain from u translates to information on the translational energy. To elucidate the chemical reaction dynamics, three properties of the $I(\theta,u)$ are worthwhile studying. First, if the energetics of the product isomers are well separated, the maximum translation energy E_{max} can be used to identify the nature of the products. Here, E_{max} is simply the sum of the reaction exoergicity obtained either from

electronic structure calculations or literature and the collision energy in the experiments. Therefore, if we subtract the collision energy from the experimentally determined E_{max}, the exoergicity of the reaction is obtained. Second, in the most favorable case, the distribution maximum of the $P(E_T)$ can give the order-of-magnitude of the barrier height in the exit channel. If a $P(E_T)$ peaks at zero or close to zero, the bond rupture has either no or only a small exit barrier (loose exit transition state). On the other hand, $P(E_T)$s can show pronounced maxima away from zero translational energy; these data suggest a significant geometry as well as electron density change from the decomposing intermediate to the products resulting in a repulsive bond rupture from a tight transition state. Third, the fraction of energy released into translational degrees of freedom is worth investigating; a fraction of about 30−40% often implies that the chemical reaction dynamics are governed by the formation of a covalently bound intermediate from reaction of the primary and secondary reactants whereas a higher fraction is often characteristic for 'direct' reaction dynamics.

The angular information of the flux contour maps gives information on the $T(\theta)$ and is of fundamental importance to elucidate the chemical reaction dynamics and the intermediates involved. These graphs show the angular-dependent flux distribution an observer would see if (s)he moves with the center of mass velocity dwelling on the center-of-mass of the system. Here, the direction of the primary beam is defined as 0° and of the secondary beam as 180°. Several shapes of the flux distributions are feasible. First, the $T(\theta)$ and corresponding flux contour map $I(\theta,u)$ shows a symmetric profile around 90°; this means the intensity of the flux distribution is the same at a center of mass angle θ and $180° - \theta$. This 'forward−backward' symmetric behavior is characteristic for a bimolecular reaction $A + BC \rightarrow AB + C$ which goes through a [ABC]* intermediate (indirect scattering dynamics; Figure 2) holding a lifetime larger than its rotation period. Here, the complex lives long enough—on the picosecond order—to rotate several times and it will have 'forgotten' the directions of the incoming collision partners. Alternatively, a symmetric distribution around 90° could be interpreted in a way that the reaction proceeds though a 'symmetric' exit transition state. In this case, the decomposing complex must have a rotation axis which interconverts, for instance, the leaving hydrogen atom. On this basis, the H atom can be released into θ and $180° - \theta$ with equal probability to result in a forward−backward symmetric flux distribution; no information on the lifetime of the fragmenting intermediate can be obtained. The actual interpretation of $T(\theta)$ goes even further. While the symmetry is an essential requirement, the shape of $T(\theta)$ is determined by the disposal of the total angular momentum and a variety of shapes are indeed possible depending on the correlation between initial and final angular momentum as well as the final rotational angular momentum. Second, the angular flux distribution can be asymmetric around 90°; often the flux at 0° is larger than that at 180°. In the simplest scenario, this suggests a so-called 'osculating complex model': here, the reaction is still indirect and proceeds via formation of an intermediate, but the lifetime of the latter is on the order of the rotation period, and multiple rotations cannot occur; here, the asymmetry can be used as a clock to estimate the lifetime of the intermediate (case 1). Another optional interpretation of this shape is that the chemical dynamics are governed by two microchannels, i.e., a forward−backward symmetric one and a second more forward-scattered contribution (case 2). Increasing the collision energy and observing the change in the center-of-mass angular distribution might help to discriminate between both cases. In many experiments, a transition from a forward−backward symmetric to a more forward distribution with increasing collision energy can be connected to an osculating complex model, whereas the reverse trend, i.e., a less pronounced forward peaking as the collision energy rises, supports case 2. Third, the center-of-mass angular flux distribution can show predominantly flux only in the forward direction, i.e., the flux peaks at 0° and is zero at larger angles ('stripping dynamics') or only in the backward direction, i.e., the flux distribution shows a maximum at 180° and falls down to zero at lower angles ('rebound dynamics'). In these cases, the reaction is 'direct' and proceeds either via a very short-lived, highly rovibrationally excited intermediate with a lifetime of less than 0.1 ps or goes through a transition state without involving an intermediate. Direct reactions are associated with repulsive or weakly attractive potential energy surfaces, whereas a long-lived intermediate experiences the deep potential energy well of a bound species.

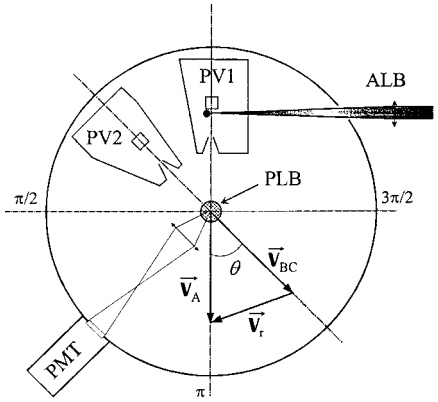

Figure 11. Schematic top view of a crossed beam machine with rotatable sources and laser-induced fluorescence detection (LIF): PV1/PV2, pulsed valves 1/2; PMT, photomultiplier tube; ALB, ablation beam; PLB, probe laser beam; $\mathbf{v}_A$, velocity vector beam A; $\mathbf{v}_{BC}$, velocity vector beam BC; $\mathbf{v}_r$, velocity vector of the relative velocity.

2. Rotatable Sources with Laser-Induced Fluorescence Detection

Figure 11 portrays a schematic top view of a crossed beam machine with two rotatable, pulsed molecular beam sources PV1 and PV2.[525] Compared to the perpendicular source geometry of the previous setup, crossed beam machines employing rotatable sources can give very low collision energies. Here, the

beam intersection angle can be varied from 135.0° to 22.5°. Recalling eq 13, this represents a powerful approach to scan the relative collision energy of both reactants down to 0.38 kJ mol^{-1} without changing the laboratory velocities of the reactants. So far, only astrochemically relevant reactions of atomic carbon with unsaturated hydrocarbons have been performed. Here, supersonic $C(^3P_j)$ beams were produced by laser ablation of graphite[526] and seeding the ablated species into helium, neon, or argon carrier gas. However, the rotatibility of both sources makes it difficult to investigate reaction with two photolytically generated species such as collisions between atom and radicals or radicals and radicals.

This setup does not utilize a quadrupole mass spectrometer coupled to an electron impact ionizer but probes the atomic hydrogen and deuterium reaction product via laser-induced fluorescence (LIF). As the reactions of atomic carbon plus unsaturated hydrocarbons are strongly expected to produce highly unsaturated hydrocarbon radicals, the a priori unknown nature of the radical products makes it difficult to probe the latter via LIF detection. Hence, in reactions which are dominated by an atomic carbon versus atomic hydrogen/deuterium exchange, the light H/D products have been sampled; in principle, if LIF detection schemes of heavier products are available, this technique can be extended to observe the latter spectroscopically. Briefly, the $D(^2S_{1/2})$ atoms produced in the reaction were probed by one-photon resonant LIF using the $(^2P_j-^2S_{1/2})$ Lyman-α transition at 121.534 nm and a photomultiplier tube as a detector. The vacuum ultraviolet photons were generated by frequency tripling of ultraviolet radiation around 365 nm in krypton gas. The VUV beam propagated perpendicular to the molecular beam scattering plane and hence perpendicular to the relative velocity vector. Note that whereas the D atom detection is essentially background free, a probing of the H atom at the $(^2P_j-^2S_{1/2})$ Lyman-α transition at 121.57 nm is limited by a hydrogen atom background arising from photodissociation of background molecules such as hydrocarbons and water in the main chamber. Relative, collision energy-dependent cross sections of the H/D atom yields were obtained by dividing the averaged signal intensities by the relative velocities of the reagents. Recall, however, that in some cases it might be difficult to elucidate if the H/D atoms originates from a carbon versus hydrogen/deuterium exchange or a three-body fragmentation in which the intermediate of a binary collision decomposes to a heavy hydrocarbon fragment, molecular hydrogen, and atomic hydrogen. Therefore, identification of the heavy product is often desirable.

C. Results

1. Reactions of $C(^3P_j)$

Reactive scattering experiments of atomic carbon $C(^3P_j)$ with alkynes [acetylene (C_2H_2),[524,527−530] methylacetylene (CH_3CCH),[524,531−533] dimethylacetylene (CH_3CCCH_3),[534] and the propargyl radical (C_3H_3)[535,536]], alkenes [ethylene (C_2H_4),[524,537,538] propylene (C_3H_6),[539,540] 1,3-butadiene (C_4H_6),[541] and the vinyl radical (C_2H_3)[542−544]], cummulenes [allene (H_2CCCH_2)[532,545] and 1,2-butadiene (methylallene; C_4H_6)[546]], benzene (C_6H_6),[547−549] and hydrogen sulfide (H_2S)[550−552] were performed and supported with electronic structure and statistical (Rice−Ramsperger−Kassel−Marcus) calculations. The prime directive of these studies was to expose the synthetic routes to small (sulfur-carrying) hydrocarbon radicals in the interstellar medium[542,553−557] and in hydrocarbon-rich atmospheres of planets and their moons.[558] The reactions with acetylene and vinyl expose possible routes to form ubiquitous interstellar C_3H and C_3H_2 isomers; collisions with three distinct C_4H_6 isomers dimethylacetylene, 1,2-butadiene, and 1,3-butadiene can unravel how various C_5H_5 isomers—potential precursors to PAH-like species—are synthesized in extraterrestrial space (sections II.A and II.D).

To untangle the chemical dynamics of complex, polyatomic reactions comprehensively, it is always useful to combine the crossed beam data with electronic structure calculations on the underlying potential energy surfaces (PES) and with statistical (RRKM) calculations.[559] Here, global potential energy surfaces can predict the energetics of distinct product isomers, intermediates, and various transition states to a chemical accuracy of about ± 5 kJ mol^{-1}. These calculations can be carried out on ground-state and excited surfaces. Statistical calculations can predict further the branching ratios of the reaction products emerging from chemically activated complexes as formed in crossed beam experiments. However, these calculations alone cannot reveal the actual reaction mechanisms involved. First, RRKM calculations superimpose a complete energy randomization in the [ABC]* intermediate of a bimolecular reaction before the latter falls apart. However, recent crossed beam studies of $C(^3P_j)$/1,2-butadiene,[546] $C(^3P_j)/CD_3CCH$,[533] $C(^3P_j)/C_6H_6$,[548] and C_6H_5/CH_3CCH (section IV.C.5) and the reactions of electronically excited carbon atoms $C(^1D_2)$ with acetylene, ethylene, and methylacetylene revealed strong discrepancies between the calculated and the experimentally observed product distributions.[560,561] Second, potential energy surfaces cannot foresee if the reaction dynamics are 'direct' or 'indirect'; therefore, they cannot account for the experimentally observed direct contributions as exposed in the reactions of ground-state carbon with acetylene, ethylene, 1,2-butadiene, and benzene. Finally, it is difficult to predict theoretically if electronically excited surfaces are involved in the actual dynamics (C_2D/C_2H_2 system; section IV.C.4). On the other hand, electronic structure calculations provide guidance if experimental enthalpies of formation of potential radical products are lacking. Further, the geometries of various exit transition states can be compared with the experimentally derived center-of-mass angular distributions to pin down the most likely reaction paths. On the basis of these considerations, crossed beam experiments and computations of the underlying potential energy surfaces are strongly complimentary to expose the reaction dynamics of complicated, polyatomic reactions comprehensively. Note that the reaction prod-

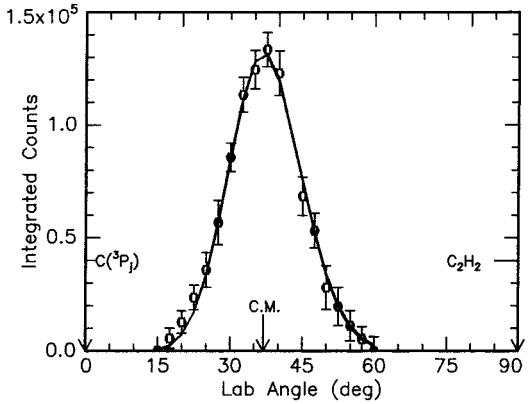

Figure 12. Laboratory angular distribution of the C_3H product of the $C(^3P_j) + C_2H_2(X^1\Sigma_g^+)$ reaction at $m/e = 37$ at a collision energy of 28.0 kJ mol^{-1}. Circles and 1σ error bars indicate experimental data; the solid lines represent the calculated distribution for the upper and lower carbon beam velocity. C.M. designates the center-of-mass angle.

ucts and intermediates are often 'nonclassical' organic molecules whose bonds cannot be simply classified as, for instance, double or triple bonds. Likewise, the radical center(s) is(are) often delocalized. Therefore, in the following figures, only single bonds are drawn; radical centers are omitted for clarity.

1.1. Reactions with Alkynes. The reaction of atomic carbon in its ^3P_j ground state with acetylene presents the prototype encounter of carbon atoms with the simplest alkyne and is discussed in detail; hereafter the reactions with methylacetylene, dimethylacetylene, and the propargyl radical are compiled briefly. The crossed beam experiments expose the existence of an atomic carbon versus hydrogen exchange pathway. The reactive scattering signal was detected at a mass-to-charge ratio $m/e = 37$ (C_3H^+) (Figure 12). A forward-convolution fitting of the data yielded weakly polarized center-of-mass angular flux distributions decreasingly forward scattered with respect to the carbon beam as the collision energy rises from 8.8 to 28.0 kJ mol^{-1} and is isotropic at 45.0 kJ mol^{-1}. Reaction dynamics inferred from the experimental data and ab initio calculations suggested two microchannels initiated by a barrierless addition of $C(^3P_j)$ either to one acetylenic carbon to form *trans*-propenediylidene (INT1) or to two carbon atoms to yield a triplet cyclopropenylidene isomer (INT2) (Figures 13 and 14). Both intermediates are stabilized by 122−137 and 190−216 kJ mol^{-1} with respect to the reactants and are connected through a transition state located 3−4 kJ mol^{-1} above INT1 (Table 6). Propenediylidene was suggested to undergo a [2,3]-H-migration to a triplet propargylene intermediate INT3 via a barrier of 0.1−11 kJ mol^{-1} followed by a C−H bond cleavage via a symmetric exit transition state to l-C_3H ($X^2\Pi_\Omega$) and H. Propargylene is the global minimum of the triplet surface and bound by 352−388 kJ mol^{-1} with respect to the reactants. Direct stripping dynamics donated to the forward-scattered, second microchannel to form the C_{2v}-symmetric c-$C_3H(X^2B_2)$ isomer and H. This contribution is quenched with rising collision energy. Both reactions to l- and c-C_3H have no exit barrier and are slightly exoergic by 1.5 and 8.6 kJ mol^{-1}. The finding of an enhanced formation of the cyclic isomer as the collision energy drops seems to be in contradiction to a quantum mechanical study of this reaction by a reduced dimensionality approach.[562] Here, the linear isomer was found to be the principal reaction product at the whole energy range from 5 to 70 kJ mol^{-1}; c-C_3H was predicted to be formed only

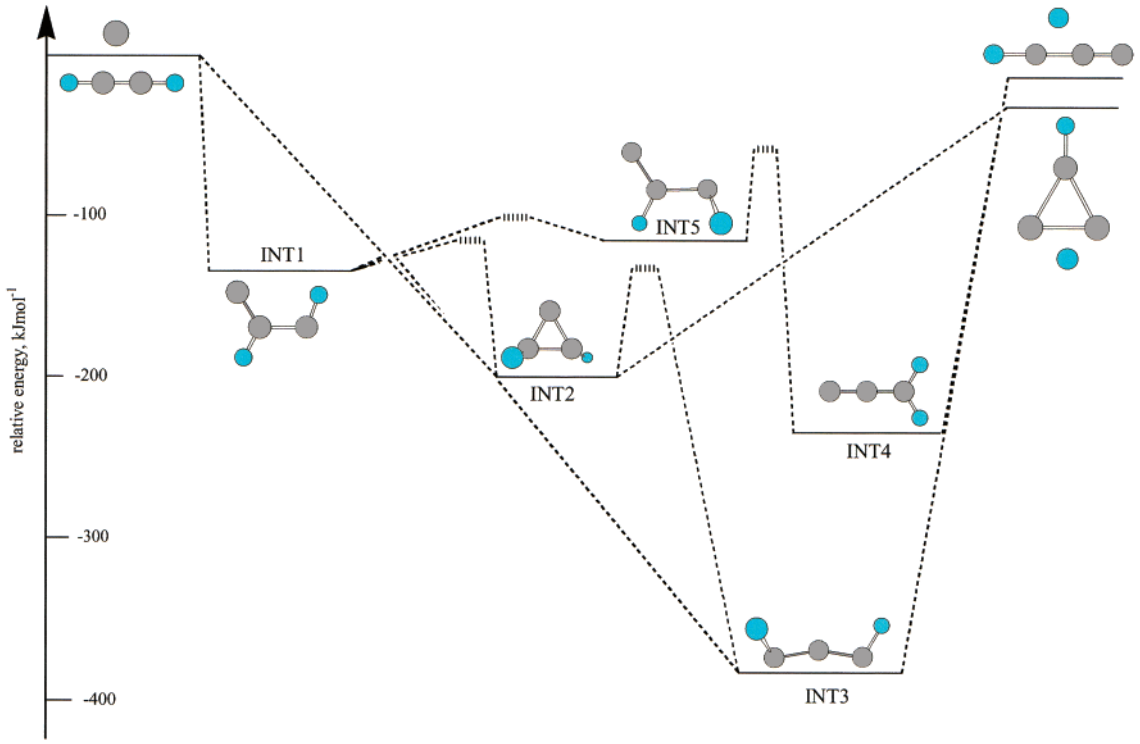

Figure 13. Schematic triplet potential energy surface of the reaction of ground-state atomic carbon with acetylene. Carbon atoms are denoted in gray and hydrogen atoms in light blue.[528−530]

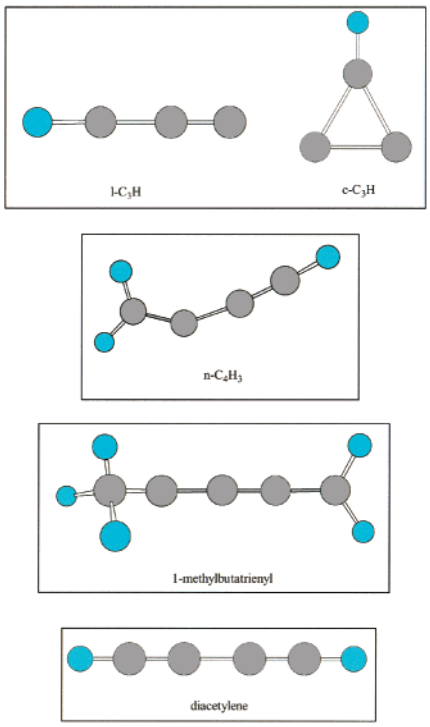

Figure 14. Hydrocarbon radicals produced via a carbon versus hydrogen exchange pathway in the reactions of atomic carbon with acetylene, methylacetylene, dimethylacetylene, and the propargyl radical. Carbon atoms are denoted in gray and hydrogen atoms in light blue.

at higher energies. However, this approach hardly treats the experimentally inferred direct reaction dynamics to the c-C_3H isomer comprehensively, and more extensive theoretical investigations accounting for a direct pathway are desirable.

Not long ago, the reaction of atomic carbon with perdeuteroacetylene was also investigated at lower collision energies down to 0.4 kJ mol^{-1} utilizing a crossed beam setup with rotatable sources and LIF detection of atomic deuterium.[563] Figure 15 depicts the normalized excitation function of the reaction of $C(^3P_j)$ with $C_2D_2(X^1\Sigma_g^+)$ obtained by this technique. Assuming that the reaction is independent of the fine structure of the carbon atoms, relative thermal rate constants were calculated and compared with low-temperature CRESU data of the $C(^3P_j)/C_2H_2(X^1\Sigma_g^+)$ system. At collision energies lower than 4.9 kJ mol^{-1}, these data compared nicely with CRESU results, verifying that the reaction is indeed barrierless. However, one fundamental difference should be stressed. Since the formation of the l-C_3D isomer was found to be endoergic by 7 kJ mol^{-1}, only the exoergic channel to form c-C_3D was open at lower collision energies. Since the CRESU studies were performed with C_2H_2, both the cyclic and linear isomer can be synthesized. Note that an investigation of the $C(^3P_j) + C_2H_2(X^1\Sigma_g^+)$ reaction at very high collision energies larger than 200 kJ mol^{-1} opened the endoergic $CH(X^2\Pi_\Omega) + C_2H(X^2\Sigma^+)$ channel.[564] This pathway was suggested to be either direct via a hydrogen abstrac-

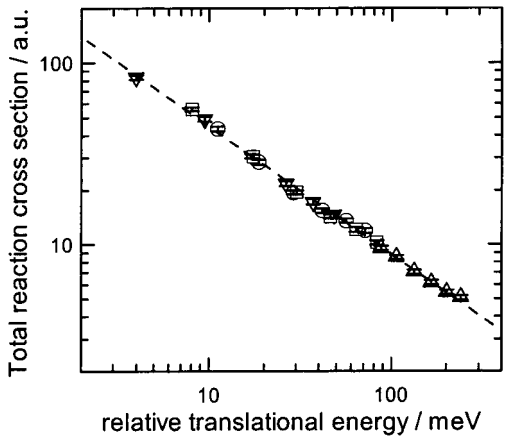

Figure 15. Normalized excitation function of the reaction of $C(^3P_j)$ with d_2-acetylene, C_2D_2 ($X^1\Sigma_g^+$). The dashed line represents the best fit.

Table 6. Relative Energies of Intermediates Involved in the Reaction of Ground-State Carbon Atoms with Acetylene, Methylacetylene, and Dimethylacetylene; TS Denotes a Transition State of an Isomerization of Two Intermediates[a]

	C_2H_2; R1 = R2 = H	CH_3CCH; R1 = H; R2 = CH_3	CH_3CCCH_3; R1 = R2 = CH_3
INT1	122−137	137	132
INT2	190−216	221	225
INT3	352−388	374	374
INT4	239−253	223	242
INT5	114	136	124
TS INT1/5 → INT2	3−4	18	1−2
TS INT1 → INT3	0.1−11	0.8	n/a
TS INT2 → INT3	55−58	61	65
TS INT1 → INT5	10	8	10
exit transition state	0	24	18

[a] All data are given in kJ mol^{-1}. n/a: the barrier of a methyl group migration to a dimethylvinylidenecarbene intermediate was not investigated.

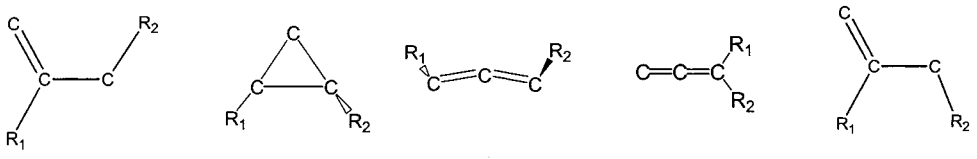

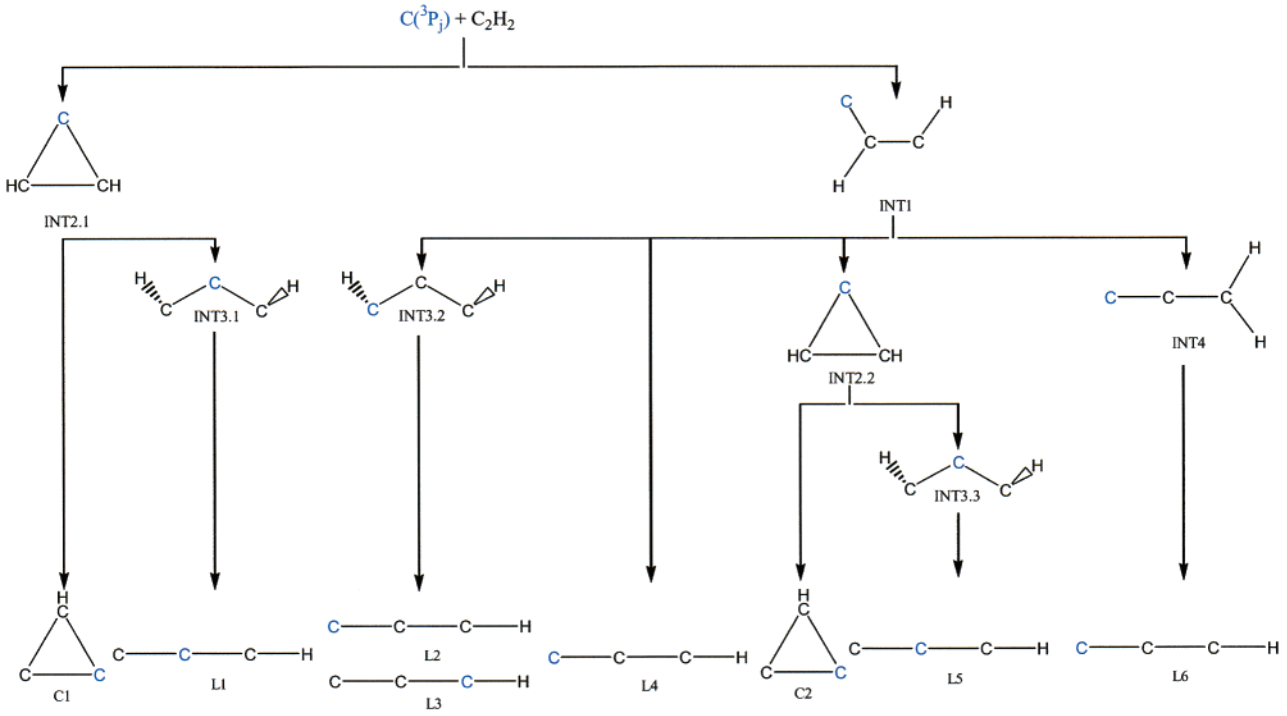

Figure 16. Feasible reaction pathways to form linear and cyclic C_3H isomers on the triplet surface via various C_3H_2 intermediates. The atomic carbon reactant is denoted in blue.

tion or indirect through a propenediylidene intermediate INT1 followed by a carbon−carbon bond rupture.

The very recent experimental verification of the $C_3(X^1\Sigma_g^+) + H_2(X^1\Sigma_g^+)$ channel, which has a branching ratio of 30−40%, showed that the suggested mechanism to form C_3H is more diverse than previously thought.[524,565] Electronic structure calculations predicted that intersystem crossing of a long-lived propargylene intermediate INT3 from the triplet to the singlet manifold is facile. The singlet propargylene intermediate can lose molecular hydrogen via a five-membered cyclic transition state or undergo a [1,3]-H shift to singlet vinylidene carbene prior to an H_2 ejection to form the tricarbon molecule. Therefore, both the propargylene and the vinylidenecarbene intermediates—which are long-lived—likely also undergo a barrierless atomic hydrogen elimination to the l-C_3H isomer. Hence, three distinct pathways might actually form l-C_3H, whereas solely direct dynamics may account for the c-C_3H isomer at lower collision energies.

However, the actual dynamics of the $C(^3P_j)/C_2H_2(X^1\Sigma_g^+)$ system might be even more complex. Figure 16 compiles nine indirect reaction pathways to form C_3H isomers. Tagging the attacking carbon atom in blue, an addition of $C(^3P_j)$ to two carbon atoms leads to c-C_3H_2 INT2.1, which in turn gives the cyclic c-C_3H isomer C1. Alternatively, INT2.1 undergoes ring opening to triplet propargylene INT3.1; the new carbon atom is located in the center of the molecule. The latter decays to the l-C_3H isomer L1 with the carbon atom at the central position. Second, $C(^3P_j)$ adds to only one acetylenic carbon atom to give INT1. This intermediate might undergo three reactions. These are (1) a hydrogen shift to propargylene INT3.2 ($C(^3P_j)$ is now in the terminal position of the carbon chain and not in the center position as found in INT3.1), this intermediate can fragment to form two distinct l-C_3H isomers L2 and L3, (2) an H atom loss to give l-C_3H L4, and (3) a ring closure to c-C_3H_2 INT2.2, which in turn loses a H atom to give c-C_3H C2 or ring opens to propargylene INT3.3; the latter ejects an H atom to l-C_3H L5. A fourth option, i.e., an H atom shift to triplet vinylidenecarbene INT4 followed by l-C_3H formation L6, can be likely ruled out due to the inherent high barrier of the hydrogen migration (28 kJ mol^{-1} with respect to INT5; the latter is connected by a trans−cis isomerization to INT1) compared to the formation of INT3.2. These options involve only indirect dynamics, and direct pathways can provide additional channels to form C_3H isomers. Finally, the intersystem crossing followed by atomic hydrogen loss might yield l-C_3H as well.

These simple considerations underline that further experimental and theoretical studies of this reaction are clearly desired. It is important to note that the linear C_3H isomers L1−L5 are formed on the triplet surface via distinct reaction pathways; they must not be considered a priori as 'equivalent'. For instance, INT3.1 could account for the symmetric angular distribution since this intermediate is 'symmetric'. However, INT3.2 is only 'symmetric' if the energy randomization is complete. These open questions should be answered soon using the following strategy. First, a reaction of atomic carbon with C_2HD has to be performed at collision energies lower than 5.8 kJ mol^{-1}. Two mass-to-charge ratios are expected, i.e., m/e = 38 (C_3D) and m/e = 37 (C_3H). Since the formation of c-C_3H is endoergic by 5.8 kJ mol^{-1}, the center-of-mass angular distributions of m/e = 38 and 37 are expected to differ strongly. This experiment can resolve further to what extent the isotropic

angular distribution to form l-C_3H is the result of a long-lived triplet propargylene or a 'symmetric' intermediate (recall since the formation of d_1-propargylene HCCCD is expected, the latter has no C_2 symmetry; this might have a profound effect on the angular distribution). Second, the linear and cyclic C_3H isomers could be photoionized selectively via tunable VUV light of a synchrotron. Lastly, performing the experiment with ^{13}C and investigating the fragmentation patterns of the C_3H isomers might unravel if $H^{13}CCCH$ or $HC^{13}CCH$ is the decomposing intermediate; this could give three distinct l-C_3H isotopomers: $H^{13}CCC$, $HC^{13}CC$, and $HCC^{13}C$.

The involved potential energy surfaces and chemical dynamics of the $C(^3P_j)$ reactions with methyl- and dimethylacetylene show strong similarities but also striking differences to the acetylene reaction. First, both reactions are governed by indirect scattering dynamics via the formation of strongly bound intermediates. $C(^3P_j)$ attacks the carbon−carbon triple bond without entrance barrier to either one or both carbon atoms (Figure 13 and Table 6). These pathways yield (substituted) propenediylidene and/or (substituted) cyclopropenylidene intermediates, which are stabilized by 132−137 and 221−225 kJ mol^{-1} with respect to the reactants (Table 6). The propenediylidene intermediate can undergo a hydrogen shift to form a methylpropargyl isomer via a low barrier of only 0.8 kJ mol^{-1}. This pathway is similar to the acetylene reaction, which involves a propargylene intermediate. Further, the substituted cyclopropenylidene isomers ring opens to substituted propargylene radicals via barriers of 61−65 kJ mol^{-1}. The latter reside in deep potential energy wells of 374 kJ mol^{-1} and decompose via H atom loss through tight transition states located 18−24 kJ mol^{-1} above the products; this order of magnitude has been verified by the crossed beam studies as the center-of-mass translational energy distributions show pronounced maxima at 20−60 kJ mol^{-1}. The reactions to form n-$C_4H_3(X^2A')$ and 1-methylbutatrienyl (X^2A') radicals are strongly exoergic by 190 and 177 kJ mol^{-1}, respectively (Figure 14). Note that at lower collision energies, a second, thermodynamically less stable c-C_4H_3 isomer might be formed in the $C(^3P_j)/CH_3CCH$ system. Compared to the acetylene reaction, no direct pathway was found.

The $C(^3P_j)/C_3H_3(X^2B_1)$ system presents the only atom−radical reaction which has been investigated comprehensively in crossed beam experiments so far. Similar to the previous systems, the dynamics are indirect and governed by an initial addition of $C(^3P_j)$ to the π-electron density at the acetylenic carbon atom of the propargyl radical, followed by a [1,2]-hydrogen migration to form a bound n-C_4H_3 intermediate. A final carbon−hydrogen bond rupture yields atomic hydrogen and diacetylene through a tight exit transition state located 30 kJ mol^{-1} above the products. To a minor amount, the carbon atom adds to two carbon atoms, forming a cyclopropenylidene derivative followed by ring opening to n-C_4H_3. The H atom loss to synthesize diacetylene is the dominating exit channel (Figure 14). Theory predicts that two minor pathways of less than a few percent might form the butatrienylidene isomer (C_4H) plus molecular hydrogen and acetylene plus ethinyl.

These investigations showed that the reactions of carbon atoms with alkynes can synthesize extremely reactive hydrocarbon radicals in distinct interstellar environments. Most important, these studies can (1) reproduce the relative ratios of the cyclic versus the linear C_3H isomers in warmer circumstellar envelopes of IRC+10216 and toward cold, dense clouds and (2) predict the formation of hitherto unobserved interstellar radicals, in particular the n-C_4H_3 species. Finally, the atom−radical reaction of carbon with propargyl presents an alternative route to form diacetylene in circumstellar envelopes; previous networks suggested a sole production path via ethinyl radicals reacting with acetylene (sections II.C and IV.C.4)

1.2. Reactions with Alkenes. The reactions of ground-state atomic carbon $C(^3P_j)$ with four olefines, ethylene (C_2H_4), propylene (C_3H_6), 1,3-butadiene (C_4H_6), and the vinyl radical (C_2H_3) were investigated in crossed beam experiments at collision energies between 17.1 and 45.0 kJ mol^{-1} and computationally to explore the formation of (substituted) propargyl radicals and C_3H_2 isomers in the interstellar medium. Propargyl itself is currently considered as the key radical involved in the formation of benzene and possibly PAHs (sections II.A and II.D). However, substituted propargyl derivatives have been contemplated only very recently as potential precursors to form substituted benzene and cyclopentadienyl as well as seven-membered ring structures.[566]

All reactions of closed-shell olefines proceed on the triplet surface via indirect scattering dynamics and are initiated by a barrierless addition of the carbon atom to the π-bond forming three-membered ring adducts cyclopropylidene, methylcyclopropylidene, and vinylcyclopropylidene (INT1) (Figure 17). These structures are stabilized by 213-218 kJ mol^{-1} with respect to the reactants and ring-open via barriers of 52−65 kJ mol^{-1} to allene, methylallene, and vinylallene (INT2) (Table 7). Competing hydrogen shifts to (substituted) cyclopropene intermediates (INT3) are unfavorable as these processes involve significant barriers of 200−210 kJ mol^{-1}. All allene derivatives reside in deep potential energy wells of 342−360 kJ mol^{-1} and decompose predominantly via tight exit transition states located 18−23 kJ mol^{-1} above the separated products by atomic hydrogen loss. The experimental data support the existence of exit barriers as the center-of-mass translation energy distributions peak at 28−60 kJ mol^{-1}. This leads to propargyl (C_3H_3 (X^2B_1); C_2H_4 system), three C_4H_5 isomers 1,3-butadienyl-2 (H_2CHCCH_2 (X^2A')), 1-methylpropargyl ((CH_3)HCCCH(X^2A'')), and 3-methylpropargyl ((CH_3)$CCCH_2$ (X^2A'')) in a ratio of about 3.7:2.8:1 (C_3H_6 system) and 1- and 3-vinylpropargyl (HCCCH(C_2H_3)(X^2A'') and $H_2CCC(C_2H_3)(X^2A'')$ (8:1; C_4H_6 system) in strongly exoergic reactions (190−210 kJ mol^{-1}) (Figure 18). Besides these common characteristics, the calculations predict further that the triplet methylallene and vinylallene intermediates decompose via homolytic cleavage of a carbon−carbon

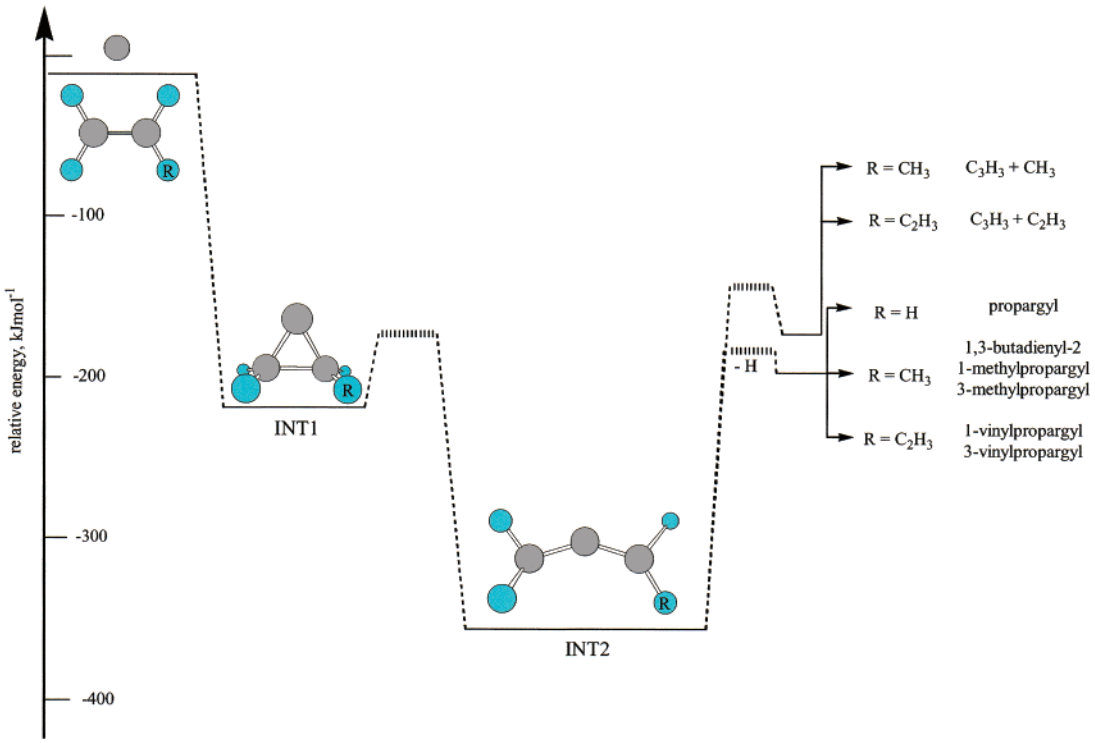

Figure 17. Common features of triplet potential energy surfaces of the reaction of ground-state atomic carbon with ethylene, propylene, and 1,2-butadiene. R denotes H, CH_3, or C_2H_3 of the olefine reactants. Carbon atoms are denoted in gray and hydrogen atoms in light blue.[538−541]

Table 7. Relative Energies of Intermediates Involved in the Reaction of Ground-State Carbon Atoms with Ethylene, Propylene, and 1,3-butadiene; TS Denotes a Transition State of an Isomerization of Two Intermediates[a]

	C_2H_4; R = H	$C_2H_3CH_3$; R = CH_3	$C_2H_3C_2H_3$; R = C_2H_3
INT1	217	218	213
INT2	343	342−344	360
TS INT1 → INT2	56	54−65	52
TS INT1 → INT3	210	203	200
exit transition state H loss	19	18−23	18−21

[a] All data are given in kJ mol^{-1}.

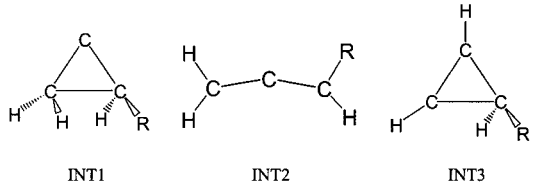

single bond to $CH_3 + C_3H_3$ (16%) and $C_2H_3 + C_3H_3$ (10%) via transition states lying 25−42 kJ mol^{-1} above the separated fragments (Figure 17). Note that the latter pathways are unobservable employing 'universal' detectors due to the significant background signal at the masses of interest from the parent molecules.

The reaction of atomic carbon with ethylene as the prototype of all olefines shows two peculiarities. First, a minor fraction of triplet allene intermediates of about 7% was found to undergo a hydrogen shift followed by fragmentation of the vinylmethylene complex (H_2CCHCH). The latter decomposed either to atomic hydrogen plus the propargyl radical or to acetylene (C_2H_2) plus triplet carbene (CH_2) (2%). The latter pathway has been confirmed indirectly in room-temperature kinetic experiments.[497] The authors demonstrated that—compared to the monitor reaction with hydrogen sulfide—the yield of atomic hydrogen was slightly less than unity. This may suggest the presence of a second, minor reaction pathway, such as the formation of acetylene and triplet carbene. Second, the reaction with ethylene shows a third pathway to form propargyl radicals via direct scattering dynamics. All these findings together reveal explicitly the complementary information provided by kinetic, dynamic, and theoretical studies of astrochemically important bimolecular reactions to form hydrocarbon radicals in the interstellar medium.

Due to the limited signal-to-noise ratio, only restricted experimental data on the atom−radical reaction of $C(^3P_j)$ plus $C_2H_3(X^2A')$ are available. Reaction products and the likely mechanisms involved are inferred predominantly from theoretical investigations. As expected, the atom−radical reaction has no entrance barrier and forms a cyclic intermediate (−468 kJ mol^{-1}) which undergoes ring opening via a barrier of 40 kJ mol^{-1} to the thermodynamically more stable propargyl radical (−636 kJ mol^{-1}). A competing hydrogen migration to the cyclopropenyl radical is unlikely as a large barrier of 212 kJ mol^{-1} inhibits this pathway. Both intermediates isomerize via transition states located well below the energy of the separated reactants to various C_3H_3 structures. The latter are predicted to decompose predominantly via H atom loss to propargylene ($HCCCH(X^3B)$; 70−77%), cyclopropenylidene (c-C_3H_2 (X^1A_1); 13−18%), vinylidenecarbene ($H_2CCC(X^1A_1)$; 4−7%) (Figure 18) and—to a minor amount—via molecular hydrogen loss

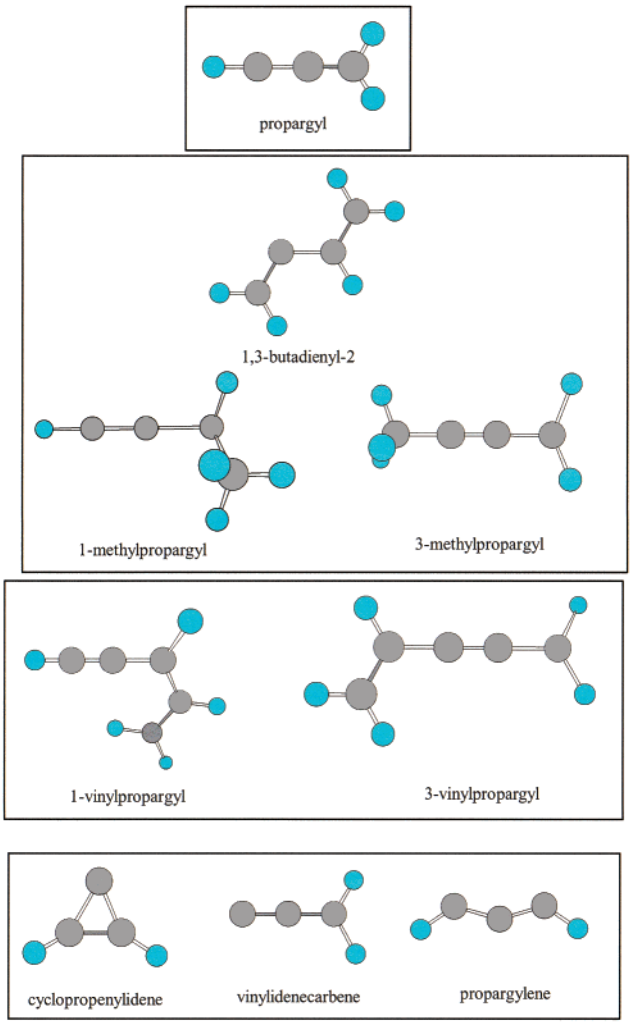

Figure 18. Hydrocarbon radicals produced via a carbon versus hydrogen exchange pathway in the reactions of atomic carbon with ethylene, propylene, 1,3-butadiene, and the vinyl radical. Carbon atoms are denoted in gray and hydrogen atoms in light blue.

to the l-C_3H isomer. Therefore, single-collision conditions of carbon atoms with vinyl radicals could form three distinct C_3H_2 isomers in the interstellar medium. Surprisingly, the dominating reaction product propargylene has not yet been observed in extraterrestrial environments (Table 1) and should be sought for.

1.3. Reactions with Allenes. The crossed molecular beams technique augmented by electronic structure and statistical calculations was employed to investigate the reaction between ground-state carbon atoms, $C(^3P_j)$, with allene (H_2CCCH_2) and 1,2-butadiene (methylallene; C_4H_6). At lower collision energies, the reaction dynamics were found to be indirect via long-lived intermediates. The carbon atom attacks—similar to the olefines—the π-system barrierless, forming cyclopropylidene-like intermediates INT1 which reside in potential energy wells of 265−281 kJ mol^{-1} (Figure 19; Table 8). Note that the double bonds in 1,2-butadiene are not equivalent; dominated by large impact parameters, $C(^3P_j)$ preferentially attacks the terminal double bond to form INT1 (top; mechanism 1); to a minor amount, small impact parameters lead to an addition of atomic carbon to form INT1 (bottom; mechanism 2). Rather than undergoing hydrogen shifts via large barriers of about 200 kJ mol^{-1}, the intermediates show an opening of the ring over barriers of only 39−58 kJ mol^{-1} yielding (substituted) triplet butatriene species INT2. These are bound 405−430 kJ mol^{-1} with respect to the reactants and decay by atomic hydrogen emission through exit transition states lying 9−24 kJ mol^{-1} above the products. Here, the reaction with allene leads to the *n*-C_4H_3 isomer. In the case of 1,2-butadiene, the situation is more complex. Although both intermediates INT1 (Figure 19; top and bottom) ring open, the triplet methylbutatriene complexes INT2 were not found to be equivalent (Table 8). The carbon atom is located at the C2 or the C3 position. INT2 with the carbon atom formally inserted at C2 is suggested to decay nonstatistically prior to a complete energy randomization via atomic hydrogen loss forming 1- and 4-methylbutatrienyl CH_3CCCCH_2 (X^2A'') and $HCCCCH(CH_3)$(X^2A'') radicals (Figure 20). The energy randomization in INT2 with the 'inserted' carbon at the C3 position is likely to be complete. This isomer decomposes via H atom loss to form predominantly 3-vinylpropargyl, $H_2CCCC_2H_3$ (X^2A'').

Recent crossed beam studies of the $C(^3P_j)/H_2CCCH_2$ system employing rotatable sources with LIF detection of the light hydrogen atom at collision energies from 0.47 to 27.1 kJ mol^{-1} [567] and low-temperature kinetic investigations provided conclusive evidence that this reaction is indeed fast and barrierless. Converting the experimentally derived excitation function, i.e., the dependence of the relative cross section of a reaction on the collision energy, to thermal rate constants yields an excellent agreement of both methods. This is a slight negative temperature dependence of the rate constants as the temperature drops. However, compared to the methylacetylene isomer, recent room-temperature kinetic studies of the allene reaction[497] depicted a slightly higher H atom yield in the latter system. This is likely attributed to the existence of a triplet methylpropargyl intermediate (CH_3CCCH) in the $C(^3P_j)$ + CH_3CCH reaction.[531−533] This intermediate decomposes predominantly via atomic hydrogen loss, but a minor much less exoergic pathway might be a homolytic bond cleavage to form the l-C_3H isomer plus a methyl group.[532] On the basis of the triplet C_4H_4 potential energy surface, this mechanism is not open in the allene system.

1.4. Reactions with Aromatic Molecules. So far, only the reaction of atomic carbon with benzene (C_6H_6;X^1A_{1g}) has been studied under single-collision conditions in crossed beam experiments,[547,548] theoretically,[548,549] and via flow studies at room temperature.[485,497] The dynamics were investigated at collision energies between 8.8 and 52.5 kJ mol^{-1} showing that—similar to the reactions with olefines and allenes—atomic carbon adds barrierless to the π-system to form a weakly stabilized intermediate INT1 (−62 kJ mol^{-1}; Figure 21). The latter ring opens via a small barrier of about only 4 kJ mol^{-1} to a seven-membered ring intermediate INT2 (−294 kJ mol^{-1}) followed by an H atom ejection to give a 1,2-didehy-

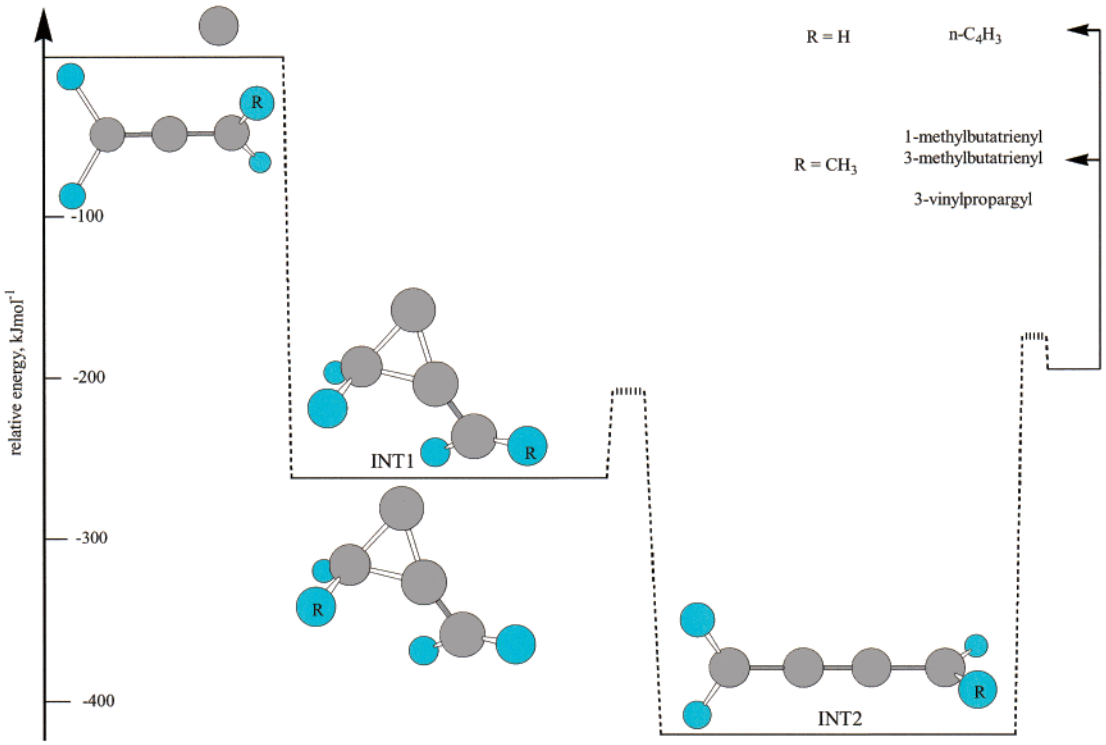

Figure 19. Common features of triplet potential energy surfaces of the reaction of ground-state atomic carbon with allene and 1,2-butadiene (methylallene). R denotes H or CH_3 of the allene reactants. Carbon atoms are denoted in gray and hydrogen atoms in light blue.[545,546]

Table 8. Relative Energies of Intermediates Involved in the Reaction of Ground-State Carbon Atoms with Allene and 1,2-Butadiene (methylallene)[a]

	H_2CCCH_2	$H_2CCCH(CH_3)$
INT1	265 (R1=R2=H)	276−281 (R1 = H; R2 =CH_3) (R1 = CH_3; R2 = H)
INT2	405 (R1=R2=H)	430 (R = CH_3)
TS INT1 → INT2	39	41−58
exit transition state H loss	9	20−24

[a] TS denotes a transition state of an isomerization of two intermediates. All data are given in kJ mol^{-1}.

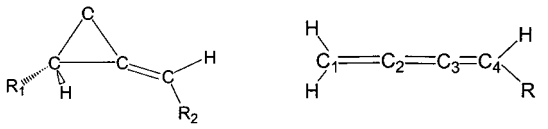

drocycloheptatrienyl radical C_7H_5 (X^2B_1) in an exoergic reaction (15.6± 4.8 kJ mol^{-1}) without exit barrier. At low collision energies the chemical dynamics are solely indirect and dominated by large impact parameters. As the collision energy rises, the smaller impact parameters become more important and the chemical dynamics are increasingly direct. At all collision energies, the reaction proceeds on the triplet surface. In case of reactions with perdeuterobenzene, the formation of a C_7D_6 adduct which has a lifetime of a few hundred microseconds is observed as a second channel; a significant background prevents the assignment of the adduct in the $C(^3P_j)/C_6H_6$ system. Statistical calculations suggest that the formation of the thermodynamically favored bicyclic

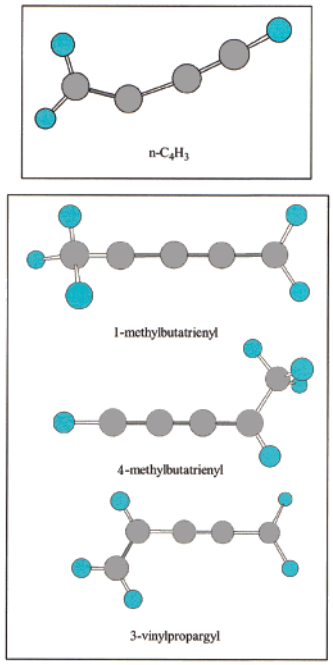

Figure 20. Hydrocarbon radicals produced via a carbon versus hydrogen exchange pathway in the reactions of atomic carbon with allene and 1,2-butadiene. Carbon atoms are denoted in gray and hydrogen atoms in light blue.

C_7H_5 radical benzocyclopropenyl (X^2B_1) might be a minor byproduct.

These studies demonstrated explicitly that the reaction of atomic carbon with benzene proceeds without an entrance barrier and is exoergic. Since all transition states involved are well below the energy of the separated reactants, this reaction may be of fundamental importance in the destruction of

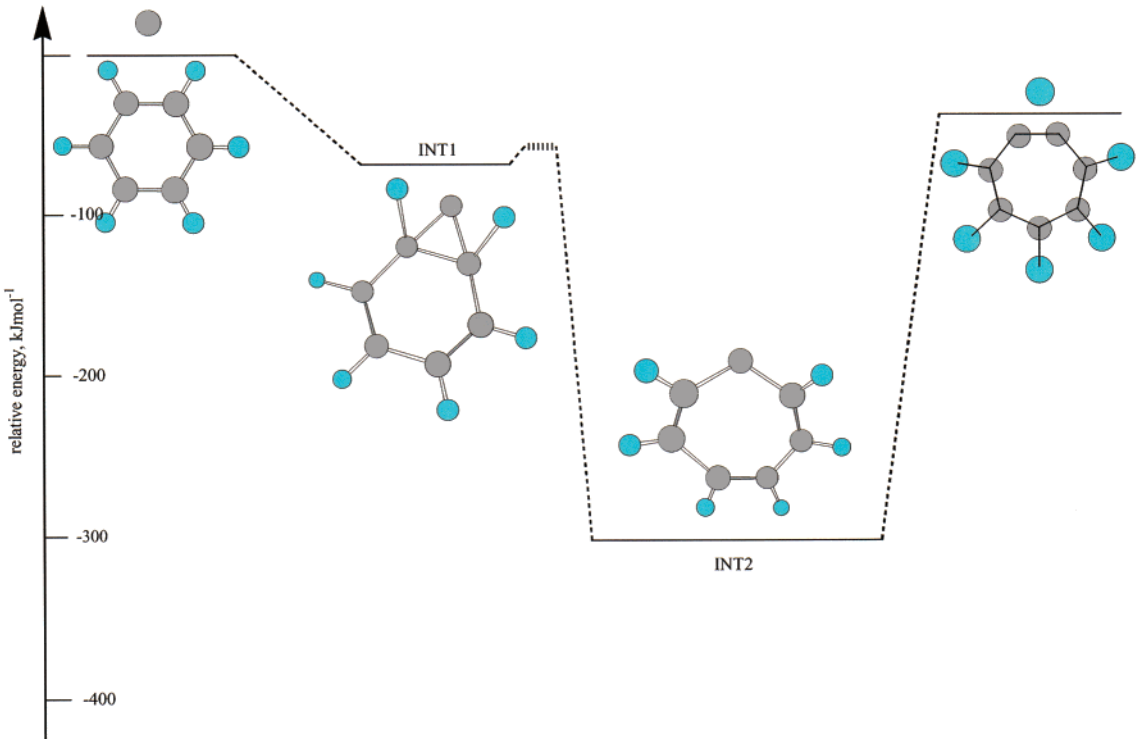

Figure 21. Simplified triplet potential energy surface of the reaction of ground-state atomic carbon with benzene. Carbon atoms are denoted in gray and hydrogen atoms in light blue.[548,549]

benzene even in the low-temperature environments of dense molecular clouds and especially in planetary nebulae where benzene was detected (Table 1). Recent kinetic investigations of this reaction support—at least at room temperature—that this reaction is very fast within gas kinetics limits. Hence, even in these coldest molecular clouds, the six-membered benzene ring might be enlarged by reaction with carbon atoms. In contrast, benzene is resistant toward attack by atomic oxygen as entrance barriers of 16.6−20.5 kJ mol^{-1} inhibit this reaction in low-temperature environments. Likewise, the reaction with ground-state atomic nitrogen, N($^4S_{3/2}$), also is expected to have an entrance barrier and cannot happen in cold molecular clouds. This underlines the special ability of atomic carbon to be incorporated into aromatic hydrocarbon molecules under expansion of the cyclic structure. However, if we go to denser interstellar environments such as circumstellar envelopes of carbon stars or planetary nebulae close to the central stars, long-lived C_7H_6 intermediates can likely be stabilized via a three-body process. Recent kinetic studies measuring the H atom yield confirmed this scenario indirectly.[497] Here, very low H atom production yields of only 0.16 ± 0.08 have been measured, suggesting that under these bulk conditions three-body processes are very efficient in stabilizing the adducts. As benzene represents the common 'building block' of ubiquitous PAH-like species in the interstellar environments, these findings propose that atomic carbon might react with these molecules as well. The situation can be more diverse, since more complex PAHs not only contain benzenoid units but also possess ethylene-like (C═C) and butadiene-like (C═C−C═C) moieties as in phenanthrene and anthracene. However, the more complicated astrochemically relevant systems are, the more difficult experimental investigations become. Therefore, it is necessary to understand simple, prototype systems, e.g., the reaction of carbon atoms with benzene, to develop versatile concepts first before attempting to unravel the chemical reactivity of more complicated molecules.

1.5. Reactions with Sulfur-Bearing Molecules. Investigating the formation of sulfur-bearing molecules in the interstellar medium is an important means to understand the history and chemical evolution of star-forming regions, dense clouds, circumstellar envelopes of carbon stars, and planetary nebulae. Compared to the cosmic carbon versus sulfur abundances of 15:1, sulfur is severely depleted, and only nine sulfur-bearing molecules have been observed so far (Table 1). The CS species and the sulfur-terminated cummulene carbenes C_2S and C_3S are of particular astrochemical interest. Although these molecules are ubiquitous in cold molecular clouds such as OMC-1 and TMC-1,[568−570] in circumstellar envelopes of the protostellar object B335[571] and carbon star IRC +10216,[572] their hydrogen-terminated species HC_nS and C_nSH have not been searched for. Therefore, these species might represent important organosulfur tracer molecules and possibly the missing source of molecular-bound sulfur in the interstellar medium.

The reaction between ground-state carbon atoms, C(^3P_j), and hydrogen sulfide (H_2S) was carried out under single-collision conditions using the crossed molecular beams technique and combining the data with electronic structure calculations.[550−552] The reaction dynamics are indirect, proceeding via a barrierless[498] addition of the carbon atom to the sulfur atom to form a weakly bound (58−64 kJ mol^{-1}) triplet CSH_2 intermediate INT1 (Figure 22). A hydrogen atom migration via a small barrier of 34 kJ mol^{-1}

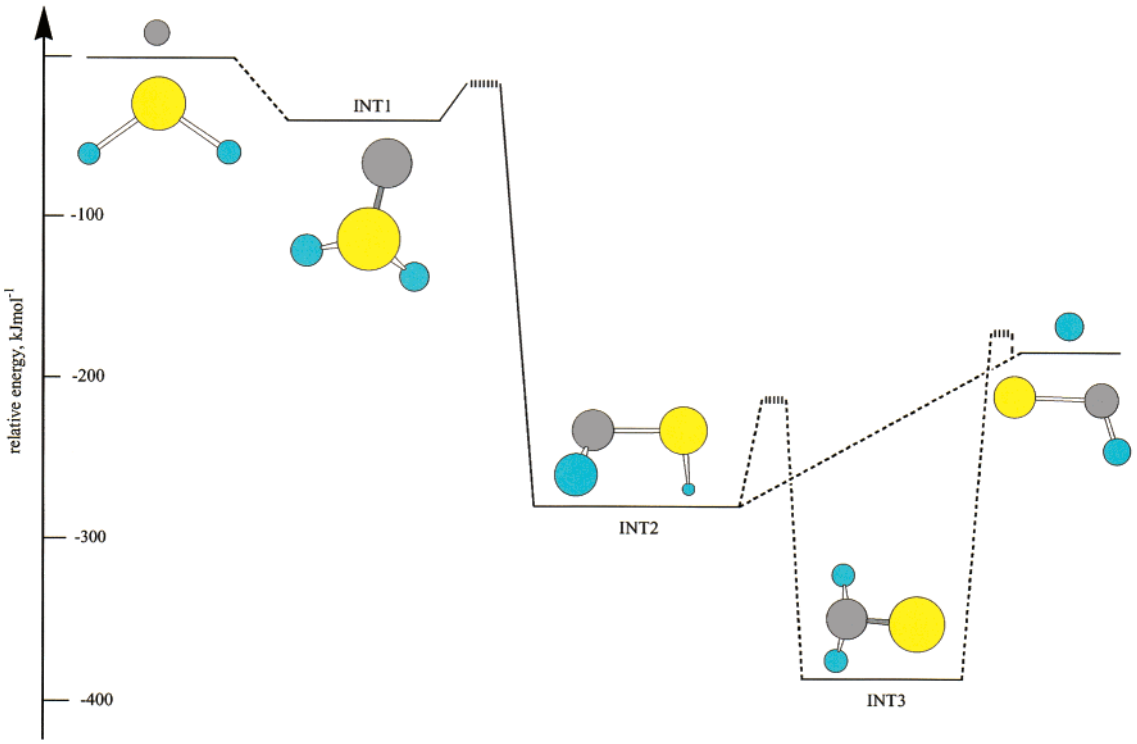

Figure 22. Simplified triplet potential energy surface of the reaction of ground-state atomic carbon with hydrogen sulfide. Carbon atoms are denoted in gray, hydrogen atoms in light blue, and sulfur atoms in yellow.[498,551]

forms a thiohydroxycarbene intermediate INT2 (HCSH) on the triplet surface. The latter is stabilized by 285−290 kJ mol^{-1} and can lose a H atom barrierless to form the thermodynamically most stable thioformyl isomer HCS (X^2A') in an exoergic reaction (169−184 kJ mol^{-1}). The authors pointed out that at lower collision energies a H shift in HCSH might yield triplet thioformaldehyde INT3 (−378−383 kJ mol^{-1}); the latter was found to fragment via a barrier of 11 kJ mol^{-1} to HCS(X^2A') plus H($^2S_{1/2}$). Recent statistical calculations suggest that two channels via triplet thiohydroxycarbene (≈80%) and triplet thioformaldehyde (≈20%) should give the HCS isomer. Further, upper limits of 10% of the thermodynamically less stable HSC(X^2A') isomer were derived under single-collision conditions; recent statistical calculations predict only minor fractions of less than 0.6%.[498] The formation of HSC(X^2A') might follow direct scattering dynamics via short-lived triplet H_2-SC intermediates which cannot be treated accurately using statistical calculations. This remains to be investigated further. In summary, these studies verify that binary collisions of atomic carbon with hydrogen sulfide are barrierless and hence rapid within the order of gas kinetics limits and are strongly suggested to form the hitherto unobserved HCS(X^2A') radical in the interstellar medium.

1.6. General Trends and Reactivity of Carbon Atoms. The crossed beam investigations provided impressive evidence that all reactions of ground-state carbon atoms with unsaturated hydrocarbons are initiated by an addition of the carbon atom to the unsaturated bonds. These hydrocarbon systems often show multiple reaction pathways via the formation of strongly bound intermediates (indirect scattering dynamics) and—in the case of acetylene, ethylene, 1,2-butadiene, and benzene—direct reaction dynamics as well. With the exception of the C(^3P_j) + C_2H_2 reaction, no indication of intersystem crossing from the triplet to singlet manifold is apparent. It was shown that upon reaction with olefines, allenes, and benzene, C(^3P_j) forms solely three-membered ring intermediates. The latter ring open but do not isomerize via hydrogen migration since the involved barriers are rather high (≈200 kJ mol^{-1}) compared to ring-opening processes of 58 kJ mol^{-1} at most. This finding is in strong contrast to the alkyne systems. Here, at least two addition pathways to either one or two acetylenic carbon atoms are feasible yielding (substituted) propenediylidene and cyclopropenylidene structures, respectively. With the exception of the dimethylacetylene reactant, the substituted propenediylidenes isomerize via a facile hydrogen shift via barriers of not more than 11 kJ mol^{-1} to substituted propargyl intermediates; the ring opening of all cyclopropenylidene structures was found to be a common pathway in all alkyne reactions investigated. Since all transition states involved lie well below the energy of the reactant molecules, the formation of these hydrocarbon radicals is exoergic, and the rate constants are fast, these reactions present compelling candidates to form complex, carbon-bearing molecules over a broad temperature range from 10 K as prevailing in dense clouds up to high-temperature settings in hot molecular cores, circumstellar envelopes, and planetary nebulae.

All intermediates decomposed mainly via atomic hydrogen elimination barrierless (C_6H_6 and C_2H_2 systems) or via transition states located up to 24 kJ mol^{-1} above the products. The reactions with ethylene, propylene, 1,3-butadiene, and possible methylacetylene also depicted—to a minor extent—carbon−

carbon bond ruptures. The versatile concept of an atomic carbon versus hydrogen atom exchange yielded 16 hydrocarbon species, among them astronomically detected l- and c-C_3H and C_3H_2 isomers. Two 'families' of synthesized radicals can formally be derived from the *n*-C_4H_3 radical (1- and 4-methylbutatrienyl) and from the propargyl radical (1- and 3-methylpropargyl; 1- and 3-vinylpropargyl). This demonstrates the unique power of experiments performed under single-collision conditions to discriminate between distinct structural isomers via the dynamics and isotopic substitution studies. Lastly, four C_5H_5 isomers were assigned unambiguously. Together with (substituted) propargyl radicals, these species are strongly expected to play a crucial role in the formation of aromatic molecules in carbon-rich circumstellar envelopes and planetary nebulae.

2. Reactions of $C_2(X^1\Sigma_g^+/a^3\Pi_u)$ and $C_3(X^1\Sigma_g^+)$

Crossed beam experiments of dicarbon and tricarbon molecules with unsaturated hydrocarbons acetylene (C_2H_2), methylacetylene (CH_3CCH), and ethylene (C_2H_4) were conducted at collision energies between 8 and 170 kJ mol^{-1} and augmented by electronic structure calculations.[565,573,588] These investigations explore synthetic routes and detailed mechanisms to hydrogen-deficient carbon clusters HC_n ($n = 0-8$) and H_2C_n ($n = 3,4,6$) in extraterrestrial environments—molecules which present a crucial link between naked carbon clusters, polycyclic aromatic hydrocarbons, and carbon-rich grain material. The reactions with acetylene and ethylene are prototype encounters of small carbon molecules with the simplest alkyne and alkene, respectively, and thus could unravel basic mechanisms of reactions with the higher members of the same series. The collisions with methylacetylene were chosen to follow the influence of a hydrogen substitutions with a methyl group on the dynamics. Since the data analysis is still in progress, only preliminary findings are reported here.

2.1. Reactions with Alkynes and Alkenes. The data suggest that all reactions with C_2H_2, C_2H_4, and CH_3CCH are governed by an initial addition of the carbon cluster to the π-molecular orbitals forming highly unsaturated cyclic structures. These intermediates are connected via various transition states, ring open to chain isomers, and decompose via atomic hydrogen emission forming CCCCH (C_2/C_2H_2), HCCCCH$_2$ (C_2/C_2H_4), and $H_2CCCCCH$ (C_2/CH_3CCH), Figure 23. Possible pathways to form the cummulene carbene CCCCH$_2$ and CCCCCH$_2$ from reaction of dicarbon and tricarbon with ethylene, respectively, via H_2 elimination are currently under investigation. The collisions of dicarbon on the singlet surface proceed without entrance barrier and are found to be exoergic. This supports recent kinetic studies at elevated temperatures proposing that the reactions are very fast within gas kinetic limits (10^{-10} cm^3 s^{-1}).[574,575] Note that the reaction of $C_2(a^3\Pi_u)$ with ethylene was found to proceed via a triplet cyclobutyne intermediate[576]—a ring-strained structure which has not been identified in previous studies. In strong contrast, the tricarbon versus atomic hydrogen replacement yielding CCCCCH (C_3/C_2H_2), $H_2CCCCCH$ (C_3/C_2H_4), and $H_2CCCCCCH$ (C_3/CH_3CCH) open up only if the collision energies are higher than 80 ± 9, 56 ± 4, and 45 ± 5 kJ mol^{-1}, respectively. Therefore, these reactions must have either (1) an entrance barrier, (2) an endoergic energy balance, or (3) both. Previous kinetic studies of $C_3(X^1\Sigma_g^+)$ verify this finding. Compared to the dicarbon molecule, rate constants of tricarbon with several alkenes and alkynes were found to be much smaller and seldom reached the 10^{-12} cm^3 s^{-1} range at room temperature.[577-579]

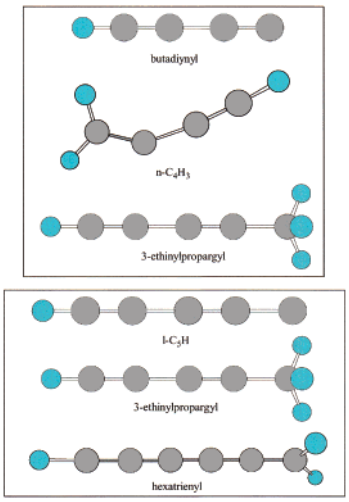

Figure 23. Structures of hydrogen-deficient carbon clusters as identified in the reactions of dicarbon and tricarbon with acetylene, ethylene, and methylacetylene. Carbon atoms are denoted in gray and hydrogen atoms in light blue.

These findings have strong implications to the chemistry in the interstellar medium. Since the data suggest that reactions of $C_2(X^1\Sigma_g^+)$ with unsaturated hydrocarbons acetylene, ethylene, and methylacetylene most likely have no entrance barrier and are exoergic, they may form hydrogen-deficient carbon clusters even in the coldest environments such as dense clouds (10 K). Therefore, the linear C_4H radical as detected in these environments and in circumstellar shells of carbon stars is likely to be synthesized via the reaction of dicarbon with acetylene. Most importantly, these studies can anticipate the formation and existence of two hitherto not identified molecules in the interstellar medium: HCCCCH$_2$ and $H_2CCCCCH$. Here, the *n*-C_4H_3 isomer, which can be also formed from the reaction of atomic carbon with allene and methylacetylene, deserves particular attention. Its ground state is bent, whereas the linear butatrienyl structure represents a transition state between two bent structures, located only 255 cm^{-1} above the *n*-C_4H_3. Since the coldest molecular clouds have averaged translational temperatures of about 10 K—about 7 cm^{-1}—*n*-C_4H_3 must be bent. In hotter interstellar environments such as molecular cores and circumstellar envelopes, internally excited C_4H_3 radicals could overcome the barrier and hence should be quasi-linear. Therefore, the microwave spectrum of the *n*-C_4H_3 radical depends strongly on the temperature of the interstellar environments. Vice versa, recording these microwave spectra could serve as a probe of the temperature in the interstellar medium.

However, since the reactions of tricarbon with unsaturated hydrocarbons involve significant thresholds, these processes are feasible only at elevated temperatures such as in outflow of carbon-rich stars or planetary nebulae. Here, the reaction of C_3 with C_2H_2 is an excellent candidate to form observed l-C_5H and possibly hitherto not detected $H_2CCCCCH$ and $H_2CCCCCCH$ isomers. These findings should encourage a search for those unidentified radicals in the circumstellar envelope of IRC+10216. These data on the C_2/C_3 reactions with acetylene suggest further that the alternating C_nH and C_mH (n = even, m = odd) abundances in distinct interstellar environments might be a result of different chemical reactivities of odd versus even carbon clusters.

2.2. Reaction with Sulfur-Bearing Molecules. The reaction of $C_2(X^1\Sigma_g^+)$ with hydrogen sulfide (H_2S) was performed at a collision energy of 46.0 kJ mol^{-1}, and preliminary results are reviewed here.[580] The dicarbon molecule adds barrierless to the sulfur atom forming a $CCSH_2$ complex. Various reaction pathways were identified. The first pathway involves indirect dynamics via strongly bound $CCSH_2$ complexes which undergo two successive hydrogen migrations on the singlet potential energy surface to give a thiohydroxyacetylene intermediate (HSCCH). The latter is stabilized by 466 kJ mol^{-1} with respect to the reactants and loses a hydrogen atom to produce the thioketenyl radical HCCS ($X^2\Pi_\Omega$). To a minor amount, HSCCH isomerizes to the thiohydroxyketene structure (H_2CCS) which in turn decomposes to HCCS ($X^2\Pi_\Omega$) plus H. All barriers involved lie clearly below the energy of the separated reactants; together with the exoergic reaction channels, this makes the reaction of dicarbon with hydrogen sulfide an important pathway to form the HCCS isomer in the interstellar medium. Lastly, the TOF spectra of the atomic and molecular hydrogen loss differ, and a fit of the latter suggests the formation of a C_2S molecule via H_2 loss. The assignment of the electronic state and structure (linear versus cyclic) is currently under investigation.

3. Reactions of CN($X^2\Sigma^+$)

Crossed beam experiments of cyano $CN(X^2\Sigma^+)$ radicals with unsaturated hydrocarbons acetylene (C_2H_2),[581,582] methylacetylene (CH_3CCH),[583,584] dimethylacetylene (CH_3CCCH_3), ethylene (C_2H_4),[585] allene (H_2CCCH_2),[583,586] and benzene (C_6H_6)[587] were performed at collision energies between 13.4 and 36.7 kJ mol^{-1} and combined with electronic structure calculations to investigate synthetic routes to form nitriles in the interstellar medium[588,589] and in hydrocarbon-rich atmospheres of planets and their moons.[590−594] The reactions with acetylene and ethylene are prototype encounters of the cyano radicals with the simplest alkyne and alkene, respectively, and thus are expected to reveal key concepts for reactions with the higher members of the same series. The reactions with methylacetylene and dimethylacetylene were selected to observe the effect of H-substitutions with one and two methyl groups on the dynamics. Binary collisions with allene, when compared to the reaction with its methylacetylene isomer, expose how distinct isomers react. Finally, the reaction with benzene is the prototype for the series of reactions of radicals with aromatic hydrocarbons.

3.1. Reactions with Alkynes. The reaction dynamics of cyano radicals with acetylene, methylacetylene, and dimethylacetylene were found to be indirect and dictated by the formation of bound intermediates (Figures 24 and 25; Table 9). The cyano

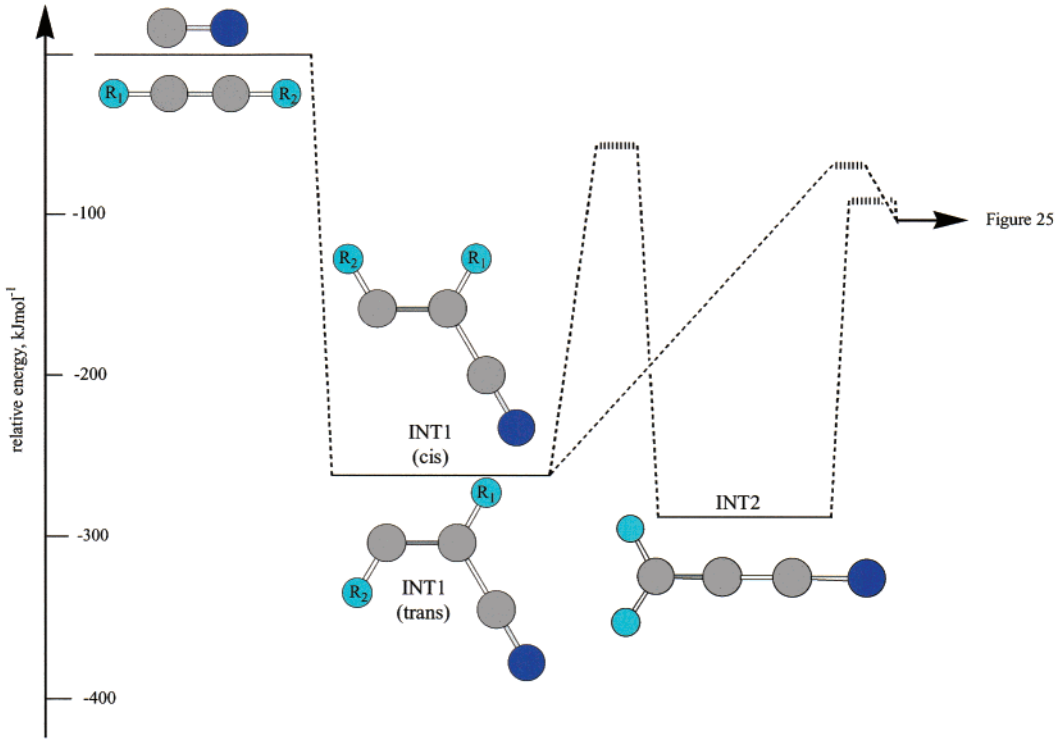

Figure 24. Common features of doublet potential energy surfaces of the reaction of ground-state cyano radicals with acetylene, methylacetylene, and dimethylacetylene. For each system, R_1 and R_2 are defined in Table 9. Carbon atoms are denoted in gray, hydrogen atoms in light blue, and nitrogen atoms in deep blue.[581−584]

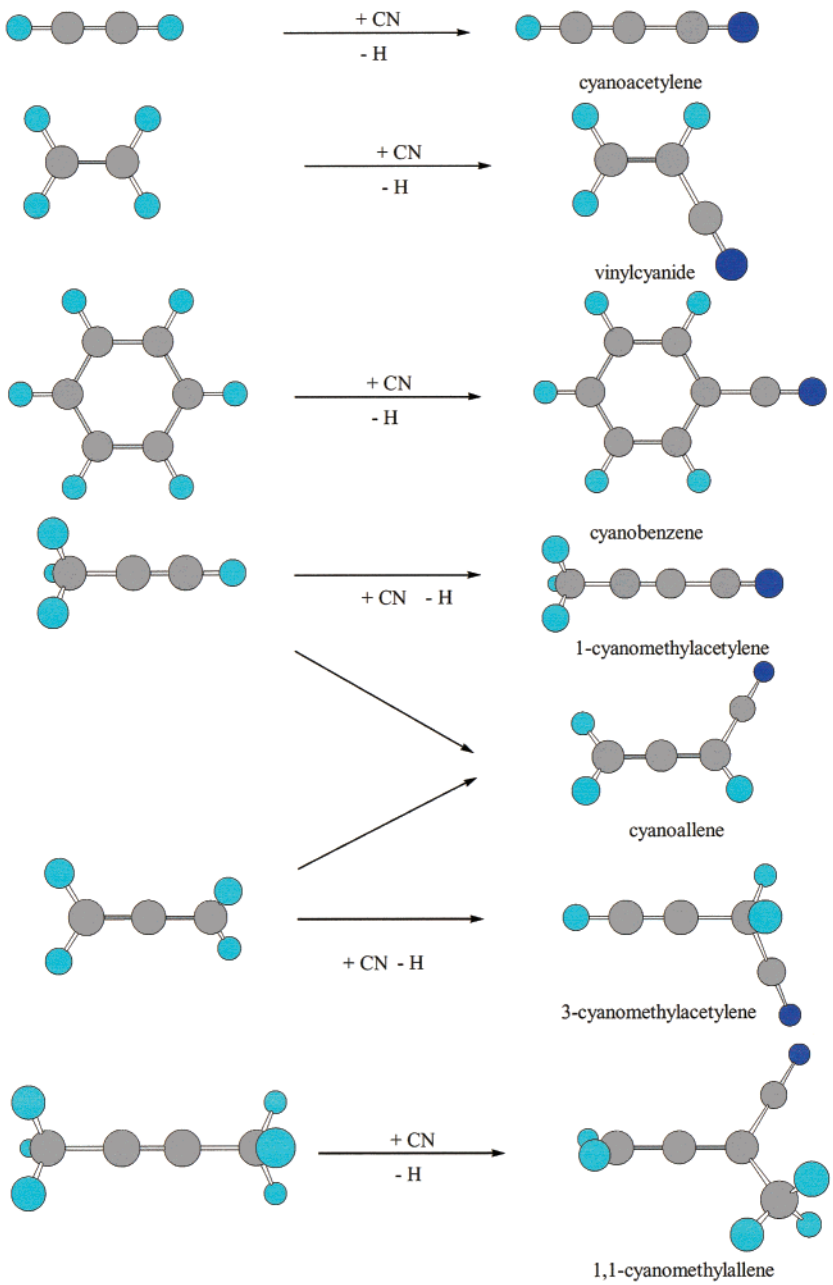

Figure 25. Nitrile products formed via the cyano- versus atomic hydrogen-exchange pathway in the reactions of cyano radicals with acetylene, ethylene, benzene, methylacetylene, allene, and dimethylacetylene. Carbon atoms are denoted in gray, hydrogen atoms in light blue, and nitrogen atoms in deep blue.

radical adds to the carbon−carbon triple bond without an entrance barrier and forms cis and trans intermediates INT1. These doublet radicals are stabilized in deep potential energy wells of 236−253 kJ mol^{-1} with respect to the separated reactants. Due to the low barrier of interconversion between the cis and trans structures of only 14−19 kJ mol^{-1}, the equilibrium concentration of both isomers is expected to be unity. Note that in the case of methylacetylene, the steric hindrance of the methyl group, the enhanced electron density of the acetylenic carbon atom, and large impact parameters likely favor an addition to the terminal acetylenic carbon atom. However, even if the cyano radical adds—to a minor amount—to the carbon atom holding the methyl group, the intermediates formed are connected via energetically accessible three- and four-membered ring isomers to INT1 and hence isomerize. Previous computational investigations of the CN/C_2H_2 system considered solely the reaction via addition and H atom elimination without considering the role of cyclic intermediates.[595−597] However, an addition of the cyano radical with the nitrogen atom to the triple bond cannot be dismissed a priori. These pathways involve no entrance barriers and yield doublet isocyano radical intermediates. Although the H atom loss to form isocyanides is closed (see below), these isocyano radical intermediates can isomerize via transition states below the separated reactants to the corresponding cyano radical structures INT1.[582] Therefore, both addition pathways involving the carbon or nitrogen atom of the cyano radical will lead to the INT1 intermediate. The latter can undergo C−H bond cleavages leading to cyanoacetylene (HCCCN),

Table 9. Relative Energies of Intermediates Involved in the Reaction of Ground-State Cyano Radicals with Acetylene, Methylacetylene, and Dimethylacetylene[a]

	C_2H_2; R1 = R2 = H	CH_3CCH; R1 = H; R2 = CH_3	CH_3CCCH_3; R1 = R2 = CH_3
INT1	242	252−253	236
INT2	288	275	n/a
TS INT1 → INT2	177	187	n/a
exit transition state H loss from INT1	22	8−19	6−8
exit transition state H loss from INT2	7	13	n/a

[a] All data are given in kJ mol^{-1}. TS denotes a transition state of an isomerization of two intermediates.

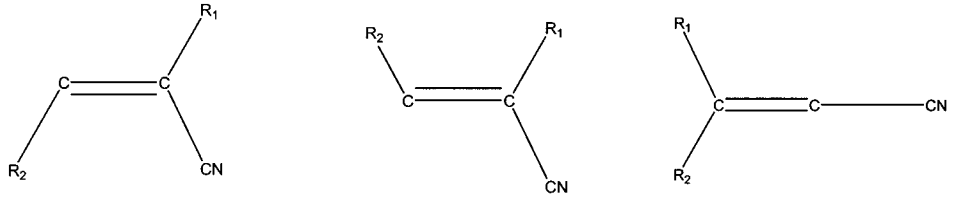

INT1(trans) INT1(cis) INT2

1-cyanomethylacetylene (CH_3CCCN) and cyanoallene (CH_2CCH CN), and 1,1-cyanomethylallene (CH_2-$CCCN(CH_3)$) via exit transition states located 6−22 kJ mol^{-1} above the products. In the case of the reaction with acetylene and methylacetylene, small fractions of INT1 of about 10−15% are found to isomerize via a [1,2]-H atom shift through barriers of 177−187 kJ mol^{-1} to form INT2; these structures are stabilized by 288 and 275 kJ mol^{-1}, respectively. In turn, INT2 decays via H atom emission through exit transition states located only 7 and 13 kJ mol^{-1} above the cyanoacetylene plus hydrogen and the 1-methylcyanoacetylene plus atomic hydrogen.

It is very interesting that the reaction of the cyano radical with methylacetylene synthesizes both the 1-cyanomethylacetylene and cyanoallene isomers in equal amounts almost invariant on the collision energy as evidenced by experiments with deuterated methylacetylene. This strongly indicates that the energy randomization in the decomposing intermediates is likely complete as the energy has to 'flow' over four bonds from the initially formed C−CN connectivity in INT1 to the carbon−hydrogen bond in the methyl group. Further, it is quite interesting to investigate the shape of the center-of-mass angular distributions when substituting one and two H atoms by a CH_3 group. At similar collision energies, the T(θ)s change from slightly forward scattered to symmetric distributions; this strongly indicates a transition from an osculating to a long-lived intermediate. This resembles a general trend, i.e., an increased lifetime of the fragmenting intermediate as the number of atoms and hence oscillators rises. Note that no methyl loss pathway has been identified due to the limited signal-to-noise of the masses of interest and the unfavorable kinematics. On the basis of the potential energy surface of the CN/CH_3CCH system, only INT2 can emit a methyl group. Since the latter is only of minor relevance for the chemical reaction dynamics, the contribution of the methyl loss pathway is expected to be small. However, statistical calculations predict that in case of the dimethylacetylene reaction, the methyl group loss should be dominant.

3.2. Reactions with Alkenes and Allenes. In the reactions of ethylene and allene, once again the cyano radical interacts with the π-electron density without entrance barriers to form a carbon−carbon σ bond and the doublet radicals INT1 (Figures 25 and 26; Table 10). The allene reaction leads to trans and cis isomers, which equilibrate rapidly to equal concentrations. The addition of CN($X^2\Sigma^+$) to the central carbon atom of allene was found to be less important due to dominating large impact parameters leading to reaction. Even if trajectories with low impact parameters follow this pathway to a minor amount, the addition product can isomerize rapidly via a three-membered ring intermediate to INT1. Likewise, similar to the reactions with (substituted) acetylenes, addition of the cyano radical with its nitrogen atom to the double bond cannot be excluded since the potential energy surfaces involved are purely attractive. However, the isocyano radical intermediates were found to isomerize via cyclic intermediates to INT1. Hence, both modes of addition of CN($X^2\Sigma^+$) to the double bond with either the carbon or nitrogen atom will yield ultimately the nitrile intermediates. The INT1 structures reside in deep potential energy wells of 216−232 kJ mol^{-1} with respect to the reactants. Considering the ethylene system, INT1 either loses an H atom via a tight exit transition state located 16 kJ mol^{-1} above the products (40% of all INT1) or rearranges via a hydrogen shift through a barrier of 136 kJ mol^{-1} to INT2 which is the global minimum of the C_3H_4N PES (−286 kJ mol^{-1}) prior to a fragmentation to form vinylcyanide plus a hydrogen atom via a rather lose transition state placed only 3 kJ mol^{-1} above the products (60% of INT1). In case of the allene reaction, the initially formed complex INT1 loses a hydrogen atom either at the CH_2 or CH_2CN group; both pathways are exothermic and the transition states lie 6−8 kJ mol^{-1} above the separated products. The channel leading to the cyanoallene ($HCCCH_2CN$) plus atomic hydrogen was found to be dominant (90%) compared to the pathway forming 3-cyanomethylacetylene ($HCCCH_2$-(CN)) (10%).[598] Note that similar to the CN/CH_3CCH system, the reaction of cyano radicals with allene,

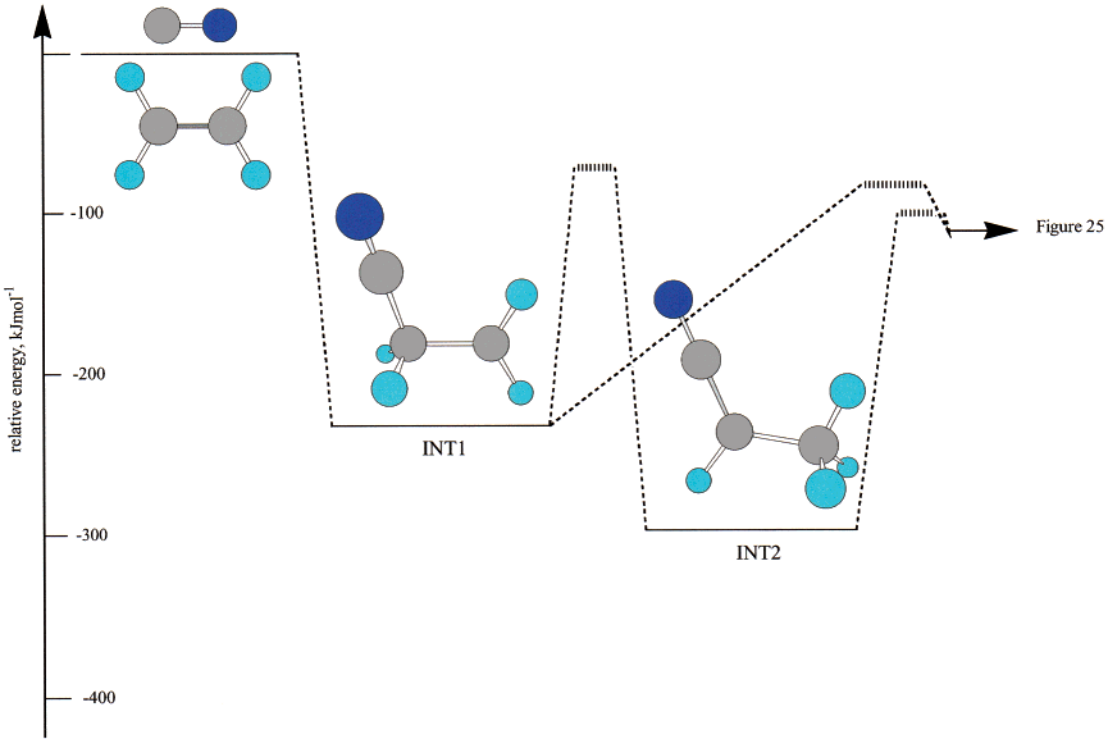

Figure 26. Schematic doublet potential energy surfaces of the reaction of ground-state cyano radicals with ethylene. Numeric data are given in Table 10. Carbon atoms are denoted in gray, hydrogen atoms in light blue, and nitrogen atoms in deep blue.[585]

Table 10. Relative Energies of Intermediates Involved in the Reaction of Ground-State Cyano Radicals with Ethylene, Allene, and Benzene[a]

	C_2H_4	H_2CCCH_2	C_6H_6
INT1	232	216−219	165
INT2	286	n/a	n/a
TS INT1 → INT2	136	n/a	n/a
exit transition state H loss from INT1	16	6−8	33
exit transition state H loss from INT2	3	n/a	n/a

[a] All data are given in kJ mol^{-1}. TS denotes a transition state of an isomerization of two intermediates.

the second C_3H_4 isomer, yields two distinct C_3H_3CN isomers, one which has been observed in the methylacetylene reaction cyanoallene plus 3-methylcyanoacetylene (Figure 25).

3.3. Reactions with Aromatic Molecules. Finally, the reaction of the cyano radical with benzene needs to be addressed. Similar to the reactions of the cyano radical with alkynes, alkenes, and allene, the interaction of CN ($X^2\Sigma^+$) with benzene is dominated by long-range dispersion forces and proceeds indirectly via a long-lived intermediate. The potential energy surface involved is similar to Figure 26, but no hydrogen migration was found to be important. Here, the initial addition is barrierless and correlates with the intermediate INT1, which is bound by 165 kJ mol^{-1} with respect to the reactants (Table 10). At all collision energies, the center-of-mass angular distributions are forward−backward symmetric and peak at $\pi/2$. This shape documents that the decomposing intermediate has a lifetime longer than its rotational period and that the hydrogen is emitted almost perpendicular to the C_6H_5CN plane, giving preferentially sideways scattering. Due to the aromaticity of the benzene molecule, INT1 resides in a shallower potential energy well compared to typical depths of 216−253 kJ mol^{-1} for the previous reactions (Tables 9 and 10). This doublet intermediate can undergo a homolytic carbon−hydrogen bond rupture through a tight exit transition state located 33 kJ mol^{-1} above the products, forming the cyanobenzene isomer (C_6H_5CN) plus atomic hydrogen in an exoergic reaction (−95 kJ mol^{-1}). The cyano radical versus atomic hydrogen replacement follows the classical patterns of an aromatic, radical substitution reaction of halogens with benzene, except that the encounter of the cyano radical with benzene proceeds without an entrance barrier.

3.4. General Trends and Reactivity of Cyano Radicals. The reactions of cyano radicals with unsaturated hydrocarbons studied share common features. First, all reactions are barrierless, dominated by long-range attractive forces in the entrance channel, and governed by indirect scattering dynamics via formation of intermediates which are bound by 165−253 kJ mol^{-1} with respect to the separated reactants. Second, these intermediates either decompose through atomic hydrogen elimination via transition states located 6−33 kJ mol^{-1} above the nitrile products and depict—in the case of acetylene, methylacetylene, and ethylene—hydrogen shifts via barriers of 136−187 kJ mol^{-1} prior to an H atom ejection. Third, about 30−42% of the total energy available was found to channel into the translational energy of the products. Fourth, the center-of-mass translational energy distributions peak well away from zero translational energy at 15−50 kJ mol^{-1}, thus verifying the electronic structure calculations of exit bar-

riers involved when the intermediates decompose. Since all transition states involved lie well below the energy of the reactant molecules and the formation of the nitriles is exoergic by 50−106 kJ mol^{-1}, these reactions present compelling candidates to form complex organic nitriles—precursors to biologically important amino acids—over a broad temperature range from 10 K as prevailing in dense clouds up to high- temperature settings in hot molecular cores, circumstellar envelopes, planetary nebulae, and shocks in circumstellar disks. Further, various important reaction intermediates were identified. Under the single-collision conditions, the lifetime of the intermediates which are formed with extremely high internal excitation is on the order of a few picoseconds at most, and hence, the intermediates fragment before the adduct can reach the detector. Therefore, in low-density interstellar environments such as dense clouds, these intermediates cannot be stabilized by a three-body reaction. In denser solar system environments such as Titan, however, three-body collisions may have a profound impact on the atmospheric chemistry and can lead to a stabilization and/or successive reaction of the intermediate(s). The reaction products, intermediates involved, and kinetic investigations at low (CRESU) and elevated temperatures[599] present provided sound experimental data which can now be included into sophisticated and updated models of distinct interstellar and solar system environments.

The versatile concept of a cyano radical versus atomic hydrogen exchange presents the first explicit experimental evidence that nitriles can be formed in reactions of cyano radicals with unsaturated hydrocarbons. This makes it even feasible to predict the formation of nitriles once the corresponding unsaturated hydrocarbons are identified in the interstellar medium and in planetary atmospheres. Here, cyanoacetylene (HCCCN), vinylcyanide (C_2H_3CN), and 1-cyanomethylacetylene (CH_3CCCN) have already been observed in the interstellar medium (Table 1); cyanoacetylene has been detected further in Titan's atmosphere. The crossed beam experiments verify that methylacetylene (CH_3CCH) is the common precursor to cyanoallene ($H_2CCCH(CN)$) and 1-cyanomethylacetylene (CH_3CCCN). Since the latter isomer has been assigned unambiguously toward TMC-1 and OMC-1, cyanoallene ($H_2CCCH(CN)$) is strongly expected to be present in dense clouds as well. This has been confirmed very recently, and an identification of cyanoallene was made toward TMC-1 with the 100 m radiotelescope in Effelsberg (Germany).[600] This demonstrates nicely that basic laboratory experiments on the chemical reaction dynamics of bimolecular, elementary reactions—especially those involving distinct isomers—can indeed predict where in the interstellar medium astrochemically important molecules are being synthesized. Therefore, these studies can foresee that hitherto unobserved nitriles (Figure 25) will certainly be present in the interstellar medium and in dense atmospheres of planets and their moons.

The formation of isonitrile isomers was not observed in the crossed beam experiments. All reactions to HCCNC, C_2H_3NC, CH_3CCNC, $H_2CCCH(NC)$, and $H_2CCCCH_3(NC)$ are endoergic by 4−13 kJ mol^{-1}. Although the formation of C_6H_5NC is exoergic by about 5 kJ mol^{-1}, the exit barrier of the final carbon−hydrogen bond rupture is 30 kJ mol^{-1} above the energy of the separated reactants. The PES of the CN/CH_3CCH system shows similar features: despite an exoergic reaction of −36 kJ mol^{-1}, the exit barrier is located 9 kJ mol^{-1} above the reactants. Therefore, in low-temperature extraterrestrial environments, the average translational energy of the reactants can neither compensate for the reaction endoergicity nor promote overcoming the exit barrier. Note that in cold planetary atmospheres, vibrationally excited cyano radicals—produced via photodissociation of atmospheric HCN—might use their internal energy to compensate for the reaction endoergicity. In addition, in high-temperature environments such as in circumstellar envelopes of carbon stars and planetary nebulae close to the photosphere, the enhanced translational energy of the reactants can overcome the endoergicity and isonitriles might be formed as well.

Further investigation of this reaction class shall focus on the role of the H atom abstraction reaction to HCN and/or HNC. The H atom abstraction from acetylene is endoergic and cannot proceed in cold molecular clouds. A cyano radical approaching the hydrogen atom of ethylene from the N-side has a transition state forming HNC and C_2H_3 located 22 kJ mol^{-1} above the energy of the reactants; this barrier closes the reaction in dense clouds. When the CN radical reacts with the radical center with ethylene, methylacetylene, allene, dimethylacetylene, and benzene, all potential energy surfaces are attractive on the B3LYP level of theory. The formation of HCN and the hydrocarbon radicals is found to be exoergic by 82, 170, 162, 176, and 75 kJ mol^{-1} without energy barriers. Therefore, these processes can form HCN even in the coldest molecular clouds holding temperatures as low as 10 K. If the cyano radical approaches the H atom of allene, methylacetylene, dimethylacetylene, or allene with its N-side, the calculations show the formation of loosely bound van der Waals complexes which are about 10 kJ mol^{-1} more stable than the separated reactants. Due to the smaller polarizability of ethylene, the intermolecular forces are found to be too weak to form this van der Waals complex. In all cases, the barrier from these complexes to HNC plus the hydrocarbon radical is slightly (3 kJ mol^{-1}) below the reactants. Therefore, HNC can be formed in dense molecular clouds. However, a preliminary statistical investigation of the CN/C_2H_4 system suggests that the hydrogen abstraction pathway is less dominant than addition to a double bond (<10%).

4. Reactions of $C_2D(X^2\Sigma^+)$

Crossed beam experiments of the d_1-ethinyl $C_2D(X^2\Sigma^+)$ radicals with unsaturated hydrocarbons acetylene (C_2H_2),[601] methylacetylene (CH_3CCH),[602,603] and allene (H_2CCCH_2)[604] were conducted at collision energies between 26.1 and 39.8 kJ mol^{-1} and augmented with electronic structure calculations to

Table 11. Relative Energies of Intermediates Involved in the Reaction of Ground-State Ethinyl Radicals with Acetylene and Methylacetylene[a]

	C_2H_2; R = H	CH_3CCH; R = CH_3
INT1	262	266−267
INT2	333	314
TS INT1 → INT2	163	174
exit transition state H loss from INT1	23	7−20
exit transition state H loss from INT2	4	9

[a] All data are given in kJ mol^{-1}. TS denotes a transition state of an isomerization of two intermediates.

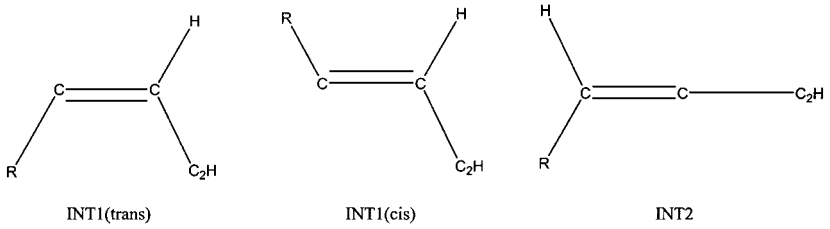

INT1(trans) INT1(cis) INT2

investigate the formation of (substituted) polyacetylenes and allenes in interstellar environments[601−603] and in atmospheres of planets and their moons.[590,594,604] Note that the actual reactions were performed with d_1-ethinyl but not with ethinyl itself. This was due to the experimental difficulties to prepare and stabilize an intense, supersonic ethinyl radical beam. In the following sections, energetics and structures are given for the nondeuterated reactants, intermediates, and products.

4.1. Reactions with Alkynes. The potential energy surfaces involved are very similar to those of the isoelectronic cyano radical reactions and discussed in terms of Figure 24. Both reactions with acetylene and methylacetylene involve indirect chemical dynamics and are initiated by a barrierless addition of the ethinyl radical to the π-electron density of acetylene and methylacetylene forming strongly bound intermediates INT1. Both intermediates are doublet radicals and stabilized by 262−267 kJ mol^{-1} with respect to the reactants (Table 11). INT1 shows a rapid cis−trans isomerization involving only small barriers of 14−19 kJ mol^{-1} or undergoes [1,2]-H shifts via barriers of 163−174 kJ mol^{-1} to INT2. The latter species reside in deep potential energy wells of 314−333 kJ mol^{-1} and thus are more stable than their predecessors. The acetylene system shows at least three distinct reaction pathways. These are (1) a predominant fragmentation of INT1 via H loss through a barrier of 23 kJ mol^{-1} forming diacetylene (HCCCCH), (2) a minor contribution of decomposing INT2 complexes via atomic hydrogen ejection to give diacetylene (HCCCCH) via a relatively lose exit transition state about 4 kJ mol^{-1} above the products, and (3) a molecular hydrogen elimination to form the butadiynyl radical (HCCCC) (1−2%). The latter pathway deserves particular attention as a H_2 elimination was not observed in the isoelectronic reaction of cyano radicals with acetylene (the H_2 + CCCN channel was found to be endoergic by +35 kJ mol^{-1} and hence not open energetically under the experimental conditions). Isotopic substitution shows explicitly that the formation of butadiynyl involves a [1,1] molecular hydrogen loss. Surprisingly, no transition state was found which connects ground-state INT2 (X^2A') to butadiynyl ($X^2\Sigma^+$) plus molecular hydrogen. However, a closer look at the excited $^2A''$ surface shows a correlation of an excited state (A^2A'') of the n-C_4H_3 intermediate to the electronically excited butadiynyl radical ($A^2\Pi$) plus molecular hydrogen. Recall that the $A^2\Pi$ state is only 72 cm^{-1} above the $X^2\Sigma^+$ ground state. Neither the molecular hydrogen loss[605] nor the role of INT2 has been addressed in previous studies of this reaction.[606−609]

Similar to the reaction with CH_3CCH (section IV.C.1), the new carbon−carbon σ bond forms at the carbon atom adjacent to the acetylenic hydrogen atom. A crossed beam experiment of d_1-ethinyl with d_3-methylacetylene shows explicitly that INT1 decomposes to form both methyldiacetylene (CH_3-CCCCH) (channel 1; 70−90%; Figure 27) and to a minor amount ethinylallene ($H_2CCCH(C_2H)$) (channel 2; 10−30%) isomers through exit transition states located 7−20 kJ mol^{-1} above the products in strongly exoergic reactions (95−135 kJ mol^{-1}). A minor reaction pathway involves an H emission from INT2 to methyldiacetylene via a barrier of about 9 kJ mol^{-1} (channel 3). A methyl group elimination was not observed experimentally, but this pathway might be present to a minor amount.

4.2. Reactions with Allenes. The reaction of the ethinyl radical with the second C_3H_4 isomer, allene, is similar to the isoelectronic reaction with the cyano radical. It is dominated by long-range dispersion forces and proceeds barrierless by an addition of ethinyl to a terminal carbon of allene. This process leads to the formation of the two radical intermediates (cis and trans forms) which are bound in deep potential energy wells of about 232 kJ mol^{-1} with respect to the reactants. These intermediates decompose via H atom elimination through exit transition states located 7−16 kJ mol^{-1} above the products into two distinct isomers: ethynylallene ($H_2CCCH(C_2H)$) and 1,4-pentadiyne ($HCCCH_2CCH$). Both reactions are exoergic by −102 and −65 kJ mol^{-1}, respectively. Branching ratios of more than 9:1 are estimated based on RRKM studies. Since the reaction is dominated by large impact parameters, the attack of the ethinyl radical at the central carbon atom of allene is likely to be less important.

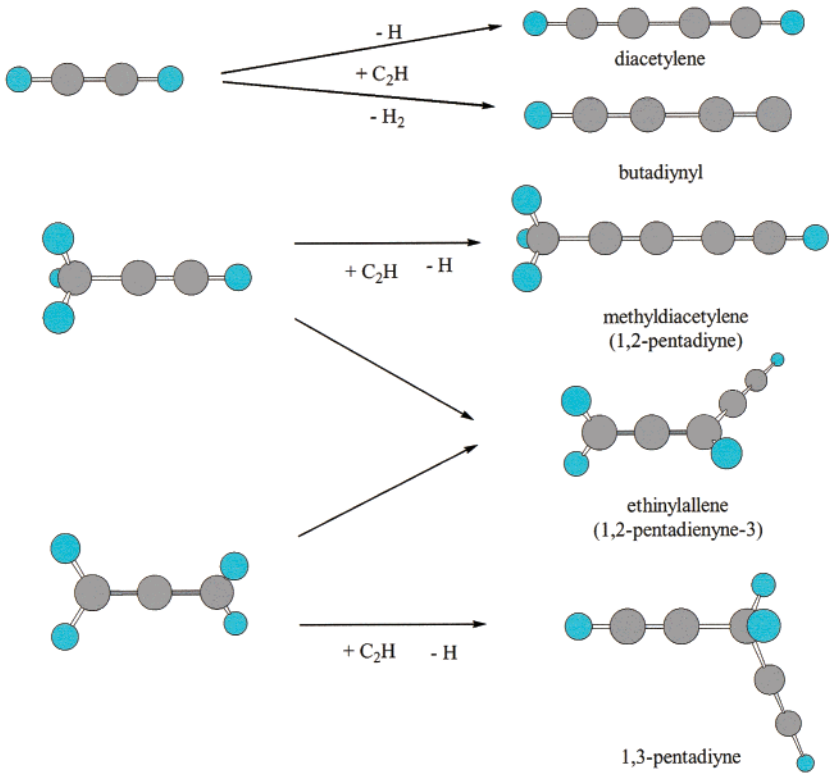

Figure 27. Products formed via the ethinyl versus atomic and molecular hydrogen-exchange pathways in the reactions of ethinyl radicals with acetylene, methylacetylene, and allene.

4.3. General Trends and Reactivity of Ethinyl Radicals. Similar to the reaction of the isoelectronic cyano radical, the reactions of ethinyl radicals with unsaturated hydrocarbons are barrierless, dominated by long-range attractive forces in the entrance channel, and dictated by indirect scattering dynamics via formation of intermediates strongly bound by 232−267 kJ mol^{-1}. However, whereas the CN/C_2H_2 and CN/CH_3CCH system goes through an osculating complex at comparable collision energies, the reactions of ethinyl depict long-lived complex behaviors. Two effects can contribute to this. First, the additional atom of the ethinyl versus cyano reactant increases the number of vibration modes by three. Second, the low-frequency wagging/bending modes of the ethinyl group might increase the lifetime even further. The intermediates formed initially fragment predominantly via an atomic hydrogen loss through exit transition states located 4−23 kJ mol^{-1} above the products; in the case of both alkynes, [1,2]-H shifts through barriers of 163−174 kJ mol^{-1} prior to an H atom emission are likely. Third, fractions of 30−40% of the total energy available were found to channel into the translational degrees of freedom of the products, and the translational energy distributions peak well away from zero at 15−45 kJ mol^{-1}. This order of magnitude supports the electronic structure calculations and verifies the presence of exit transition states. Most importantly, all transition states are located well below the energy of the reactant molecules and the formation of the unsaturated hydrocarbons is found to be exoergic by 65−135 kJ mol^{-1}. Finally, the reactions of both ethinyl and cyano radicals with methylacetylene form two distinct isomers each (Figures 25 and 27). However, the branching ratio of the formation of the $CH_3-C\equiv C-X$ versus H_2CCCHX is unity for X = CN but increases for X = C_2H. This can be rationalized in terms of a larger difference in the energetics of the exit transition states to both isomers in the ethinyl reaction (22 kJ mol^{-1}) compared to the CN/CH_3CCH reaction (2 kJ mol^{-1}) and hence inherent larger unimolecular rate constants for the decomposition of the involved intermediates to the products.

The experimental assignment of the ethinyl versus atomic hydrogen (and in the case of acetylene, molecular hydrogen) pathway expose for the very first time that these reactions can indeed synthesize (substituted) polyacetylenes and allenes in interstellar environments as well as in planetary atmospheres. Here, diacetylene (HCCCCH), butadiynyl (HCCCC), and methyldiacetylene (CH_3CCCH) have been observed in the interstellar medium (Table 1) and diacetylene in Titan's atmosphere. On the basis of the versatile concept of an initial addition of the ethinyl radical to the unsaturated double or triple bond together with kinetic studies at ultralow and elevated temperatures,[610−612] the existence of butenine ($C_2H_3C_2H$), ethinylallene ($H_2CCCH(C_2H)$), 1,4-butadiyne ($HCCCH_2(C_2H)$), and phenylacetylene ($C_6H_5C_2H$) upon reaction with ethylene, allene, and benzene can be predicted in extraterrestrial environments. Their identification will be a peerless task of further astronomical observations and especially of the Cassini−Huygens mission to Titan which is scheduled to arrive in 2004.

In addition, various intermediates were identified. Under the single-collision conditions, the lifetime of the internally excited intermediates is mostly a few picoseconds; therefore, they fragment before reaching

the detector or before they can be stabilized in low-density interstellar environments as in dense clouds. In denser solar system environments such as Titan's atmosphere, however, three-body collisions may have a crucial consequence on the atmospheric chemistry and can lead to a stabilization of the intermediate-(s). Most importantly, these free radicals can undergo subsequent reactions with distinct trace gases C_2H_2, C_2H, or C_4H_2 to form even more complex molecules such as C_6H_5, C_6H_4, C_6H_5, C_8H_5, and C_8H_4 isomers—extremely unstable species which have been only partly included into chemical reaction networks of solar system and interstellar environments.

Finally, it should be noted that the CRESU rate constants of cyano radical reactions with unsaturated hydrocarbons are systematically larger compared to ethinyl reactions. In the case of acetylene and ethylene, cyano species react at similar temperatures by a factor of ca. 2 faster than the ethinyl counterparts. This can be likely attributed to a simple 'geometrical factor' and the potential energy surfaces involved as visualized explicitly on the acetylene reactions. The cyano radical can add to the unsaturated bond with the carbon and nitrogen atoms, thus forming a cyano or isocyano intermediate. Since the formation of isonitriles is forbidden energetically, those isocyano intermediates were found to rearrange to the corresponding cyano intermediates, which in turn lose an H atom to form the nitrile. However, the ethinyl radical can add to the π-bond barrierless only with the radical center located at the carbon atom; an addition of the HC-group[609] involves a barrier of 32 kJ mol^{-1},[609] which cannot be passed in the low-temperature CRESU experiments. This can lead to a simple model predicting that—compared to the cyano reactant—only one-half of the collisions of ethinyl radicals with unsaturated hydrocarbons are reactive.

5. Reactions of $C_6H_5(X^2A')$

5.1. Reactions with Alkynes. The reaction of phenyl radicals with methylacetylene presents the only system of this reaction class studied under single-collision conditions at a relatively high collision energy of 140 kJ mol^{-1}.[613−615] The experimental data were combined with electronic structure calculations revealing that this reaction has an entrance barrier of about 17 kJ mol^{-1}. This finding correlates nicely with recent kinetic data upon reactions with olefines and alkynes showing very low rate constants at temperature ranges up to 1100 K ranging between 10^{-12} and 10^{-14} cm^3 s^{-1}.[616] Similar to the cyano and ethinyl radical reactions, the unpaired electron of the phenyl radical is located in a centrosymmetrical orbital and adds to the triple bond of the methylacetylene molecule forming a cis−trans intermediate. Since the chemical reaction dynamics were found to be on the boundary between an osculating complex and a direct reaction, the highly rovibrationally excited $(C_6H_5)HCCCH_3$ intermediate is very short lived and does not experience the deep potential energy well of 150−160 kJ mol^{-1}. It loses a hydrogen atom to form the phenylmethylacetylene molecule on the $^2A'$ surface. A crossed beam reaction of phenyl radicals with d_3-methylacetylene demonstrated convincingly that the phenylallene isomer was not observed experimentally. This can be compared to the cyano and ethinyl radical reactions. Whereas their reactions with methylacetylene proceed via indirect scattering dynamics through long-lived and/or osculating complexes holding lifetimes of ca. 1−2 ps, the phenyl radical shows direct dynamics via a short-lived (<0.1 ps) intermediate. This translates into reactive scattering signal preferentially in the forward hemisphere with respect to the phenyl radical beam. The shorter lifetime of the $CH_3CCH(C_6H_5)$ intermediate compared to CH_3CCHC_2H and CH_3-CCHCN precludes an energy 'flow' into the methyl group. Hence, only the $CH_3CCC_6H_5$ isomer is observed experimentally at these high collision energies and no phenylallene isomer is formed. This finding can be rationalized comparing the average collision energies of the reactive encounters. As a general trend, the lifetime of an intermediate decreases as the collision energy rises, and as an extreme, the reaction goes from a long-lived intermediate through an osculating complex, and finally via direct scattering dynamics. However, statistical calculations demonstrate a dramatic energy/temperature dependence: at lower temperatures, the bicyclic indene isomer is the sole reaction product; no phenylmethylacetylene is formed. However, when the temperature is increased to 1000 K, indene diminishes completely in favor of phenylmethylacetylene and phenylallene (Figure 28). As the temperature increases to 2000 K, phenylmethylacetylene is formed almost exclusively—in strong analogy as observed in the crossed beam study.

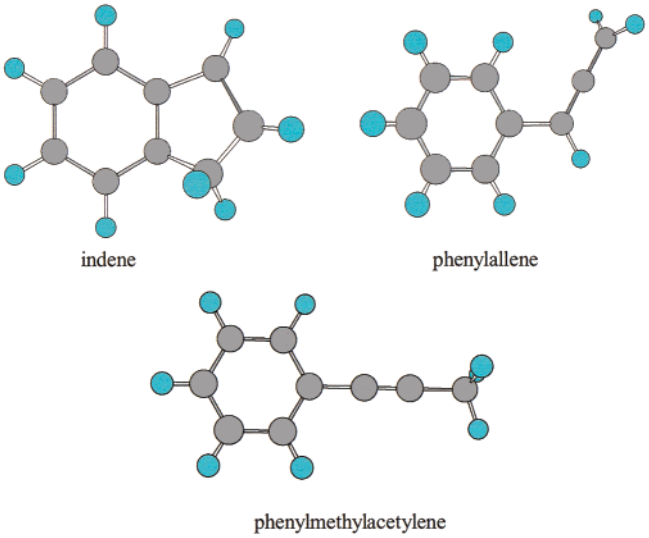

Figure 28. Structures of three C_9H_8 isomers formed at low (indene), intermediate (phenylallene and phenylmethylacetylene), and high temperatures/collision energies (phenylmethylacetylene). Carbon atoms are denoted in gray and hydrogen atoms in light blue.

The combined crossed beam and theoretical investigation explicitly demonstrated that the branching ratios of the indene, phenylallene, and phenylmethylacetylene isomers depend strongly on the collision energy (and hence temperature) in the actual environment of interest. Since this reaction holds an entrance barrier of 17 kJ mol^{-1}, it is irrelevant for

the formation of PAHs in cold molecular clouds or hydrocarbon-rich atmospheres of Jupiter, Saturn, and Titan because this entrance barrier inhibits the reaction. However, temperatures close to the photosphere of carbon stars and planetary nebulae can reach up to 4500 K, and the reactions might be important in these environments. The actual effect on PAH synthesis must be verified in refined chemical modeling of these scenarios including, in particular, the strong temperature dependence of the branching ratios of distinct isomers.

V. Implications for Solar System Chemistry

The reactions of the isoelectronic cyano $CN(X^2\Sigma^+)$ and ethinyl radicals $C_2H(X^2\Sigma^+)$ are of fundamental relevance to the chemical processing of hydrocarbon-rich atmospheres of planets and their satellites. The atmospheric composition of Saturn's satellite Titan, for instance, is dominated by nitrogen (N_2) and methane (CH_4) together with trace amounts of acetylene (C_2H_2), ethane (C_2H_6), propane (C_3H_8), methylacetylene (CH_3CCH), hydrogen cyanide (HCN), cyanoacetylene (HCCCN), and C_2N_2.[617−626] The chemistry of the cyano and ethinyl radicals is thought to be initiated by photolysis of HCN and C_2H_2, respectively, to generate reactive radicals in their $^2\Sigma^+$ electronic ground state. Since their reactions proceed fast even at low temperatures as present in Titan's atmosphere and without entrance barrier, are exoergic, and all transition states involved lie below the energy of the separated reactants, cyano and ethinyl radicals are strongly expected to react with unsaturated hydrocarbons to nitriles, (substituted) polyacetylenes, and allenes as observed in crossed beam experiments (Figures 25 and 27). These experiments present the very first experimental evidence that neutral−neutral reactions of $CN(X^2\Sigma^+)$ and C_2H $(X^2\Sigma^+)$ radicals with unsaturated hydrocarbons can synthesize nitriles and complex hydrocarbons in Titan's atmosphere and possibly in Jupiter, Saturn, Uranus, Neptune, Pluto, and Triton.

However, two fundamental differences between reactions in the interstellar medium and solar system environments should be noted. Due to the low density of only 10^4-10^6 cm^{-3} in dense clouds, only binary collisions are relevant in these environments. The reaction intermediates, which have lifetimes of a few picoseconds at the most, fragment exclusively. In the denser planetary atmospheres, however, a third-body collision might divert the internal energy to stabilize the radical intermediates. This collision-induced stabilization of the intermediate(s) strongly depends on the temperature as well as density profile of each atmosphere and hence on the mean collision frequency of the complexes with the bath molecules. Therefore, the actual influence on the organic chemistry must be investigated in future reaction networks modeling the chemistry in Titan's atmosphere. So far, no network has considered the chemistry of these radical intermediates, although they could play a significant role in the stepwise growth to larger molecules or even in aerosol production. Since all models rely heavily on laboratory measurements, sophisticated data on rate constants, intermediates involved, and reaction products are crucial to obtain a legitimate and realistic picture of the prevailing chemistry in our solar system now and in the future. Note that a recent study on the hydrocarbon chemistry in Neptune's stratosphere clearly demonstrates the necessity of these laboratory data.[627] Here, a thorough error analysis of the input data exposed substantial shortcomings of currently existing models. For instance, C2 compounds were found to be 'reproduced' only within error limits of 100%. The situation becomes even scarier considering species with three carbon atoms and errors of 200% were derived. Even in astronomical scales, inaccuracies of 2000% for more complex molecules expose the severe limitations of current reaction networks of planetary and satellite atmospheres. Therefore, without sophisticated laboratory data, models will never reproduce the actual observations. In addition, reactions of electronically excited atoms are important in solar system environments. Note, for instance, reactions of $O(^1D_2)$ atoms in the terrestrial atmosphere, of $N(^2D_j)$ in the upper layers of Titan's atmosphere, and of $C(^1D_2)$ in comets approaching perihelon, cf. refs 518 and 519.

The experimental results can be employed further to set up a systematic database of reaction products and predict the formation of hitherto unobserved gas-phase molecules in solar system environments. Therefore, future surveys in the framework of the Cassini−Huygens mission to Titan and analytical devices for upcoming space missions can be designed. This provides a crucial link between basic laboratory experiments and applied space exploration. These applications of the crossed beam method to planetary chemistry problems have just begun to scratch the surface. In this millennium, laboratory experiments of the kind presented here combined with planetary space mission data will undoubtedly unravel the complex chemical processes prevailing in planetary atmospheres of our solar system.

VI. Implications for Combustion Processes and Chemical Vapor Deposition

The laboratory experiments have strong links to terrestrial combustion processes and chemical vapor deposition. Although the rovibrationally excited reaction intermediates fragment before a three-body collision takes place in low-density interstellar clouds, the conditions are more complex in actual combustion scenarios. Here, number densities of typically 10^{17} cm^{-3} prevail at temperatures of a few thousand Kelvin, and three-body reactions can stabilize the intermediates efficiently. The elevated temperatures open further reaction pathways which, like the elementary reactions of $C_3(X^1\Sigma_g^+)$, are either endoergic or involve significant entrance barriers. These data propose that under oxygen-poor conditions, chemistry in combustion processes, carbon-rich circumstellar envelopes, and planetary nebulae are remarkably alike.

The explicit identification of the hydrogen replacement by atomic carbon, dicarbon, and tricarbon suggests that hydrogen-deficient hydrocarbon molecules might be formed also in combustion environ-

ments. This has been confirmed very recently as small hydrocarbons C_4H_3 (1), C_3H_2 (2), C_3H (3), HCCCCH (4), C_6H_3 (5), C_2 (6), C_2H_3 (7), C_6H_5 (8), CH (9), $CCCCH_2$ (10), C_5H_2 (11), and C_8H_2 (12) have been scavenged in ethylene flames.[628−630] Note that molecules 1−5 were detected in crossed beam experiments; species 6−8 represented reactants. This situation compares nicely to chemical vapor deposition employing, for instance, acetylene/oxygen/argon flames. Here, atomic hydrogen and methyl radicals are strongly considered to be the key species involved.[631] In addition, C_3H_3, C_4H_3, C_2, C_3, CH, and C_xH_2 ($x = 4, 6, 8$) might play a crucial role in diamond growth.[632−634] Note that elementary reactions of boron are of potential importance to chemical vapor deposition of boron-rich systems, cf. refs 635 and 636.

Further, the polyatomic products of the crossed beam reactions can be grouped nicely in three 'families' of radicals which might provide suitable precursors to form the first (substituted) aromatic ring molecule, polycyclic aromatic hydrocarbon-like species, and ultimately carbonaceous nanoparticles (soot). These are (1) the '*C_3H_3 family*' (propargyl; 1- and 3-methylpropargyl; 1- and 3-vinylpropargyl), (2) the '*n-C_4H_3 family*' (*n*-C_4H_3; 1- and 3-methylbutatrienyl), and (3) the '*C_5H_5 family*' (1- and 4-methylbutatrienyl; 1,3-butadienyl-2). The reaction of two propargyl radicals is strongly believed to give benzene via various chain structures (sections II.A and II.D) However, no attention has been devoted so far to the unique synthetic power of substituted propargyl radicals. Radical−radical reactions of members of the '*C_3H_3 family*' might synthesize methylbenzene (toluene), *o*- and *p*-dimethylbenzene (xylene), *o*- and *p*-methylvinylbenzene, and *o*- and *p*-divinylbenzene.[566] Likewise, reactions of acetylene with species of the '*n*-C_4H_3 *family*' could lead to benzene and toluene, whereas collisions of these radicals with members of the same or the '*C_3H_3 family*' are expected to form seven- and eight-membered ring structures. None of these pathways has yet been contemplated in chemical models of combustion flames. Lastly, the '*C_5H_5 family*' is likely to be involved in the production of (substituted) cyclopentadienyl radicals—potential precursors to naphthalene-like molecules in combustion flames, carbon-rich circumstellar envelopes, and planetary nebulae.

Finally, the H−C−S system is of particular importance as organosulfur molecules are thought to be transient species in the combustion of sulfur-containing fuel and coal. Hitherto, only simple di- and triatomic sulfur-bearing species S_2, SH, CS, H_2S, OCS, and SO_2 have been characterized explicitly in combustion flames and in kinetic models of these settings.[637] However, more complex hydrogen-deficient organosulfur species such as HCS and the isomers HCCS and C_2S could present important reaction intermediates in combustion processes which might ultimately lead to sulfur-bearing polycyclic aromatic hydrocarbons and—after oxidation—acid rain. Compared to dense clouds, the chemistry in combustion flames is expected to be more diverse. Due to the denser combustion environments, intermediates involved can be stabilized and primary products can undergo secondary reactions. As the HCCS radical has a $^2\Pi$ electronic ground state, a barrierless reaction with the propargyl radical is strongly expected. This might lead to a $HCCCH_2$-SCCH molecule which could rearrange to form sulfur-carrying heterocycles. This process might be closely related to the reaction of two propargyl radicals forming first linear C_6H_6 isomers and in a later stage possibly benzene. In a similar manner, HCCS could react with acetylene to form a 1-thiophenyl radical via a chain isomer and successive isomerization via ring closure. This remains to be investigated further.

VII. Summary and Outlook

This review concentrated on the newly emerging field of astrochemistry and compiled the latest trends in laboratory experiments to unravel the formation of carbon-bearing molecules in distinct interstellar environments via neutral−neutral reactions. Kinetic studies and crossed beam experiments provided highly complementary data on rate constants, reaction intermediates, and product isomer(s). The kinetic investigations help to determine rate constants of astrophysically important reactions over a wide temperature range from 13 K as characteristic for dark (molecular) clouds to a few thousand Kelvin (simulating the chemical processing in planetary nebulae and circumstellar envelopes close to the photosphere of the central star). Crossed beam experiments are conducted at characteristic collision energies, so far from 0.38 to 150 kJ mol^{-1}. Formally, this would correspond to an average kinetic temperature of the reactants as low as 45 K. Both kinetic and dynamic studies furnished compelling evidence that the reactions of carbon atoms, dicarbon molecules, cyano radicals, and ethinyl species with unsaturated hydrocarbons are fast within gas kinetics limits even at temperatures as low as those prevailing in dense clouds. Those bimolecular collisions lead a broad product spectrum ranging from hydrogen-deficient hydrocarbon radicals via nitriles to (substituted) polyacetylenes and allenes. The reactions of atomic carbon with unsaturated hydrocarbons deserve particular attention, since complex organic molecules can be built-up sequentially over a wide range of collision energies and, hence, temperatures in interstellar environments from 10 to 4500 K. On the contrary, reactive collisions of oxygen and nitrogen atoms with closed-shell hydrocarbons play no role in the chemistry of dense clouds as these processes involve significant entrance barriers. This demonstrates nicely the unique reactivity of carbon atoms and the unmatched ability to formally 'insert' into carbon−carbon bonds of alkynes, olefines, and aromatic molecules such as benzene. These results provide further basic mechanisms and generalized concepts on how complex molecules can be synthesized in the interstellar medium. Likely routes to, for instance, interstellar C_3H and C_3H_2 isomers, (substituted) polyacetylenes, and nitriles have been exposed, and a multitude of hydrocarbons, nitriles, and allenes undetected so far in interstellar space or in our solar system have been identified. Prospective spectroscopic surveys toward dense clouds, hot cores, carbon-

rich circumstellar envelopes, and planetary nebulae will very likely identify these elusive molecules soon.

The implications of these findings to astrobiological enigmas such as the formation of 'prebiotic' ozone and precursors to amino acids have been also addressed, and connections to the chemical processing of hydrocarbon-rich atmospheres of planets and satellites were presented. Related problems of combustion processes and chemical vapor deposition have been exposed, in particular elementary steps to form precursors to PAH molecules and sulfur-bearing species. These numerous implications clearly demonstrate the strongly interdisciplinary character of this research ranging from distant extraterrestrial environments via our solar system to terrestrial-bound scenarios such as combustion chemistry and even fundamental gas-phase reactions in organic chemistry, which cannot be performed employing traditional techniques.

The applications of crossed beam experiments and kinetic studies to numerous unsolved enigmas in astrochemistry have just begun to scratch the surface. In the coming decades, significant improvements in the production techniques of atoms and free radicals, possibly a direct identification of intermediates involved, and an assignment of high- and low-mass reaction products will certainly extend the contemporary limitations of currently existing setups. The low-mass products of astrochemically relevant reactions should be probed in crossed beam experiments. This is of particular importance with respect to atomic carbon, dicarbon, and tricarbon reacting with hydrocarbons and their radicals. Here, substantial background counts from dissociative ionization of the reactant molecules in the electron impact ionizer themselves makes it impracticable to detect low-mass products if they have the same mass-to-charge ratio as the reagent fragments. Here, a resonant or nonresonant ionization of the product(s) coupled with ion imaging, for instance, could provide an answer. Recent crossed beam reactions of chlorine atoms with propane leading to hydrogen chloride plus propyl radicals overcame this limitation by employing nonresonant photoionization of the propyl products via tunable UV/VUV synchrotron radiation and detecting the ions via a quadrupole mass spectrometer in the TOF mode.[638,639] This approach allowed ionizing the propyl radical selectively. Alternatively, pulsed UV/VUV photoionization detection has been coupled to a crossed beam machine with a QMS to probe reactively and inelastically scattered species in transition-metal−hydrocarbon systems.[640−646] Third, velocity map imaging, which in principle allows for the simultaneous measurements of angular and velocity distributions of state-specific reaction products, combined with single-photon ionization has been applied successfully to detect the alkoxy products of chlorine reactions with alcohols [647,648] However, these principles have not been applied so far to study astrochemically relevant reactions.

In the coming decades, laboratory experiments under single-collision conditions augmented by astronomical observations, space mission, and theoretical investigations will revolutionize the understanding of complex chemical processes prevalent in extraterrestrial environments further. Implementing substantial experimental upgrades is strongly expected to expand the limits to multichannel atom−radical and radical−radical reactions, especially in the carbon−hydrogen system. This is of paramount importance as the modeling community and the correct outcome of chemical reaction networks of interstellar environments depend on comprehensive input data. Cutting-edge laboratory experiments are crucial to untangle the remaining secrets in astrochemistry.

VIII. Acknowledgments

R.I.K. is indebted to the Deutsche Forschungsgemeinschaft (DFG) for a Habilitation fellowship (IIC1-Ka1081/3-1) and D. Gerlich (University Chemnitz, Germany), Y. T. Lee (Academia Sinica, Taiwan), and A. G. Suits (Stony Brook, USA) for support. The author thanks (in alphabetic order) O. Asvany, N. Balucani, C. C. Chiong, L. C. L. Huang, and D. Stranges for experimental assistance. Special thanks to (in alphabetic order) H. F. Bettinger, M. Head-Gordon, A. M. Mebel, C. Ochsenfeld, Y. Osamura, H. F. Schaefer, P. v. R. Schleyer, and F. Stahl for fruitful collaborations on electronic structure calculations. Special thanks to N. Balucani, M. Boediger, H. Bettinger, D. Williams, I. W. M. Smith, I. R. Sims, M. Costes, J. C. Loison, and D. Hussain for comments on parts of this manuscript and to K. Noris (York) for helping with the reference compilation. Finally, the author acknowledges the permission from SEDS (J. Ware; background cover image), NOAO (National Optical Astronomy Observatory, Figure 1 images upper line right, center line second from left, bottom line center), BIMA (Berkeley Illinois Maryland Association, image bottom line left: Pound, M.; Dayal, A.; Bieging, J. H. *Astrophys. J.* **1995**, *439*, 996. Dayal, A.; Bieging, J. H. *Astrophys. J. Lett.* **1993**, *407*, 37), M. McCall (UC Berkeley, upper line center), STSI (Space Telescope Science Institute; images bottom line left, center line left, center line right, center line second from right, top line left), D. Husain (Figure 4), D. C. Clary (Figure 5), J. C. Loison (Figures 6 and 7), I. W. M. Smith and I. R. Sims (Figures 8 and 9), and M. Costes (Figures 11 and 15) for permission to utilize images and/or figures in this article.

IX. References

(1) Chemistry and Physics of Molecules and Grains in Space. *Faraday Discuss.***1998**, *109*.
(2) Hollenbach; D. J.; Thronson, H. A. *Interstellar Processes*; Reidel: Dordrecht, 1987.
(3) Tielens, A. G. G. M.; Allamandolla, L. J. In *Interstellar Processes*; Hollenbach, D. J., Thronson, H. A., Eds.; Reidel: Dordrecht, 1987; pp 397−469.
(4) *Carbon in the Galaxy: Studies from Earth and Space*; NASA-SP-3061, NASA: Washington, D.C.,1990.
(5) *Interstellar Dust*; NASA-SP-3036, NASA: Washington, D.C., 1989.
(6) Wilson, T. L.; Matteucci, F. *Astron. Astrophys. Rev.* **1992**, *4*, 1−33.
(7) http://www.cv.nrao.edu/~awootten/allmols.html.
(8) Turner, B. E. *Astrophys. J.*, in press.
(9) Winnewisser, G.; Armstrong, J. T. *The Physics and Chemistry of Interstellar Molecular Clouds*; Springer: Berlin, 1989.
(10) Mampaso, A.; Prieto, M.; Sanchez, F. *Infrared Astronomy*; Cambridge University Press: Cambridge, 1993.

(11) Ehrenfreund, P.; et al. *Laboratory Astrophysics and Space Research*; Kluwer: Dordrecht, 1999.
(12) Jorgensen, U. G. *Molecules in the Stellar Environment*; Springer: Berlin, 1994.
(13) Greenberg, J. M. *The Cosmic Dust Connection*; NATO ASI Series 487; Reidel: Dordrecht, 1996.
(14) Guenther, E. W.; Stecklum, B.; Klose, S. *Optical and Infrared Spectroscopy of Circumstellar Matter*; ASP Conference Series 188; ASP: San Francisco, 1999.
(15) Greenberg, J. M.; Pirronello, V. *Chemistry in Space*; NATO ASI Series 323; Reidel: Dordrecht, 1991.
(16) Diercksen, G. H. F.; Huebner, W. F.; Langhoff, P. W. *Molecular Astrophysics*; NATO ASI Series 157; Reidel: Dordrecht, 1985.
(17) Minh, Y. C.; van Dishoek, E. F. *Astrochemistry: From Molecular Clouds to Planetary Systems*; ASP: San Fancisco, 2000.
(18) Watt, G. D.; Williams, P. M. *Circumstellar Matter*; Kluwer: Dordrecht, 1995.
(19) Haschick, A. D.; Ho, P. L. P. *Atoms, Ions, and Molecules: New Results in Spectral Line Astrophysics;* ASP Conference Series 16*;* San Francisco, 1991.
(20) Ehrenfreund, P.; Charnley, S. B. *Annu. Rev. Astronomy Astrophysics.* **2000**, *38*, 427−483.
(21) Bakes, E. L. O. *The Astrochemical Evolution of the Interstellar Medium*; Twin Press: Vledder, 1997.
(22) Hollenbach, D. J.; Thronson, H. A. *Interstellar Processes*; Reidel: Dordrecht, 1987.
(23) Millar, T. J.; Williams, D. A. *Rate Coefficients in Astrochemistry*; Kluwer: Dordrecht, 1988.
(24) Van Dishoeck, E. F. In *The Molecular Astrophysics of Stars and Galaxies*; Hartquist, T. W., Williams, D. A., Eds.; Oxford Science Publications: Oxford, 1998; pp 53−100.
(25) Altwegg, K.; Ehrenfreund, P.; Geiss, J.; Huebner, W. *Composition and Origin of Cometary Materials*; Kluwer: Dordrecht, 1999.
(26) Scheffler, H.; Esässer, H. *Physics of the Galaxy and Interstellar Matter*; Springer: Berlin, 1988.
(27) Boehme, D. K.; Herbst, E.; Kaifu, N.; Saito, S. *Chemistry and Spectroscopy of Interstellar Molecules*; University of Tokyo Press: Tokyo, 1992.
(28) Millar, T. J.; Williams, D. A. *Dust and Chemistry in Astronomy*; IOP: Bristol, 1993.
(29) Ferrara, A.; McKee, C. F.; Heiles, C.; Shapiro, P. R. *The Physics of the Interstellar Medium and Intergalactic Medium*; ASP Conference Series 80; ASP: San Francisco, 1995.
(30) Blitz, L. *The Evolution of the Interstellar Medium*; ASP Conference Series 12; ASP: San Francisco, 1990.
(31) Gustafson, B. A. S.; Hanner, M. S. ASP Conference Series 104; ASP: San Francisco, 1996.
(32) Watanabe, T.; et al. *Molecular Processes in Space*; Plenum: New York, 1999.
(33) Somerville, W. B.; Crawford, I. A. *J. Chem. Soc., Faraday Trans.* **1993**, *89*, 2261−2268.
(34) Klisch, E.; et al. *Astron. Astrophys.* **1995**, *304*, L5−8 and references therein.
(35) Viti, S.; Williams, D. A.; O'Neill, P. T. *Astron. Astrophys.* **2000**, *354*, 1062−1070.
(36) Maier, J. P.; et al. *Astrophys. J.* **2001**, *553*, 267−273.
(37) Turner, B. E. *Astrophys. J.* **2000**, *542*, 837−860.
(38) Charnley, S. B.; Ehrenfreund, P.; Kuan, Y. J. *Spectrochim. Acta A* **2001**, *57*, 685−704.
(39) Ikeda, M.; et al. *Astrophys. J.* **1999**, *527*, L59−62.
(40) Flower, D.; LeBourlot, J.; Pineau des Forets, G.; Roueff, E. *Astron. Astrophys.* **1994**, *282*, 225−232.
(41) Schilke, P.; Keene, J.; LeBourlot, J.; Pineau des Forets, G.; Roueff, E. *Astron. Astrophys.* **1995**, *294*, L17−20.
(42) Tatematsu, K.; et al. *Astrophys. J.* **1999**, *526*, 295−306.
(43) Schönberner, D.; Blöcker, T. In *The Molecular Astrophysics of Stars and Galaxies*; Oxford Science Publisher: Oxford, 1998; pp 237−264.
(44) Caselli, P.; Hasegawa, T. I.; Herbst, E. *Astrophys. J.* **1993**, *408*, 548−558.
(45) Millar, T. J.; Hernst, E.; Charnley, S. B. *Astrophys. J.* **1991**, *369*, 147−156.
(46) Wallerstein, G.; Noriega-Crespo, A. *Stellar and Circumstellar Astrophysics;* ASP Conference Series 57; ASP: San Francisco, 1994.
(47) Lee, H. H.; Herbst, E.; des Fortes, G. P.; Roueff, E.; Le Bourlot, J. *Astron. Astrophys.* **1996**, *311*, 690−707.
(48) Williams, D. A.; Hartquist, T. W. *Acc. Chem. Res.* **1999**, *32*, 334−341.
(49) Hartquist, T. W.; Caselli, P.; Rawlings, J. M. C.; Ruffle, D. P.; Williams, D. A. In *The Molecular Astrophysics of Stars and Galaxies;* Hartquist, T. W., Williams, D. A., Eds.*;* Oxford Science Publications: Oxford, 1998; pp 102−140.
(50) Van Dishoek, E. F.; et al. In *Universe as Seen by ISO*; ESA-SP-*427*, ESA: Paris, 437−448, 1999.
(51) Charnley, S. B. *Astrophys. J.* **1997**, *481*, 396−405.
(52) El-Nawawy, M. S.; Howe, D. A.; Millar, T. J. *Mon. Not. R. Astron. Soc.* **1997**, *292*, 481−489.
(53) Van der Tak, F. F. S.; van Dishoek, E. F.; Caselli, P. *Astron. Astrophys.* **2000**, *362*, 327−339.
(54) Charnley, S. B. *Astophys. Space Sci.* **1995**, *224*, 251−254.
(55) Van Dishoek, E. F.; et al. *Astron. Astrophys.* **1996**, *315*, L349−352.
(56) Yun, J. L.; Liseau, R. *ASP Conference Series 132*; ASP: San Francisco, 1998.
(57) Lai, S. P.; Crutcher, R. M. *Astrophys. J., Suppl. Ser.* **2000**, *128*, 271−286.
(58) Charnley, S. B.; Kress, M. E.; Tielens, A. G. G. M.; Millar, T. J. *Astrophys. J.* **1995**, *448*, 232−239.
(59) Dickens, J. E.; et al. *Astrophys. J.* **1997**, *489*, 753−757.
(60) Nummelin, A.; et al. *Astron. Astrophys.* **1998**, *337*, 275−286.
(61) Pan, J.; Albert, S.; Sastry, K. V. L. N.; Herbst, E.; de Lucia, F. C. *Astrophys. J.* **1998**, *499*, 517−519.
(62) Charnley, S. B.; Kaufman, M. J. *Astrophys. J. L.* **2000**, *529*, 111−114.
(63) Butler, R. A. H.; et al. *Astrophys. J., Suppl. Ser.* **2001**, *134*, 319−321.
(64) Kollis, J. M.; et al. *Astrophys. J. L.* **2001**, *554*, 81−85.
(65) Hollis, J. M.; Lovas, F. J.; Jewell, P. R. *Astrophys. J. L.* **2000**, *540*, 107−110.
(66) Mehringer, D. M.; Snyder, L. E.; Miao, Y.; Lovas, F. *Astrophys. J. L.* **1997**, *480*, 71−74.
(67) Liu, S. Y.; Mehringer, D. M.; Snyder, L. E. *Astrophys. J.* **2001**, *552*, 654−663.
(68) Wyrowski, F.; Schilke, P.; Walmsley, C. M. *Astron. Astrophys.* **1999**, *341*, 882−895.
(69) Gwenlan, C.; et al. *Astron. Astrophys.* **2000**, *354*, 1127−1133.
(70) Nummelin, A.; Bergman, P. *Astron. Astrophys.* **1999**, *341*, L59−62.
(71) Minh, Y. C.; Dickens, J. E.; Irvine, M.; McGonagle, D. *Astron. Astrophys.* **1995**, *298*, 213−218.
(72) Turner, B. E. *Astrophys. J. L.* **1990**, *362*, 29−33.
(73) Ceccarelli, C.; et al. *Astron. Astrophys.* **1998**, *338*, L43−46.
(74) Dickens, J. E.; Irvine, W. M. *Astrophys. J.* **1999**, *518*, 733−739.
(75) Rodgers, S. D.; Charnley, S. B. *Astrophys. J.* **2001**, *553*, 613−617.
(76) Charnley, S. B.; Tielens, A. G. G. M.; Rodgers, S. D. *Astrophys. J. L.* **1997**, *482*, 203−206.
(77) Teixeira, T. C.; Devlin, J. P.; Buch, V.; Emerson, J. P. *Astron. Astrophys.* **1999**, *347*, L19−22.
(78) Schutte, W. A.; Greenberg, J. M. *Astron. Astrophys.* **1991**, *244*, 190−204.
(79) Schutte, W. A. In *Solid Interstellar Matter: The ISO Revolution*; d'Hendecourt, L., Joblin, C., Jones, A., Eds.*;* Springer: Berlin, 1999; pp 183−198.
(80) Kessler, M. F.; et al. *Astron. Astrophys.* **1996**, *315*, L27−L31.
(81) Lahuis, F.; van Doshoek, E. F. *Astron. Astrophys.* **2000**, *355*, 699−712.
(82) Ehrenfreund, P.; Schutte, W. A. Minh, Y. C.; van Dishoek, E. F. *Astrochemistry: From Molecular Clouds to Planetary Systems*; ASP: San Francisco, 2000; pp 135−146.
(83) Ehrenfreund, P.; Dartois, E.; Demyk, K.; d'Hendecourt, L. *Astron. Astrophys.* **1998**, *339*, L17−20.
(84) Gibb, E. L. *Astrophys. J.* **2000**, *536*, 347−356.
(85) Boudin, N.; Schutte, W. A.; Greenberg, J. M. *Astron. Astrophys.* **1998**, *331*, 749−759.
(86) Gibb, E. L.; et al. *Astrophys. J.* **2000**, *536*, 347−356.
(87) Ehrenfreund, P.; et al. *Icarus* **1997**, *123*, 1−15.
(88) Whittet, D. C. B.; et al. *Astrophys. J. L.* **1998**, *498*, 159−163.
(89) Gerakines, P. A.; et al. *Astrophys. J.* **1999**, *522*, 357−377.
(90) Whittet, D. C. B.; et al. *Astrophys. J. L.* **1998**, *498*, 159−163,
(91) Boogert, A. C. A.; et al. *Astron. Astrophys.* **2000**, *353*, 349−362.
(92) Teixeira, T. C.; Emerson, J. P.; Palumbo, M. E. *Astron. Astrophys.* **1998**, *330*, 711−725.
(93) Ehrenfreund, P.; et al. *Astron. Astrophys.* **1996**, *315*, L341−344.
(94) Boogert, A. C. A. *Astron. Astrophys.* **1996**, *315*, L377−380.
(95) Boogert, A. C. A.; et al. *Astron. Astrophys.* **1998**, *336*, 352−358.
(96) Schutte, W. A.; Gerakines, P. A.; Geballe, T. R.; van Dishoek, E. F.; Greenberg, J. M. *Astron. Astrophys.* **1996**, *309*, 633−647.
(97) Palumbo, M. E.; Geballe, T. R.; Tielens, A. G. G. M. *Astrophys. J.* **1997**, *479*, 839−844.
(98) Dartois, E.; et al. *Astron. Astrophys.* **1999**, *342*, L32−35.
(99) Schutte, W. A.; et al. *Astron. Astrophys.* **1996**, *315*, L333−336.
(100) Schutte, W. A.; et al. *Astron. Astrophys.* **1999**, *343*, 966−976.
(101) Nejad, L. A. M.; Millar, T. J. *Astron. Astrophys.* **1987**, *183*, 279−286,.
(102) Lindqvist, M.; Schöier, F. L.; Lucas, R.; Olofsson, H. *Astron. Astrophys.* **2000**, *361*, 1036−1057.
(103) Jorgensen, U. G.; Hron, J.; Loidl, R. *Astron. Astrophys.* **2000**, *356*, 253−266.
(104) Monnier, J. D.; Danchi, W. C.; Hale, D. S.; Tuthill, P. G.; Townes, C. H. *Astrophys. J.* **2000**, *543*, 868−879.
(105) Cernicharo, J.; Guelin, M.; Kahane, *Astron. Astrophys. J, Suppl. Ser.* **2000**, *142*, 181−215.
(106) Guelin, M.; Neininger, N.; Cernicharo, J. *Astron. Astrophys.* **1998**, *335*, L1−4.

(107) Alksne, Z. K.; Alksnis, A. K.; Dzervitis, U.K. *Properties of Galactic Carbon Stars*; Orbit: Malabar, 1991.
(108) Millar, T. J.; Herbst, E.; Bettens, R. P. A. *Mon. Not. R. Astron. Soc.* **2000**, *316*, 195−203.
(109) Cernicharo, J.; et al. *Astron. Astrophys.* **1996**, *315*, L201−204.
(110) Herpin, F.; Cernicharo, J. *Astrophys. J. L.* **2000**, *530*, 129−132.
(111) Latter, W. B.; Charnley, S. B. *Astrophys. J. L.* **1996**, *463*, 37−40.
(112) Le Bertre, T. *Astron. Astrophys.* **1997**, *324*, 1059−1070.
(113) Doty, S. D.; Leung, C. M. *Mon. Not. R. Astron. Soc.* **1997**, *286*, 1003−1011.
(114) Groenewegen, J. *AA.* **1997**, *317*, 503−520.
(115) Williams, D. A. *Chem. Eur. J.* **1997**, *3*, 1929−1932.
(116) Wing, R. F. *The Carbon Star Phenomenon*; IAU, Kluwer: Dordrecht, 2000.
(117) Hasegawa, YT.; Volk, K.; Kwok, S. *Astrophys. J.* **2000**, *532*, 994−1005.
(118) Kwok, S. *The Origin and Evolution of Planetary Nebulae*; Cambridge University Press: Cambridge, 2000.
(119) Gammie, C. F.; Knapp, G. R.; Young, K.; Phillips; T. G.; Falgarone, E. *Astrophys. J. L.* **1989**, *345*, 87−89.
(120) Yan, M.; Federman, S. R.; Dalgarno, A.; Bjorkman, J. E. *Astrophys. J.* **1999**, *515*, 640−648.
(121) Cernicharo, J.; et al. *Astrophys. J. L.* **2001**, *546*, 123−126.
(122) Cernicharo, J.; et al. *Astrophys. J. L.* **2001**, *546*, 127−130.
(123) Billing, G. D.; Mikkelsen, K.V. *Introduction to Molecular Dynamics and Chemical Kinetics;* Wiley: New York, 1996.
(124) House, J. E.; Brown, W. C. *Principles of Chemical Kinetics*; Publisher: Dubuque, 1997.
(125) EspensonJ. H. *Chemical Kinetics and Reaction Mechanisms;* McGraw-Hill: New York, 1995.
(126) Pilling, M. J.; Seakins P. W. *Reaction Kinetics*; Oxford University Press: Oxford, 1995.
(127) Billing, G. D.; Mikkelsen, K. V. *Advanced Molecular Dynamics and Chemical Kinetics*; Wiley: New York, 1997.
(128) Steinfeld, J. I.; Francisco, J. S.; Hase, W. L. *Chemical Kinetics and Dynamics*; Prentice Hall: New York, 1989.
(129) Houston, P. I. *Chemical Kinetics and Reaction Dynamics*; McGraw-Hill: Boston, 2001.
(130) McQuarrie, D. A.; Simons, J. D. *Physical Chemistry−A Molecular Approach*; University Science Books: Sausalito, 1997.
(131) Bernstein,R. B. *Atom-Molecule Collision Theory;* Plenum Press: New York, 1984.
(132) Child, M. S. *Molecular Collision Theory*; Dover: New York, 1974.
(133) Stone, A.J. *The Theory of Intermolecular Forces*; Clarendon Press: Oxford, 1996.
(134) Wyatt, R. E.; Zhang J. Z. J. H. *Dynamics of Molecules and Chemical Reactions*; Marcel Dekker: New York, 1996.
(135) Lee, Y.T. In *Atomic and Molecular Beams*; Scoles, G., Ed.; Oxford University Press: Oxford, 1988; Vol. 1, pp 553−568.
(136) *Atomic and Molecular Beams*; Scoles, G., Ed.; Oxford University Press: Oxford, 1992; Vol. 2.
(137) Levine, R. D.; Bernstein, R.B. *Molecular Reactions and Chemical Reactivity*; Oxford University Press: Oxford, 1987.
(138) *Symposium on Titan* 1992; ESA-SP-338. Huygens−Science, Payload, and Mission, ESA- SP-1177, 1997.
(139) Whittet, D. C. B. *Dust in the Galactic Environments;* IOP: Bristol, 1992.
(140) Tielens, A. G. G. M.; Allamandola, L. J. In *Interstellar Processes*; Hollenach, D. J., Thronson, H. A., Eds.; Reidel, Dordrecht, 1987; pp 397−410.
(141) Schmitt, B. In *Molecules and Grains in Space*; Nenner, I., Ed.; AIP Press, New York, 1994, pp 735−750.
(142) Manico, G.; Raguni, G.; Pirronello, V.; Roser, J. E.; Vidali, G. *Astrophys. J. L.* **2001**, *548*, 253−256.
(143) Biham, O.; Furman, I.; Katz, N.; Pirronello, V.; Vidali, G. *Mon. Not. R. Astron. Soc.* **1998**, *296*, 869−872.
(144) Pirronello, V.; Liu, C.; Shen, L.; Vidali, G. *Astrophys. J. L.* **1997**, *475*, 69−72.
(145) Biham, O.; Furman, I.; Pirronello, V.; Vidali, G. *Astrophys. J.* **2001**, *553*, 595−603.
(146) Rutigliano, M.; Cacciatore, M.; Billing, G. D. *Chem. Phys. Lett.* **2001**, *340*, 13−20.
(147) Kim, Y. H.; Ree, J.; Shin, H. K. *Chem. Phys. Lett.* **1999**, *314*, 1−8.
(148) Smoluchowski, R. *Astrophys. Space Sci.* **1981**, *75*, 353−363.
(149) Katz, N.; Furman, I.; Biham, O.; Pirronello, V.; Vidali, G. *Astrophys. J.* **1999**, *522*, 305−312.
(150) Pirronello, V.; Liu, C.; Roser, J. E.; Vidali, G. *Astron. Astrophys.* **1999**, *244*, 681−686.
(151) Smith, R. *Atomic and Ion Collisions in Solids and at Surfaces*; Cambridge University Press: Cambridge, 1997.
(152) Takahashi, J.; Masuda, K.; Nagaoka, M. *Mon. Not. R. Astron. Soc.* **1999**, *306*, 22−30.
(153) Pirronello, V.; Biham, O.; Liu, C.; Shen, L.; Vidali, G. *Astrophys. J. L.* **1997**, *483*, 131−134.
(154) Hasegawa, T. I.; Herbst, E. *Mon. Not. R. Astron. Soc.* **1993**, *263*, 589−606.
(155) Lee, H. H.; Bettens, R. P. A.; Herbst, E. *Astron. Astrophys. S. S.* **1996**, *119*, 111−114.
(156) Hasegawa, T. I.; Herbst, E.; Leung, C. M. *Astrophys. J.* **1992**, *82*, 167−195.
(157) Hasegawa, T. I.; Herbst, E. *Mon. Not. R. Astron. Soc.* **1993**, *261*, 83−102.
(158) Flower, D. R. *Mon. Not. R. Astron. Soc.* **1997**, *288*, 627−630.
(159) Ruffle, D. P.; Williams, D. A.; Duley, W. W. *Mon. Not. R. Astron. Soc.* **1998**, *296*, 746.
(160) Thi, W. F.; et al. *Astrophys. J. L.* **1999**, *521*, 63−66.
(161) Wright, C. M.; van Dishoek, E. F.; Cox, P.; Sidher, S. D.; Kessler, M. F. *Astrophys. J. L.* **1999**, *515*, L29−35.
(162) Cesarsky, D.; Cox, P.; Pineau des Forets, G.; van Dishoek, E. F.; Boulanger, F.; Wright, C. M. *Astron. Astrophys.* **1999**, *348*, 945−949.
(163) Wright, C. M.; Drapatz, S.; Timmermann, R.; van der Werf, R. P.; Katterloher, R.; de Graauw, T. *Astron. Astrophys.* **1996**, *315*, L301−304.
(164) Thi, W. F.; et al. *Nature* **2001**, *409*, 60−62.
(165) Wesselius, P. R. *Astron. Astrophys.* **1996**, *315*, L197−200.
(166) Federman, S. R.; Cardelli, J. A.; van Dishoek, E. F.; Lambert, D. L.; Black, J. H. *Astrophys. J.* **1995**, *445*, 325−329.
(167) Takahiahi, J.; Masuda, K.; Nagaoka, M. *Astrophys. J.* **1999**, *520*, 724−731.
(168) Le Bourlot, J. *Astron. Astrophys.* **2000**, *360*, 656−662.
(169) Parneix, P.; Brechignac, P. *Astron. Astrophys.* **1998**, *334*, 363−375.
(170) Field, D. *Astron. Astrophys.* **2000**, *362*, 774−779.
(171) Weingartner, J. C.; Draine, B. T. *Astrophys. J., Suppl. Ser.* **2001**, *134*, 263−281.
(172) Hiraoka, K.; et al. *Astrophys. J.* **1998**, *498*, 710−715.
(173) Hiraoka, K. *Astrophys. J.* **1995**, *443*, 363−370.
(174) Tielens, A. G. G. M.; Hagen, W. *Astron. Astrophys.* **1982**, *114*, 245−260.
(175) Ruffle, D. Herbst, E. *Mon. Not. R. Astron. Soc.* **2000**, *319*, 837−850.
(176) Miao, Y.; Snyder, L. E. *Astrophys. J. L.* **1997**, *480*, 67−70.
(177) D'Hendecourt, L. B.; Allamandolla, L. J.; Greenberg, J. M. *Astron. Astrophys.* **1985**, *152*, 130−150.
(178) Hollis, J. M.; Churchwell, E. *Astrophys. J.* **2001**, *551*, 803−806.
(179) Hiraoka, K.; et al. *Astrophys. J.* **2000**, *532*, 1029−1037.
(180) Dartois, E.; Demyk, K.; d'Hendecourt, L.; Ehrenfreud, P. *Astron. Astrophys.* **1999**, *351*, 1066−1069.
(181) Gerakines, P. A.; Schutte, W. A.; Ehrenfreund, P. *Astron. Astrophys.* **1996**, *312*, 289−305.
(182) Grim, R. J. A.; et al. *Astron. Astrophys. J., Suppl. Ser.* **1989**, *78*, 161−186.
(183) Watanabe, N.; Horii, T.; Kouchi, A. *Astrophys. J.* **2000**, *541*, 772−778.
(184) Allamandolla, L. J.; Bernstein, M. P.; Sandford, S. A.; Walker, R. L. *Space Sci. Rev.* **1999**, *90*, 219−232.
(185) Roessler, K. In *Solid State Astrophysics 'Suprathermal Chemistry in Space'*; Bologna, 1991.
(186) Johnson, R. E. *Energetic Charged Particle Interactions with Atmospheres and Surfaces;* Springer: Berlin, 1990.
(187) Palumbo, M. E.; Castorina, A. C.; Strazzulla, G. *Astron. Astrophys.* **1999**, *342*, 551−562.
(188) Hudson, R. L.; Moore, M. H. *Icarus* **1999**, *140*, 451−461.
(189) Palumbo, M. E.; Pendleton, Y. J.; Strazzulla, G. *Astrophys. J.* **2000**, *542*, 890−893.
(190) Gerakines, P. A.; Moore, M. H.; Hudson, R. L. *Astron. Astrophys.* **2000**, *357*, 793−800.
(191) Brucato, J. R.; Palumbo, M. E.; Strazzulla, G. *Icarus* **1997**, *125*, 135−144.
(192) Strazzulla, G.; et al. *Astron. Astrophys.* **1998**, *338*, 292−294.
(193) Palumbo, M. E.; et al. *Astron. Astrophys.* **1998**, *334*, 247−252.
(194) Kaiser, R. I.; Mahfouz, R. M.; Roessler, K. *Nucl. Instrum. Methods* **1992**, *B65*, 468−471.
(195) Strazzulla, G.; Palumbo, M. E. *Planet. Space Sci.* **1998**, *46*, 1339−1348.
(196) Pirronello, V. In *Chemistry in Space*; Pirronello, V., Greenberg, J. M., Eds.; Kluwer: New York, 1991; pp 263−303.
(197) Roessler, K. In *Solid State Astrophysics*; Italiana di Fisica, 1991; pp 197−266.
(198) Hudson, R. L.; Moore, M. H. *Icarus* **1997**, *126*, 233−235.
(199) Notesco, G.; Laufer, D.; Bar-Nun, A. *Icarus* **1997**, *125*, 471−473.
(200) Johnson, R. E. *Rev. Mod. Phys.* **1996**, *68*, 305−312.
(201) Heyl, M. *Rep. Jül.* **1990**, *2409*.
(202) Kaiser, R. I.; Eich, G.; Gabrysch, A.; Roessler, K. *Astrophys. J.* **1997**, *484*, 487−498.
(203) Kaiser, R. I.; Roessler, K. *Astrophys. J.* **1998**, *503*, 959−975.
(204) Kaiser, R. I.; Roessler, K. *Astrophys. J.* **1997**, *475*, 144−154.
(205) Schutte, W. A.; Greenberg, J. M. *Astron. Astrophys.* **1991**, *244*, 190−195.
(206) Dzegelinko, F.; Herbst, E. *Astrophys. J. L.* **1995**, *443*, 81−83.
(207) Galloway, E. T.; Herbst, E. *Astron. Astrophys.* **1994**, *287*, 633−640.

(208) Gindulyte, A.; Massa, L.; Banks, B. A.; Rutledge, S. K. *J. Phys. Chem. A.* **2000**, *104*, 9976−9982.
(209) Westey, M. S.; Baragiola, R. A.; Johnson, R. E.; Baratta, G. A. *Nature* **1995**, *373*, 405−407.
(210) Herbst, E.; Klemperer, W. *Astrophys. J.* **1973**, *185*, 505−515.
(211) Herbst, E.; Adams, N. G.; Smith, D. *Astrophys. J.* **1984**, *285*, 618−632.
(212) Klemperer, W. *Annu. Rev. Phys. Chem.* **1995**, *46*, 1−26.
(213) Smith, D. *Chem. Rev.* **1992**, *92*, 1473−1485.
(214) Dalgarno, A. *Int. J. Mass. Spectrom. Ion Processes* **1995**, *149/150*, 429−437.
(215) Flower, D. R. *Int. Rev. Phys. Chem.* **1995**, *14*, 421−443.
(216) Gerlich, D. *J. Chem. Soc., Faraday Trans.* **1993**, *89*, 2199−2208.
(217) Herbst, E. *Angew. Chem.* **1990**, *102*, 627−641.
(218) Gerlich, D.; Horning, S. *Chem. Rev.* **1992**, *92*, 1509−1539.
(219) Mark, S.; Gerlich, D. *Chem. Phys.* **1996**, *209*, 235−257.
(220) Herbst, E. *Annu. Rev. Phys. Chem.* **1995**, *46*, 27−53.
(221) Babb, J. F.; Kirby, K. P. In *The Molecular Astrophysics of Stars and Galaxies;* Oxford Science Publications: Oxford, 1998; pp 11−36.
(222) Gerlich, D. *J. Chem. Phys.* **1989**, *90*, 3574−3581.
(223) Tosi, P.; Dmitriev, O.; Bassi, D.; Wick, O.; Gerlich, D. *J. Chem. Phys.* **1994**, *100*, 4300−4307.
(224) Mark, S.; et al. *J. Phys. Chem.* **1995**, *99*, 15587−15594.
(225) Winnewisser, G.; Herbst, E. *Top. Curr. Chem.* **1989**, *137*, 121−139.
(226) Gerlich, D.; Disch, R.; Scherbarth, S. *J. Chem. Phys.* **1987**, *87* 350−359.
(227) Mark, S.; Gerlich, D. *C. P. L.* **1996**, *209*, 235−257.
(228) Dalgarno, A. *J. Chem. Soc., Faraday Trans.* **1993**, *89*, 2111−2117.
(229) Andreazza, C. M.; Singh, P. D. *Mon. Not. R. Astron. Soc.* **1997**, *287*, 287−292.
(230) Bettens, R. P. A.; Herbst, E. *M. S. I. P.* **1995**, *149/150*, 321−343.
(231) Tennyson, J.; Miller, S.; Schild, H. *J. Chem. Soc., Faraday Trans.* **1993**, *89*, 2155−2159.
(232) Cordonnier; et al. *J. Chem. Phys.* **2000**, *113*, 3181−3193.
(233) Stark, R.; van der Tak, F. F. S.; van Dishoeck, E. F. *Astrophys. J. L.* **1999**, *521*, 67−70.
(234) Oka, T.; Jagod, M. F. *J. Chem. Soc., Faraday Trans.* **1993**, *89*, 2147−2154.
(235) Geballe, T. R.; McCall, B. J.; Hinkle, K. H.; Oka, T. *Astrophys. J.* **1999**, *510*, 251−257.
(236) Geballe, T. R.; Oka, T. *Nature* **1996**, *384*, 334−335.
(237) McCall, B. J.; Geballe, T. R.; Hinkle, K. H.; Oka, T. *Astrophys. J.* **1999**, *522*, 338−348.
(238) McCall, B. J.; Geballe, T. R.; Hinkle, K. H.; Oka, T. *Science.* **1998**, *279*, 1910−1913.
(239) McCall, B. J.; Hinkle, K. H.; Geballe, T. R.; Oka, T. *Faraday Discuss.* **1998**, *109*, 267.
(240) Takagi, N.; Fukuzawa, K.; Osamura, Y.; Schaefer, H. F. *Astrophys. J.* **1999**, *525*, 791−798.
(241) Yamamoto, S.; et al. *Astrophys. J.* **1990**, *348*, 363−369.
(242) Yamamoto, S.; Saito, S. *Astrophys. J.* **1990**, *363*, L13−16.
(243) Maluendes, S. A.; McLean, A. D.; Herbst, E. *Astrophys. J.* **1993**, *417*, 181−186.
(244) Osamura, Y.; Fukuzawa, K.; Terzieva, R.; Herbst, E. *Astrophys. J.* **1999**, *519*, 679−704.
(245) Millar, T. J.; Herbst, E. *Astron. Astrophys.* **1994**, *288*, 561−571.
(246) Umemoto, H.; et al. *Bull. Chem. Soc. Jpn.* **1986**, *59*, 1449−1454.
(247) Sato, K.; et al. *J. Phys. Chem. A* **1999**, *103*, 8650−8656.
(248) Takayanagi, T.; et al. *J. Phys. Chem. A* **1998**, *102*, 10391−10398.
(249) Kurosaki, Y.; et al. *J. Phys. Chem. A* **1998**, *102*, 254−259.
(250) Takayanagi, T.; et al. *J. Phys. Chem. A* **1999**, *103*, 250−255.
(251) Kurosaki, Y.; Takayanagi, T. *J. Phys. Chem. A* **1999**, *103*, 436−442.
(252) Takayanagi, T.; et al. *J. Phys. Chem. A* **1998**, *102*, 6251−6258.
(253) Huang, X.; Xing, G.; Bersohn, R. *J. Chem. Phys.* **1994**, *101*, 5818−5823.
(254) Schmoltner, A. M.; Chu, P. M.; Lee, Y. T. *J. Chem. Phys.* **1989**, *61*, 5365−5373.
(255) Yarkony, D. R. *J. Phys. Chem. A* **1998**, *102*, 5305−5311.
(256) Dyke, J. M.; Shaw, A. N.; Wright, T. G. *J. Phys. Chem.* **1995**, *99*, 14207−14216.
(257) Harding, L. B.; Wagner, A. F. *J. Phys. Chem.* **1986**, *90*, 2974−2987.
(258) Xing, G.; Huang, X.; Wang, X.; Bersohn, R. *J. Chem. Phys.* **1996**, *105*, 488−495.
(259) Schmoltner, A. M.; Chu, P. M.; Brudzynski, R. J.; Lee, Y. T. *J. Chem. Phys.* **1989**, *91*, 6926−6936.
(260) Abou-Zied, O. K.; McDonald, J. D. *J. Chem. Phys.* **1998**, *109*, 1293−1301.
(261) Dupuis, M.; Wendoloski, J. J.; Takada, T.; Lester, W. A. *J. Chem. Phys.* **1982**, *76*, 481−487.
(262) Quandt, R.; Min, Z.; Wang, X.; Berson, R. *J. Phys. Chem. A* **1998**, *102*, 60−64.
(263) Corchado, J. C.; et al. *J. Phys. Chem. A* **1998**, *102*, 4899−4910.
(264) Hodgson, D.; Zhang, H. Y.; Nimlos, M. R.; McKinnon, J. T. *J. Phys. Chem. A* **2001**, *105*, 4316−4327.
(265) Roberto-Neto, O.; Machado, F. B. C.; Truhlar, D. G. *J. Chem. Phys.* **1999**, *111*, 10046−10052.
(266) Wrobel, R.; Sander, W.; Kraka, E.; Cremer, D. *J. Phys. Chem. A* **1999**, *103*, 3693−3705.
(267) Bettens, R. P. A.; Lee, H. H.; Herbst, E. *Astrophys. J.* **1995**, *443*, 664−674.
(268) Moskaleva, L. V.; Lin, M. C. *J. Phys. Chem. A* **1998**, *102*, 4687−4693.
(269) Barone, V.; Orlandini, L. *Chem. Phys. Lett.* **1995**, *246*, 45−52.
(270) Thorn, R. P.; et al. *J. Phys. Chem. A* **1998**, *102*, 846−851.
(271) Payne, W. A.; Monks, P. S.; Nesbitt, F. L.; Stief, L. J. *J. Chem. Phys.* **1996**, *104*, 9808−9815.
(272) Donaldson, D. J.; Okuda, I. V.; Sloan, J. *J. Chem. Phys.* **1995**, *193*, 37−45.
(273) Gonzales, C.; Schlegel, H. B. *J. Am. Chem. Soc.* **1992**, *114*, 9118−9122.
(274) Knyazev,; Slagle, I. R. *J. Phys. Chem. A* **2001**, *105*, 3196−3204.
(275) Herbst, E.; Terzieva, R.; Talbi, D. *Mon. Not. R. Astron. Soc.* **2000**, *311*, 869−876
(276) Keene, J.; et al. *Astrophys. J.* **1993**, *415*, L131−134.
(277) Van der Keen, W. E. C. J.; Huggins, P. J.; Matthews, H. E. *Astrophys. J.* **1998**, *505*, 749−755.
(278) Ingallis, J. G.; et al. *Astrophys. J.* **1997**, *479*, 296−302.
(279) Wilson, C. D. *Astrophys. J. L.* **1997**, *487*, 49−52.
(280) Young, K., *Astrophys. J.* **1997**, *488*, L157−160.
(281) Sofia, U. J.; et al. *Astrophys. J. L.* **1997**, *482*, 105−108.
(282) White, G. J.; Sandell, G. *Astron. Astrophys.* **1995**, *299*, 179−192.
(283) Lambert, D. L.; Sheffer, Y.; Federman, S. R. *Astrophys. J.* **1995**, *438*, 740−749.
(284) Crawford, I. A. *Mon. Not. R. Astron. Soc.* **1997**, *290*, 41−48.
(285) Maier, J. P.; Lakin, N. M.; Walker, G. A. H.; Bohlender, D. A. *Astrophys. J.* **2001**, *553*, 267−273.
(286) Haffner, L. M.; Meyer, D. M. *Astrophys. J.* **1995**, *453*, 450−453.
(287) Van Dishoek, E. F.; Black, J. *Astrophys. J.* **1989**, *343*, 273−297.
(288) Van Orden, A.; Saykally, R. J. *Chem. Rev.* **1998**, *98*, 2313−2357.
(289) Weltner, W.; van Zee, R. J. *Chem. Rev.* **1989**, *89*, 1713−1747.
(290) Crawford, I. A. *Mon. Not. R. Astron. Soc.* **1990**, *244*, 646−651.
(291) Combi, M. R.; Fink, U. *Astrophys. J.* **1997**, *484*, 879−890.
(292) Hinke, K. H.; Keady, J. J.; Bernath, P. F. *Science* **1988**, *241*, 1319−1322.
(293) Giesen, T. F.; et al. *Astrophys. J. L.* **2001**, *551*, 181−184.
(294) Huggins, W. *Proc. R. Soc.* **1982**, *33*, 1−5.
(295) Sorkhabi, O.; et al. *Planet. Space Sci.* **1997**, *45*, 721−730.
(296) Swamy, K. S. K. *Astron. Astrophys.* **1996**, *313*, 323−326.
(297) Rousselot, P.; et al. *Icarus* **2000**, *146*, 263−269.
(298) Swamy, K. S. K. *Astrophys. J.* **1997**, *481*, 1004−1006.
(299) Brown, S. T.; Rienstra-Kiracofe, J. C.; Schaefer, H. F. *J. Phys. Chem. A.* **1999**, *103*, 4065−4077.
(300) Crawford, T. D.; Stanton, J. F.; Saeh, J. C.; Schaefer, H. F. *J. Am. Chem. Soc.* **1999**, *121*, 1902−1911.
(301) Apponi. A. J.; et al. *Astrophys. J. L.* **2001**, *547*, 65−68.
(302) Bell, M. B.; et al. *Astrophys. J.* **1999**, *518*, 740−747.
(303) Travers, M. J.; McCarthy, M. C.; Gottlieb, C. A.; Thaddeus, P. *Astrophys. J. L.* **1997**, *483*, 135−138.
(304) McCarthy, M. C.; et al. *Science* **1997**, *275*, 518−520.
(305) Seburg, R. A.; McMahon, R. J.; Stanton, J. F.; Gauss, J. *J. Am. Chem. Soc.* **1997**, *119*, 10838−10845.
(306) Turner, B. E. *Astrophys. J.* **1989**, *347*, L39−42.
(307) Doty, S. D.; Leung, C. M. *Astrophys. J.* **1998**, *502*, 898−908.
(308) Terzieva, R.; Herbst, E. *Astrophys. J.* **1998**, *501*, 207−220.
(309) Blanksby, S. J.; et al. *J. Phys. Chem. A* **1998**, *102*, 9949−9956.
(310) Ohishi, M.; Kaifu, N. *Faraday Discuss.* **1998**, *109*, 205−221.
(311) Langer, W. D.; et al. *Astrophys. J. L.* **1997**, *480*, 63−66.
(312) Thaddeus, P.; et al. *Astrophys. J. L.* **1985**, *294*, 49−53.
(313) Magnum.; Wotton, A. *Astron. Astrophys.* **1990**, *239*, 319−325.
(314) Yamamoto, S.; Saito, S.; Ohishi, M.; Suzuki, H.; Ishikawa, S. I.; Kaifu, N.; Murakami, A. *Astrophys. J.* **1987**, *322*, L55−58.
(315) Kuiper, T. B. H.; et al. *Astrophys. J.* **1993**, *416*, L33−36.
(316) Cox, P.; Walmsley, C. M.; Güsten, R. *Astron. Astrophys.* **1989**, *209*, 382−390.
(317) Bell, M. B.; et al. *Astrophys. J.* **1988**, *326*, 924−930.
(318) Broillet, N.; Baudry, A.; Daigne, G. *Astron. Astrophys.* **1988**, *199*, 312−317.
(319) Fosse, D.; Cernicharo, J.; Gerin, M.; Cox, P. *Astrophys. J.* **2001**, *552*, 168−174.
(320) Lucas, R.; Liszt, H. S. *Astron. Astrophys.* **2000**, *358*, 1069−1076.
(321) Thaddeus, P.; Vrtilek, J. M.; Gottlieb, C. A. *Astrophys. J. L.* **1985**, *299*, L63−66.
(322) Turner, B. E.; Rickard, L. J.; Xu, L. P. *Astrophys. J.* **1989**, *344*, 292−305.
(323) Cernicharo, J.; et al. *Astrophys. J. L.* **1991**, *368*, 39−41.
(324) Foltin, M.; et al. *J. Chem. Phys.* **1997**, *107*, 6246−6256.
(325) Pascoli, G.; Polleux, A. *Astron. Astrophys.* **2000**, *359*, 799−810.
(326) Lin, Y. T.; Mishra, R. K.; Lee, S. L. *J. Phys. Chem. B* **1999**, *103*, 3151−3155.
(327) Saunders, M.; et al. *Science* **1996**, *271*, 1693−1697.

(328) Suzuki, H.; et al. *Astrophys. J.* **1992**, *392*, 551−570.
(329) Ohishi, M.; Kaifu, N. *Faraday Discuss.* **1998**, *109*, 205−216.
(330) Ungerechts, H.; et al. *Astrophys. J.* **1997**, *482*, 245−266.
(331) Bachiller, R.; et al. *Astron. Astrophys.* **1997**, *319*, 235−243.
(332) Bakker, E. J.; et al. *Astron. Astrophys.* **1997**, *323*, 469−487.
(333) Lavasseur-Regourd, A. C.; Raulin, F. *Prebiotic Chemistry in Space;* Elsevier: New York, 1995.
(334) *Exobiology*; Chela-Flores, J., Raulin, F., Eds.; Kluwer: Dordrecht, 1998.
(335) Yson, F. *Origins of Life;* Cambridge University Press: Cambridge, 1999.
(336) Thomas, P. J.; Chyba, C. F.; McKay, C. P. *Comets and the Origin of Life*; Springer: Berlin, 1997.
(337) *Exobiology in the Solar System;* ESA-SP-*1231*, Paris.
(338) Tucker, K. D.; Kunter, M. L.; Thaddeus, P. *Astrophys. J.* **1994**, L115, 193.
(339) Saleck. A. H.; Simon, R.; Winnewisser, G.; Wouterloot, J. G. A. *Can. J. Phys.* **1994**, *72*, 747−754.
(340) Fuente, A.; Cernicharo, J.; Omont, A. *Astron. Astrophys.* **1998**, *330*, 232−242.
(341) De Graauw, Th.; et al. *Astron. Astrophys.* **1997**, *321*, L13−16.
(342) Bandy, R. E.; Lakshiminaragan, C.; Frost, R. K.; Zwier, T. S. *Science* **1992**, *258*, 1630.
(343) Allamandola, L.; Tielens, J.; Barker, J. R. *Astrophys. J., Suppl. Ser.* **1989**, *71*, 733−775.
(344) De Muizon, M. J.; d'Hendecourt, L. B.; Geballe, T. R. *Astron. Astrophys.* **1990**, *235*, 367−378.
(345) Bernard, J. P.; d'Hendecourt, L. B.; Leger, A. *Astron. Astrophys.* **1998**, *220*, 245−248.
(346) Cossart-Magos, C.; Leach, S. *Astron. Astrophys.* **1990**, *233*, 559−569.
(347) Verstraete, L.; Leger, A. *Astron. Astrophys.* **1992**, *2656*, 513−519.
(348) Hudgins, D. M.; Sandford, S. A. *J. Phys. Chem. A* **1998**, *102*, 344−352.
(349) Salama, F.; Joblin, C.; Allamandola, L. *J. Planet. Space Sci.* **1995**, *43*, 1165−1173.
(350) Moutou, C.; et al. *Astron. Astrophys.* **2000**, *354*, L17−20.
(351) Joblin, C.; et al. *Astron. Astrophys.* **1995**, *299*, 835−846.
(352) Coupanec, P. L.; Rouan, D.; Moutou, C.; Leger, A. *Astron. Astrophys.* **1999**, *347*, 669−675.
(353) Schlemmer, S.; Cook, D. J.; Harrison, J. A.; Wurfel, B.; Chapman, W.; Saykally, R. J. *Science* **1994**, *265*, 1686−1689.
(354) Jourdain de Muizon, M.; d'Hendecourt, L. B.; Geballe, T. R. *Astron. Astrophys.* **1990**, *227*, 526−541.
(355) Ehrenfreund, P.; Cami, J.; Dartois, E.; Foing, B. H. *Astron. Astrophys.* **1997**, *317*, L28−31.
(356) Joblin, C.; Tielens, A. G. G. M.; Allamandola, L. J.; Léger, A., d'Hendecourt, L.; Geballe, T. R.; Boissel, P. *Planet. Space Sci.* **1995**, *43*, 1189−1194.
(357) Salama, F.; Allamandola, L. J. *J. Chem. Soc., Faraday Trans.* **1993**, *89*, 2277−2284.
(358) Cook, D. J.; et al. *Nature* **1996**, *380*, 227−229.
(359) Mennella, V.; Colangeli, L.; Bussoletti, E. *Astrophys. J. L.* **1992**, *391*, 45−48.
(360) Duley, W. W. *Astrophys. J.* **1994**, *429*, L91−L93.
(361) Pino, T.; et al. *Chem. Phys. Lett.* **2001**, *339*, 64−70.
(362) Halasinski, T. M.; Hudgins, D. M.; Salama, F.; Allamaodola, L. J.; Bally, T. *J. Phys. Chem. A* **2000**, *104*, 7484−7491.
(363) Chillier, X. D. F.; Stone, B. M.; Salama, F.; Allamandolla, L. J. *J. Chem. Phys.* **1999**, *111*, 449−451.
(364) Salama, F.; Alalmandola, L. J. *Nature* **1992**, *358*, 42−43.
(365) Oomens, J.; van Roij, A. J. A.; Maijer, G.; von Helden, G. *Astrophys. J.* **2000**, *542*, 404−410.
(366) Hudgins, D. M.; Sandford, S. A. *J. Phys. Chem. A* **1998**, *102*, 329−343.
(367) Ehrenfreund, RP.; Foing, B. H.; d'Hendecourt, L.; Jenniskens, P.; Desert, F. X. *Astron. Astrophys.* **1995**, *299*, 213−221.
(368) Hudgins, D. M.; Bauschlicher, C. W.; Allamandola, L. J.; Fetzer, J. C. *J. Phys. Chem. A* **2000**, *104*, 3655−3669.
(369) Joblin, C.; Tielens, A. G. G. M.; Geballe, T. R.; Wooden, D. H. *Astrophys. J.* **1996**, *460*, L119−L122.
(370) Sloan, G. C.; et al. *Astrophys. J. L.* **1999**, *513*, 65−68.
(371) Hudgins, D. M.; Allamandola, L. J. *J. Phys. Chem. A* **1997**, *101*, 3472−3477,
(372) Bauschlicher, C. W.; Langhoff, S. R. *Spectrochim. Acta A* **1997**, *53*, 1225−1240.
(373) Hudgins, D. M.; Sandford, S. A.; Alalmandola, L. J. *J. Phys. Chem.* **1994**, *98*, 4243−4253.
(374) Hudgins, D. M.; Allamandolla, L. J. *J. Phys. Chem.* **1995**, *99*, 8978−8986.
(375) Robinson, M. S.; Beegle, L. W.; Wdowiak, T. J. *Astrophys. J.* **1997**, *474*, 474−478.
(376) Salama, F.; Joblin, C.; Allamandola, L. J. *J. Chem. Phys.* **1994**, *101*, 10252−10262.
(377) Hudgins, D. M.; Sandford, S. A. *J. Phys. Chem. A* **1998**, *102*, 353−360.
(378) Cook, D. J.; Saykally, R. J. *Astrophys. J.* **1998**, *493*, 793−802.
(379) Parisel, O.; Berthier, G.; Ellinger, Y. *Astron. Astrophys.* **1992**, *266*, L1−L4.
(380) Lee, W.; Wdowiak, T. J. *Astrophys. J.* **1993**, *410*, L127−L130.
(381) Salama, F.; Allamandola, L. J. *Astrophys. J.* **1992**, *395*, 301−306.
(382) Szczepanski, J.; Vala, M. *Nature* **1993**, *363*, 699−701.
(383) Hudgins, D. M.; Allamandolla, L. J. *Astrophys. J. L.* **1999**, *516*, 41−44.
(384) Romanini, D.; et al. *Chem. Phys. Lett.* **1999**, *303*, 165−170.
(385) Brechnignac, P.; Pino, T. *Astron. Astrophys.* **1999**, *343*, L49−52.
(386) Bernstein, M. P.; Sandford, S. A.; Allamandola, L. J. *Astrophys. J.* **1996**, *472*, L127− L130.
(387) Pauzat, F.; Talbi, D.; Ellinger, Y. *Astron. Astrophys.* **1997**, *319*, 318−330,
(388) Bauschlicer, C. W.; Langhoff, S. R. *Chem. Phys.* **1998**, *234*, 79−86.
(389) De Muizon, M. J.; d'Hendecourt, L. B.; Geballe, T. R. *Astron. Astrophys.* **1990**, *227*, 526−541.
(390) Buch, V. *Astrophys. J.* **1989**, *343*, 208−211.
(391) Seahra, S. S.; Duley, W. W. *Astrophys. J.* **1999**, *520*, 719−723.
(392) Sandford, S. A. *Astrophys. J.* **1991**, *376*, 599−607.
(393) Pauzat, F.; Talbi, D.; Ellinger, Y. *Mon. Not. R. Astron. Soc.* **1999**, *304*, 241−253.
(394) Sloan, G. C.; et al. *Astrophys. J.* **1997**, *474*, 735−740.
(395) Joblin, C.; Tielens, A. G. G. M.; Allamandola, L. J.; Geballe, T. R. *Astrophys. J.* **1996**, *458*, 610−620.
(396) Snow, T. P.; Witt, A. N. *Science* **1995**, *270*, 1455−1460.
(397) Joblin, C.; Leger, A.; Martin, P. *Astrophys. J. L.* **1992**, *393*, 79−82.
(398) Salama, F.; et al. *Astrophys. J.* **1999**, *526*, 265−273.
(399) Moreels, G.; et al. *Astron. Astrophys.* **1994**, *282*, 643−656.
(400) Hony, S.; et al. *Astron. Astrophys.* **2001**, *370*, 1030−1043.
(401) Natta, A.; Krügel, E. *Astron. Astrophys.* **1995**, *302*, 849−860.
(402) Roelfsema, P. R.; et al. *Astron. Astrophys.* **1996**, *315*, L289−292.
(403) Molster, F. J.; et al. *Astron. Astrophys.* **1996**, *315*, L373−376.
(404) Siebenmorgen, R.; Krügel, E. *Astron. Astrophys.* **1992**, *259*, 614−626.
(405) Cohen, M.; et al. *Astrophys. J. L.* **1999**, *513*, 135−138.
(406) Allain, T.; Sedlmayr, E.; Leach, S.; *Astron. Astrophys.* **1997**, *323*, 163−176.
(407) Molster, F. J. *Astron. Astrophys. L.* **1996**, *315*, 373−376.
(408) Tielens, A. G. G. M. *Astrophys. Space Sci.* **1997**, *251*, 1−13.
(409) Beintema, D. *Astron. Astrophys. A* **1996**, *315*, L369−372.
(410) Beintema, D. A.; van den Ancker, M. E.; Waters, L. B. F. M.; et al. *Astron. Astrophys.* **1996**, *315*, L369−L372.
(411) Buss, R. H.; Tielens, A. G. G. M.; Snow, T. P. *Astrophys. J.* **1991**, *372*, 281−290.
(412) Hanner, M. S.; Tokunaga, A. T.; Geballe, T. R. *Astrophys. J. L.* **1992**, *395*, 111−113.
(413) Schutte, W. A.; Tielens, A. G. G. M.; Allamandola, L. J.; Cohen, M.; Wooden, D. H. *Astrophys. J.* **1990**, *360*, 577−589.
(414) Schutte, W. A.; et al. *Astron. Astrophys.* **1998**, *337*, 261−274.
(415) Cook, D. J.; Saykally, R. J. *Astrophys. J.* **1998**, *493*, 793−802.
(416) Kim, H. S.; Wagner, D. R.; Saykally, R. J. *Phys. Rev. Lett.* **2001**, *86*, 5691−5694.
(417) Wagner, D. R.; Kim, H. S.; Saykally, R. J. *Astrophys. J.* **2000**, *545*, 854−860.
(418) Allain, T.; Sedlmayr, E.; Leach, S. *Astrophys. Space Sci.* **1995**, *224*, 417−418.
(419) Caro, C. N. N.; et al. *Astron. Astrophys.* **2001**, *367*, 347−354.
(420) Allain, T.; Leach, S.; Sedlmayr, E. *Astron. Astrophys.* **1996**, *305*, 602−615.
(421) Allain, T.; Leach, S.; Sedlmayr, E. *Astron. Astrophys.* **1996**, *305*, 616−630.
(422) Jochims, H. W.; Baumgärtel, H.; Leach, S. *Astrophys. J.* **1999**, *512*, 500−510.
(423) Sorkhabi, O.; et al. *J. Am. Chem. Soc.* **2001**, *123*, 671−676.
(424) Ekern, S. P.; Marshall, A. G.; Szczepanski, J.; Vala, M. *Astrophys. J.* **1997**, *488*, L39− L41.
(425) Guo, X.; Sievers, H.; Grützemacher, H. F. *Int. J. Mass. Spectrom.* **1999**, *185/186/187*, 1−10.
(426) Bernstein, M. P.; et al. *Science* **1999**, *283*, 1135−1138.
(427) Bakes, E. L. O.; Tielens, A. G. G. M. *Astrophys. J.* **1998**, *499*, 258−266.
(428) Bohme, D. K.; Wlodek, S.; Wincel, H. *Astrophys. J. L.* **1989**, *342*, 91−93.
(429) Jochims, H. W.; Baumgärtel, H.; Leach, S. *Astron. Astrophys.* **1996**, *314*, 1003−1009.
(430) Duley. W. W.; Seahra, S. *Astrophys. J.* **1998**, *507*, 874−888.
(431) Scott, A.; Duley, W. W. *Astrophys. J. L.* **1996**, *472*, 123−125.
(432) Mennella, V.; et al. *Astron. Astrophys.* **2001**, *367*, 335−361.
(433) Duley, W. W. *Astrophys. J.* **2000**, *528*, 841−848.
(434) Colangeli, L.; Mennella, V.; Baratta, G. A.; Bussoletti, E.; Strazzulla, G. *Astrophys. J.* **1992**, *396*, 369−377.
(435) Sonnentrucker, P.; Cami, J.; Ehrenfreund, P.; Foing, B. H. *Astron. Astrophys.* **1997**, *327*, 1215−1221.
(436) Scott, A. D.; Duley, W. W.; Jahani, H. R. *Astrophys. J. L.* **1997**, *490*, 175−177.

(437) Schnaiter, M.; et al. *Astrophys. J.* **1999**, *519*, 687−696.
(438) Duley, W. W.; Scott, A. D.; Seahra, S.; Dadswell, G. *Astrophys. J.* **1998**, *503*, L183−L185.
(439) Galazutdinov, G. A.; et al. *Mon. Not. R. Astron. Soc.* **2000**, *317*, 750−758.
(440) Ehrenfreund, P.; Foing, B. H. *Planet. Space Sci.* **1995**, *43*, 1183−1187.
(441) Petrie, S.; Bohme, D. K. *Astrophys. J.* **2000**, *540*, 869−885.
(442) Moutou, C.; Sellgren, K.; Verstraete, L.; Leger, A. *Astron. Astrophys.* **1999**, *347*, 949−956.
(443) Clayton, G. S. *Astron. J.* **1995**, *109*, 2069−2103.
(444) Herbig, G. H. *Astrophys. J.* **2000**, *542*, 334−343.
(445) Guillois, O.; Ledoux, G.; Reynaud, C. *Astrophys. J. L.* **1999**, *521*, 133−136.
(446) Andersen, A. C.; et al. *Astron. Astrophys.* **1998**, *330*, 1080−1090.
(447) Hill, H. G. M.; Jones, A. P.; d'Hendecourt, L. B. *Astron. Astrophys.* **1998**, *336*, L41−44.
(448) Allamandolla, L. J.; Sandford, S. A.; Wopenka, B. *Science* **1987**, *237*, 56−59.
(449) Sephton, M. A.; *Gilmour, Astrophys. J.* **2000**, *540*, 588−591.
(450) Messenger, S.; et al. *Astrophys. J.* **1998**, *502*, 284−295.
(451) Frenklach, M.; Feigelson, E. D. *Astron. Astrophys.* **1989**, *341*, 372−384.
(452) Richter, H.; et al. *J. Phys. Chem. A* **2001**, *105*, 1561−1573.
(453) Melius, C. F.; et al. *26th Symp. (Int.) Combust.* **1996**, 685−692.
(454) Wang, R.; Cadman, P. *Combust. Flame* **1998**, *112*, 359−370.
(455) Wang, R.; Cadman, P. *Combust. Flame* **1998**, *112*, 359−370.
(456) Siegmann, K.; Sattler, K. *J. Chem. Phys.* **2000**, *112*, 698−709.
(457) Bauschlicher, C. W.; Ricca, A. *Chem. Phys. Lett.* **2000**, *326*, 283−287.
(458) Böhm, H.; Jander, H. *Phys. Chem. Chem. Phys.* **1999**, *1*, 3775−3781.
(459) Fröchtenicht, R.; Hippler, H.; Troe, J.; Toennies, J. P. *J. Photobiol. A* **1994**, *80*, 33−37.
(460) Morter, C. L.; et al. *J. Phys. Chem.* **1994**, *98*, 7029−7035.
(461) Adamson, J. D.; et al. *J. Phys. Chem.* **1996**, *100*, 2125−2128.
(462) Cherchneff, I.; Barker, J. R.; Tielens, A. G. G. M. *Astrophys. J.* **1992**, *401*, 269−287.
(463) Cherchneff, I.; Barker, J. R. *Astrophys. J.* **1992**, *394*, 703−716.
(464) Blitz, A.; et al. *Phys. Chem. Chem. Phys.* **2000**, *2*, 805−812.
(465) Marinov, N. M.; Castaldi, M. J.; Melius, C. F.; Tsang, W. *Combust. Sci. Technol.* **1997**, *128*, 295−342.
(466) Babushok, V.; Tsang, W. *Combust. Flame* **2000**, *123*, 488−506.
(467) Kazakov, A.; Frenklach, M. *Combust. Flame* **1998**, *112*, 270−274.
(468) Weilmünster, P.; Keller, A.; Homann, K. H. *Combust. Flame* **1999**, *116*, 62−83.
(469) McEnally, C. S.; Pfefferle, L. D. *Combust. Flame* **1998**, *112*, 545−558.
(470) Olten, N.; Senkan, S. *Combust. Flame* **1999**, *118*, 500−507.
(471) Marinov, N. M.; et al. *Combust. Sci. Technol.* **1996**, *116/117*, 211−287.
(472) Melton, T. R.; Inal, F.; Senkan, S. M. *Combust. Flame* **2000**, *121*, 671−678.
(473) Richter, H.; Grieco, W. J.; Howard, J. B. *Combust. Flame* **1999**, *119*, 1−22.
(474) McEnally, C. S.; Pfefferle, L. D.; Robinson, A. G.; Zweir, T. S. *Combust. Flame* **2000**, *123*, 344−357.
(475) Marinov, N. M.; et al. *Combust. Flame* **1998**, *114*, 192−213.
(476) Arrington, C. A.; Ramos, C.; Robinson, A. D., Zwier, T. S. *J. Phys. Chem. A* **1998**, *102*, 3315−3322.
(477) Ristorcelli, I.; Klotz, A. *Astron. Astrophys.* **1997**, *317*, 962−967.
(478) Shebaro, L.; Bhalotra, S. R.; Herschbach, D. *J. Phys. Chem. A* **1997**, *101*, 6775−6780.
(479) McEwan, M. J.; et al. *Astrophys. J.* **1999**, *513*, 287−293.
(480) Park, J.; Burova, S.; Rodgers, A. S.; Lin, M. C. *J. Phys. Chem. A* **1999**, *103*, 9036−9041.
(481) Park, J.; Chakrabortky, D.; Bhusari, D. M.; Lin, M. C. *J. Phys. Chem. A* **1999**, *103*, 4002−4008.
(482) Tokmakov, I, V.; Park, J.; Gheyas, S.; Lin, M., C. *J. Phys. Chem. A* **1999**, *103*, 3636−3645.
(483) Mebel, A. M.; Lin, M. C.; Yu, T.; Morokuma, K. *J. Phys. Chem. A* **1997**, *101*, 3189−3196.
(484) Park, J.; Dyakov, I. V.; Lin, M. C. *J. Phys. Chem. A* **1997**, *101*, 8839−8843.
(485) Haider, N.; Husain, D. *J. Chem. Soc., Faraday Trans.* **1993**, *89*, 7−14.
(486) Haider, N.; Husain, D. *Int. J. Chem. Kinet.* **1993**, *25*, 423−435.
(487) Haider, N.; Husain, D. Z. *Phys. Chem.* **1992**, *176*, 133−150.
(488) Husain, D.; Ioannou, A. X. *J. Chem. Soc., Faraday Trans.* **1997**, *93*, 3625−3629.
(489) Haider, N.; Husain, D. *J. Photobiol. A Chem.* **1993**, *70*, 119−124.
(490) Husain, D.; Kirsch, L. J. *J. Chem. Soc., Faraday Trans.* **1971**, *67*, 2025−2035.
(491) Husain, D.; Young, A. N. *J. Chem. Soc., Faraday Trans.* **1975**, *71*, 525−531.
(492) Haider, N.; Husain, D. *Bunsen-Ges. Phys. Chem., Ber.* **1993**, *97*, 571−577.
(493) Husain, D. *J. Chem. Soc., Faraday Trans.* **1993**, *89*, 2164.
(494) Clary, D. C.; Haider, N.; Husain, D.; Kabir, M. *Astrophys. J.* **1994**, *422*, 416−422.
(495) Husain, D.; Ioannou, A. X. *J. Photochem. Photobiol. A* **1999**, *129*, 1−7.
(496) Bergeat, A.; Calvo, T.; Dorthe, G.; Loison, J. C. *Chem. Phys. Lett.* **1999**, *308*, 7−15.
(497) Bergeat, A.; Loison, J. C. *Phys. Chem. Chem. Phys.* **2001**, *3*, 2038−2042.
(498) Galland, N.; et al. *J. Phys. Chem. A* **2001**, *105*, 9893−9900.
(499) Chastaing, D.; James, P. L.; Sims; I. R.; Smith; I. W. M. *Phys. Chem. Chem. Phys.* **1999**, *1*, 2247−2256.
(500) Chastaing, D.; Le Picard, S. D.; Sims, I. R.; Smith, I. W. M. *Astron. Astrophys.* **2001**, *365*, 241−247.
(501) Rowe, B.; Parent, D. C. *Planet. Space Sci.* **1995**, *43*, 105−114.
(502) Sims, I. R.; et al. *Chem. Phys. Lett.* **1993**, *211*, 461−468.
(503) Rowe, B.; Canosa, A.; Sims, I. R. *J. Chem. Soc., Faraday Trans.* **1993**, *89*, 2193−2198.
(504) Smith, I. W. M.; Sims, I. R.; Rowe, B. R. *Chem. Eur. J.* **1997**, *3*, 1925−1928.
(505) Chastaing, D.; James, P. L.; Sims; I. R.; Smith; I. W. M. *Faraday Discuss.* **1996**, *109*, 165−182.
(506) Sims, I. R.; Smith, I. W. M. *Annu. Rev. Phys. Chem.* **1995**, *46*, 109−137.
(507) Smith, I. W. M. *Int. J. Mass Spectrom. Ion Processes* **1995**, *149/150*, 231−249.
(508) Smith, I. W. M.; Rowe, B. R. *Acc. Chem. Res.* **2000**, *33*, 261−268.
(509) Smith, M. *J. Phys. Chem. A* **1997**, *101*, 3356.
(510) Vakhtin, A. B.; Heard, D. E.; Smith, I. W. M.; Leone, S. R. *Chem. Phys. Lett.* **2001**, *344*, 310−316.
(511) Vakhtin, BA. B.; Heard, D. E.; Smith, I. W. M.; Leone, S. R. *Chem. Phys. Lett.* **2001**, *344*, 317−324.
(512) Guadagnini, R.; Schatz, G. C.; Walch, S. P. *J. Phys. Chem. A* **1998**, *104*, 5857−5862.
(513) Liao, Q.; Herbst, E. *Astrophys. J.* **1995**, *444*, 694−699.
(514) Canosa, A.; Sims, I. R.; Travers, D.; Smith, I. W. M.; Rowe, B. R. *Astron. Astrophys.* **1997**, *323*, 644−651
(515) Liao, WQ.; Herbst, E. *Astrophys. J.* **1995**, *444*, 694−701.
(516) Aalgia, M.; et al. *J. Chem. Soc., Faraday Trans.* **1995**, *91*, 575−596.
(517) Lee, Y. T. *Angew. Chem., Int. Ed.* **1987**, *26*, 939−951.
(518) Casavecchia, P.; et al. *Acc. Chem. Res.* **1999**, *32*, 503−511.
(519) Casavecchia, P.; Balucani, N.; Volpi, G. G. *Annu. Rev. Phys. Chem.* **1999**, *50*, 347−376.
(520) Kaiser, R. I.; et al. *Astrochemistry: From Molecular Clouds to Planetary Systems*; ASP: San Fancisco, 2000; pp 251−264.
(521) Kaiser, R. I.; et al. *Faraday Discuss.* **1998**, *109*, 183−204.
(522) Kaiser, R. I.; Suits, A. G. *Rev. Sci. Instrum.* **1995**, *66*, 5405−5410.
(523) Kaiser, R. I.; Ting, J.; Huang, L. C. L.; Balucani, N.; Asvany, O.; Lee, Y. T.; Chan, H.; Stranges, D.; Gee, D. *Rev. Sci. Instrum.* **1999**, *70*, 4185−4191.
(524) Casavecchia, P.; et al. *Faraday Discuss.* **2001**, *119*, 27−50.
(525) Naulin, C.; Costes, M. *Chem. Phys. Lett.* **1999**, *310*, 231−239.
(526) Naulin, C.; Costes, M. J. *Chin. Chem. Soc.* **1995**, *42*, 215−219.
(527) Kaiser, R. I.; Lee, Y. T.; Suits, A. G. *J. Chem. Phys.* **1995**, *103*, 10395−10398.
(528) Kaiser, R. I.; Ochsenfeld, C.; Head-Gordon, M.; Lee, Y. T.; Suits, A. G. *Science* **1996**, *274*, 1508−1511.
(529) Kaiser, R. I.; Ochsenfeld, C.; Head-Gordon, M.; Lee, Y. T.; Suits, A. G. *J. Chem. Phys.* **1997**, *106*, 1729−1741.
(530) Ochsenfeld, C.; Kaiser, R. I.; Suits, A. G.; Lee, Y. T.; Head-Gordon, M. *J. Chem. Phys.* **1997**, *106*, 4141−4151.
(531) Kaiser, R. I.; Stranges, D.; Lee, Y. T.; Suits, A. G. *J. Chem. Phys.* **1996**, *105*, 8721−8733.
(532) Mebel, A. M.; Kaiser, R. I.; Lee, Y. T. *J. Am Chem. Soc.* **2000**, *122*, 1776−1788.
(533) Kaiser, R. I.; Mebel, A. M.; Lee, Y. T.; Chang, A. H. H. *J. Chem. Phys.* **2001**, *115*, 5117−5125.
(534) Huang, L. C. L.; Lee, H. Y.; Mebel, A.; Lin, S. H.; Lee, Y. T.; Kaiser, R. I. *J. Chem. Phys.* **2000**, *113*, 9637−9648.
(535) Kaiser, R. I.; Sun, W.; Suits, A. G.; Lee, Y. T. *J. Chem. Phys.* **1997**, *107*, 8713−8716.
(536) Lee, T. N.; Mebel, A. M.; Kaiser, R. I. *J. Comput. Chem.* **2001**, *22*, 1522−1535.
(537) Kaiser, R. I.; Lee, Y. T.; Suits, A. G. *J. Chem. Phys.* **1996**, *105*, 8705−8720.
(538) Lee, T. N.; Lee, H. Y.; Mebel, A. M.; Kaiser, R.I. *J. Phys. Chem. A* **2001**, *105*, 1847−1856.
(539) Kaiser, R. I.; Stranges, D.; Bevsek, H. M.; Lee, Y. T.; Suits, A. G. *J. Chem. Phys.* **1997**, *106*, 4945−4953.
(540) Le, T. N.; Mebel, A. M.; Kaiser, R. I. *J. Phys. Chem. A* **2002** (in press).
(541) Hahndorf, I.; Lee, H. Y.; Mebel, A.; Lin, S. H.; Lee, Y. T.; Kaiser, R. I. *J. Chem. Phys.* **2000**, *113*, 9622−9636.
(542) Kaiser, R. I.; Ochsenfeld, C.; Stranges, D.; Head-Gordon, M.; LeeFaraday Y. T. *Faraday Discuss.* **1998**, *109*, 183−204.

(543) Nguyen, T. L.; Mebel, A. M.; Kaiser, R. I. *J. Phys. Chem. A* **2001**, *105*, 3284−3299.
(544) Nguyen, T. L.; Mebel, A. M.; Lin, S. H.; Kaiser, R. I. *J. Phys. Chem. A* **2001**, *105*, 11549−11559.
(545) Kaiser, R. I.; Mebel, A.; Chang, A. H. H.; Lin, S. H.; Lee, Y. T. *J. Chem. Phys.* **1999**, *110*, 10330−10344.
(546) Balucani, N.; Lee, H. Y.; Mebel, A.; Lee, Y. T.; Kaiser R. I. *J. Chem. Phys.* **2001**, *115*, 5107−5116.
(547) Kaiser, R. I.; Hahndorf, I.; Huang, L. C. L.; Lee, Y. T.; Bettinger, H. F.; Schleyer, P. V. R.; Schaefer, H. F. *J. Chem. Phys.* **1999**, *110*, 6091−6094.
(548) Hahndorf, I.; Lee, Y. T.; Kaiser, R. I.; Vereecken, L.; Peeters, J.; Bettinger, H. F.; Schleyer, P. V. R.; Schaefer, H. F., III *J. Chem. Phys.* **2002**, *116*, 3248−3262.
(549) Bettinger, H. F.; Schleyer, P. V. R.; Schreiner, P. R.; Schaefer, H. F., III; Kaiser, R. I.; Lee, Y. T. *J. Chem. Phys.* **2000**, *113*, 4250−4263.
(550) Kaiser, R. I.; Sun, W.; Suits, A.G. *J. Chem. Phys.* **1997**, *106*, 5288−5291.
(551) Ochsenfeld, C.; Kaiser, R. I.; Lee, Y. T. Head-Gordon, M. *J. Chem. Phys.* **1999**, *110*, 9982−9988.
(552) Kaiser, R. I.; Ochsenfeld, C.; Head-Gordon, M.; Lee, Y. T. *J. Chem. Phys.* **1999**, *110*, 2391−2403.
(553) Kaiser, R. I.; Nguyen, T. L.; Le, T. N.; Mebel, A. M. *Astrophys. J.* **2001**, *561*, 858−863.
(554) Kaiser, R. I.; Ochsenfeld, C.; Head-Gordon, M.; Lee, Y. T. *Astrophys. J.* **1999**, *510*, 784−788.
(555) Kaiser, R. I.; Stranges, D.; Lee, Y. T.; Suits, A. G. *Astrophys. J.* **1997**, *477*, 982−989.
(556) Mebel, A. M.; Kaiser, R. I. *J. Am. Chem. Soc.* **2002** (in press).
(557) Kaiser, R. I.; Lee, H. Y.; Mebel, A. M.; Lee, Y. T. *Astrophys. J.* **2001**, *548*, 852−860.
(558) Kaiser, R. I.; Ochsenfeld, C.; Head-Gordon, M.; Lee, Y. T. *Science* **1998**, *279*, 1181−1184.
(559) Baer, T.; Hase, W. L. *Unimolecular Reaction Dynamics;* Oxford University Press: Oxford, 1996.
(560) Kaiser, R. I.; Mebel, A.; Lee, Y. T. *J. Chem. Phys.* **2001**, *114*, 231−239.
(561) Kaiser, R. I.; Nguyen, T. L.; Mebel, A. M.; Lee, Y. T. *J. Chem. Phys.* **2002**, *116*, 1318−1324.
(562) Buonomo, E.; Clary, D. C. *J. Phys. Chem. A* **2001**, *105*, 2694−2707.
(563) Geppert, W.; Naulin, C.; Costes, M. *Chem. Phys. Lett.* **2001**, *333*, 51−56.
(564) Scholefield, M. R.; et al. *Chem. Phys. Lett.* **1998**, *288*, 487−493.
(565) Kaiser, R. I.; et al. *Faraday Discuss.* **2001**, *119*, 51−66.
(566) Kaiser, R. I. *Faraday Discuss.* **2001**, *119*, 273−274.
(567) Chastaing, D; et al. *Chem. Phys. Lett.* **2000**, *331*, 170−176.
(568) Chernicharo J.; et al. *Astron. Astrophys.* **1987**, *181*, L9−11.
(569) Millar, T. J.; Herbst, E. *Astron. Astrophys.* **1990**, *231*, 466−472.
(570) Petrie, S. *Mon. Not. R. Astron. Soc.* **1996**, *281*, 666−681.
(571) Velusamy, T.; Kuiper, T. B. H.; Langer, W. D. *Astrophys. J.* **1995**, *451*, L75−78.
(572) Markwick, A. J.; Millar, T. J.; Charnley, S. B. *Astrophys. J.* **2000**, *535*, 256−259.
(573) Chiong, C. C.; Asvany, O.; Balucani, N.; Lee, Y. T.; Kaiser, R. I. *Proceedings of the Eighth Asia-Pacific Physics Conference, A. P. P. C. 2000*; World Scientific Press: 2001; pp 167−169.
(574) Reisler, H.; Mangir, M.; Wittig, C. *J. Chem. Phys.* **1980**, *73*, 2280−2286.
(575) Martin M. *J. Photochem. Photobiol. A: Chem.* **1992**, *66*, 263−289.
(576) Balucani, N.; Mebel, A. M.; Lee, Y. T.; Kaiser, R. I. *J. Phys. Chem. A* **2001**, *105*, 9813−9818.
(577) Nelson, H. H.; Helvajian, H.; Pasternack, L.; McDonald, J. R. *Chem. Phys.* **1982**, *73*, 431−438.
(578) Nelson, H. H.; Pasternack, L.; Eyler, J. R.; McDonald, J. R. *Chem. Phys.* **1981**, *60*, 231−237.
(579) Lesiecki, M. L.; Hicks, K. W.; Orenstein, A.; Guillory, W. A. *Chem. Phys. Lett.* **1980**, 72−76.
(580) Kaiser, R. I.; Osamura, Y. *J. Phys. Chem. A* **2002** (in press).
(581) Huang, L. C. L.; Lee, Y. T.; Kaiser, R. I. *J. Chem. Phys.* **1999**, *110*, 7119−7122.
(582) Huang, L. C. L.; Chang, A. H. H.; Asvany, O.; Balucani, N.; Lin, S. H.; Lee, Y. T.; Kaiser, R. I.; Osamura, Y. *J. Chem. Phys.* **2000**, *113*, 8656−8666.
(583) Huang, L. C. L.; Balucani, N.; Lee, Y. T.; Kaiser, R. I.; Osamura, Y. *J. Chem. Phys.* **1999**, *111*, 2857−2860.
(584) Balucani, N.; Asvany, O.; Kaiser, R. I.; Osamura, Y. *J. Phys. Chem. A* **2002** (in press).
(585) Balucani, N.; Asvany, O.; Chang, A. H. H.; Lin, S. H.; Lee, Y. T.; Kaiser, R. I.; Osamura, Y. *J. Chem. Phys.* **2000**, *113*, 8643−8655.
(586) Balucani, N.; Asvany, O.; Chang, A. H. H.; Lin, S. H.; Lee, Y. T.; Kaiser, R. I.; Bettinger, H. F.; Schleyer, P. v. R.; Schaefer, H. F., III *J. Chem. Phys.* **1999**, *111*, 7472−7479.
(587) Balucani, N.; Asvany, O.; Chang, A. H. H.; Lin, S. H.; Lee, Y. T.; Kaiser, R. I.; Bettinger, H. F.; Schleyer, P.v. R.; Schaefer, H. F., III *J. Chem. Phys.* **1999**, *111*, 7457−7471.
(588) Kaiser, R. I.; Balucani, N.; Asvany, O.; Lee Y. T. In *Astrochemistry: From Molecular Clouds to Planetary Systems*; Minh, Y. C., van Dishoeck, E. F., Eds.: IAU Series 197; 2000; pp 251−264.
(589) Balucani, N.; Asvany, O.; Huang, L. C. L.; Lee, Y. T.; Kaiser, R. I.; Osamura, Y.; Bettinger, H. F.; Schleyer, P.v. R.; Schaefer, H. F., III *Astrophys. J.* **2000**, *545*, 892−906.
(590) Kaiser, R. I.; Balucani, N. *Int. J. Astrobiol.* **2002**, *1*, 15−23.
(591) Kaiser, R. I.; Lee, Y. T. *Highlights of Astronomy, Astronomical Society of the Pacific* **2002**, *12*, 88−91.
(592) Kaiser, R. I.; Balucani, N. *Acc. Chem. Res.* **2001**, *34*, 699−706.
(593) Balucani, N.; Asvany, O.; Huang, L. C. L.; Lee, Y. T.; Kaiser, R. I.; Osamura, Y. *Planet. Space Sci.* **2000**, *48*, 447−462.
(594) Kaiser, R. I. *ESA Spec. Publ.* **2001**, *496*, 145−153.
(595) Woon, D. E.; Herbst, E. *Astrophys. J.* **1997**, *477*, 204−208.
(596) Fukuzawa, K.; Osanura, Y.; Schaefer, H. F. *Astrophys. J.* **1998**, *505*, 278−285.
(597) Fukuzawa, K.; Osamura, Y. *Astrophys. J.* **1997**, *489*, 113−121.
(598) Chang, A. H. H. Private communication, 2001.
(599) Yang, D. L.; Lin, M. C. In *The Chemical Dynamics and Kinetics of Small Radicals*; Liu, K., Wagner, A., Eds.; World Scientific: 1995; pp 164−213.
(600) Chin, Y.; Lemme, C.; Kaiser R. I. Unpublished results.
(601) Kaiser, R. I.; Chiong, C. C.; Asvany, O.; Lee, Y. T.; Stahl, F.; Schleyer, P.v. R.; Schaefer, H. F. *Phys. Chem. Chem. Phys.* **2002** (in press).
(602) Kaiser, R. I.; Chiong, C. C.; Asvany, O.; Lee, Y. T.; Stahl, F.; Schleyer, P.v. R.; Schaefer, H. F. *J. Chem. Phys.* **2001**, *114*, 3488−3496.
(603) Stahl, F.; Schleyer, P.v. R.; Kaiser, R. I.; Lee, Y. T.; Schaefer, H. F., III *J. Chem. Phys.* **2001**, *114*, 3476−3487.
(604) Kaiser, R. I.; Stahl, F.; Schleyer, P.v. R.; Schaefer, H. F. *Planet. Space Sci.*, submitted for publication.
(605) van Look, H.; Peeters, J. *J. Phys. Chem.* **1995**, *99*, 16284−16289.
(606) Pedersen, O. P.; Opansky, B. J.; Leone, S. R. *J. Phys. Chem.* **1993**, *97*, 6822−6829.
(607) Herbst, E.; Woon, D. E. *Astrophys. J.* **1997**, *489*, 109−112.
(608) Koshi, M.; et al. *J. Phys. Chem.* **1992**, *96*, 9839−9843.
(609) Ceursters, B.; Nguyen, H. M. T.; Peeters, J.; Nguyen, M. T. *Chem. Phys.* **2000**, *262*, 243−252.
(610) Hoobler, R. J.; Leone, S. R. *J. Phys. Chem.* **1991**, *95*, 1342−1346.
(611) Lander, D. R.; Unfried, K. G.; Glass, G. P.; Curl, R. F. *J. Phys. Chem.* **1990**, *94*, 7759−7763.
(612) Opansky, B. J.; Leone, S. R. *J. Phys. Chem.* **1996**, *100*, 19904−19910.
(613) Kaiser, R. I.; Hahndorf, I.; Lee, Y. T.; Vereecken, L.; Peeters, J.; Bettinger, H. F.; Schleyer, P.v. R.; Schaefer, H. F. *Astron. Astrophys.*, submitted for publication.
(614) Kaiser, R. I.; Asvany, O.; Lee, Y. T.; Bettinger, H. F.; Schleyer, P. v. R.; Schaefer, H. F., III *J. Chem. Phys.* **2000**, *112*, 4994−5001.
(615) Kaiser, R. I.; Asvany, O.; Lee, Y. T. *Planet. Space Sci.* **2000**, *48*, 483−492.
(616) Yu, T.; Lin, M. *J. Phys. Chem.* **1995**, *99*, 8599−8606.
(617) Morrison, D. *Satellites of Jupiter*; University of Arizona Press: Tucson, 1992.
(618) Barbieri, C.; et al. *The Three Galileos: The Man, the Spacecraft, the Telescope*; Kluwer: Dordrecht, 1997.
(619) Marov, M. Y; et al. *Nonequilibrium Processes in the Planetary and Cometary Atmospheres: Theory and Applications*; Kluwer: Dordrecht, 1997.
(620) *Uranus*; Bergstralh, J. T., Miner, E. D., Matthews, M. S., Eds.; University of Arizona Press: Tucson, 1991.
(621) *Pluto and Charon;* Stern, S. A., Tholen, D. J., Eds.; University of Arizona Press: Tucson, 1997.
(622) *Origin and Evolution of Planetary and Satellite Atmospheres;* Atreya, S. K., Pollack, J. B., Matthews, M. S., Eds.; University of Arizona Press: Tucson, 1989.
(623) Cruikshank, D. P. *Neptune and Triton*; University of Arizona Press: Tucson, 1995.
(624) Coustenis, A.; Taylor, F. *Titan−The Earth-Like Moon*; World Scientific: London, 1999.
(625) Yung, Y. L.; DeMore, W. B. *Photochemistry of Planetary Atmospheres;* Oxford University Press: Oxford, 1999.
(626) *ESA's Report to the 33rd COSPAR Meeting*; ESA-SP-*1241*, 2000.
(627) Dobriejevic, M.; Parisot, J. P. *Planet. Space Sci.* **1998**, *46*, 491−505.
(628) Baukal, C. E. *Oxygen-Enhanced Combustion*; CRC Press: Boca Raton, 1998.
(629) Hausmann, M.; Homann, K. H. *Ber. Bunsen-Ges. Phys. Chem.* **1990**, *94*, 1308−1312.
(630) Harris, S. J.; Shin, S. H.; Goodwin, D. G. *Appl. Phys. Lett.* **1995**, *66*, 891−893.
(631) Redman, S. A.; et al. *Phys. Chem. Chem. Phys.* **1999**, *1*, 1415−1424.
(632) Löwe, A. G.; Hartlieb, A. T.; Brand, J.; Atakan, B.; Höinghaus, K. *Combust. Flame* **1999**, *118*, 37−50.
(633) De Theije, F. K.; Schermer, J. J.; van Enckevort, W. J. P. *Diamond Relat. Res.* **2000**, *9*, 1439−1449.

(634) Celii, F. G.; Butler, J. E. *Annu. Rev. Phys. Chem*. **1991**, *42*, 643−684.
(635) Balucani, N.; Asvany, O.; Lee, Y. T.; Kaiser, R. I.; Galland, N.; Hannachi, Y. *J. Am. Chem. Soc.* **2000**, *122*, 11234−11235.
(636) Balucani, N.; Asvany, O.; Lee, Y. T.; Kaiser, R. I.; Galland, N.; Hannachi, Y. N *J. Comput. Chem.* **2001**, *22*, 1359−1365.
(637) Schofield, K. *Combust. Flame* **2001**, *124*, 137−145.
(638) Hemmi, N.; Suits, A. G. *J. Chem. Phys.* **1998**, *109*, 5338−5343.
(639) Blank, D. A.; Hemmi, N.; Suits, A. G.; Lee, Y. T. *Chem. Phys.* **1998**, *231*, 261−278.
(640) Hinrichs, R. Z.; Willis, P. A.; Stauffer, H. U.; Schroden, J. J.; et al. *J. Chem. Phys.* **2000**, *112*, 4634−4643.
(641) Willis, P. A.; Stauffer, H. U.; Hinrichs, R. Z.; Davis, H. F. *J. Chem. Phys.* **1998**, *108*, 2665−2668.
(642) Willis, P. A.; Stauffer, H. U.; Hinrichs, R. Z.; Davis, H. F. *J. Phys. Chem. A* **1999**, *103*, 3706−3720.
(643) Stauffer, H. U.; Hinrichs, R. Z.; Willis, P. A.; Davis, H. F. *J. Chem. Phys.* **1999**, *111*, 4101−4112.
(644) Stauffer, H. U.; Hinrichs, R. Z.; Schroden, J. J.; Davis, H. F. *J. Chem. Phys.* **1999**, *111*, 10758−10761.
(645) Willis, P. A.; Stauffer, H. U.; Hinrichs, R. Z.; Davis, H. F. *Rev. Sci. Instrum*. **1999**, *70*, 2606.
(646) Stauffer, H. U.; Hinrichs, R. Z.; Schroden, J. J.; Davis, H. F. *J. Phys. Chem. A* **2000**, *104*, 107−116.
(647) Ahmed, M.; Peterka, D. S.; Suits, A. G. *Chem. Phys. Lett.* **2000**, *317*, 264−268.
(648) Ahmed, M.; Peterka, D. S.; Suits, A. G. *Phys. Chem. Chem. Phys.* **2000**, *2*, 861−868.

CR970004V